NOTE TO USERS

Transverse Magnetic Wave Scattering by Elliptic Chiral Cylinder

Biglar Najjar-Khatirkolaei

A Thesis

in

The Department

of

Electrical and Computer Engineering

Presented in Partial Fulfillment of the Requirements
for the Degree of Master of Applied Science
(Electrical and Computer Engineering) at
Concordia University
Montreal, Quebec, Canada

August 2005

Your file Votre référence
ISBN: 0-494-10245-4
Our file Notre référence
ISBN: 0-494-10245-4

Abstract

The electromagnetic scattering problem of normal incident waves on an elliptic chiral cylinder is considered. The cylinder is assumed to be homogeneous and isotropic and extends infinitely long in the z direction. An exact boundary value solution for the scattering problem of the TM wave by the elliptic chiral cylinder is analyzed and presented. The solution is based on the separation of variable technique in the elliptic cylinder coordinates system, and expressed in terms of Mathieu and modified Mathieu functions. The incident, transmitted and scattered electromagnetic waves are expressed in terms of an infinite series of wave functions. The matrix forms of the expansion coefficients are found by applying the boundary conditions and orthogonality of the Mathieu functions. The expression of the radar cross section (RCS) per unit length or echo width of electromagnetic wave scattering by elliptic chiral cylinder for co- and cross-polarized waves are derived by using the asymptotic expansions for modified Mathieu functions. Validation of the developed formulation and computer program are investigated by considering many limiting cases such as circular dielectric, circular perfect conducting, and circular chiral cylinders, as well as elliptic dielectric and elliptic perfect conducting cylinders. Numerical results of the forward and back scattered echo widths for both co- and cross-polarized waves for various cases are presented and discussed. The numerical results show the co- and cross-polarized bistatic and monostatic echo widths depend on the frequency and incidence angle of the incident wave, constitutive parameters and geometry of the elliptic chiral cylinder. In general, the echo widths decrease by increasing the chirality admittance, and increase by increasing the axes of the elliptic chiral cylinder.

Table of Contents

List of Figures

1. Introduction

1.1 Motivations

Chiral media is a subclass of the more general bi-anisotropic media and contains an additional electrical material parameter besides the permitivity and permeability. This media is a reciprocal medium characterized by different phase velocities for right and left circularly polarized waves. Considerable attention has been given to chiral media in the recent years because of its unique properties in affecting the behavior of electromagnetic fields. Electromagnetic chirality and chiral materials have been investigated for a variety of potential applications, e.g. scattering and waveguides. Chiral media is used to control electromagnetic scattered fields due to its additional electrical material parameter which is an advantage for some applications. This is because chiral media responds with both electric and magnetic polarization to either electric or magnetic excitation. Also extensive research have been carried out for scattering by non-chiral media of elliptical cross-section. Elliptical cylinders have one more degree of freedom compared to circular cylinders.

The solution of the problem of electromagnetic scattering by an elliptic chiral cylinder can be used to represent six kinds of cylinders by choosing appropriate parameters. Examples include circular non-chiral cylinders (perfect conducting and dielectric cylinders), circular chiral cylinders, elliptic non-chiral cylinders (perfect conducting and dielectric cylinders), and elliptic chiral cylinders. This is a motivating reason that we are interested to find a solution for the electromagnetic scattering wave by an elliptic chiral cylinder.

2. Objectives

The main objective of this thesis is to develop an exact solution for the electromagnetic wave scattering by an elliptic chiral cylinder. The focus on the development of exact closed form solution for the transverse magnetic (TM) polarized electromagnetic scattering case. To achieve such objective, the elliptic cylinder coordinates system, and solution of the wave equations in this system using the separation of variables technique are introduced. Expressions of the wave equation in chiral media using elliptic coordinates and expressions of incident, transmitted and scattered electromagnetic waves in terms of an infinite series of wave functions are derived. The expansion coefficients are found by applying the boundary conditions and the orthogonality of the Mathieu functions. The expressions of echo widths for co- and cross-polarized are presented. Another objective of this work is to present numerical results of the bistatic (forward scattering) and monostatic (back-scattered) echo widths for co- and cross-polarized for a variety of cases by changing the incidence angle, the size of cylinders, and the constitutive parameters of the elliptic chiral cylinder.

1.3 Literature Review

1.3.1 Scattering by Chiral Media

An integral equation and method of moments solution to the problem of scattering by an inhomogeneous chiral material of arbitrary cross section and its numerical results, including echo width and internal fields, for the scattering by chiral slabs and circular cylinders were presented in [1]. An efficient recursive eigenfunction solution for the problem of scattering by a multilayer chiral circular cylinder, with or without a surface

impedance center cylinder, for a transverse magnetic (TM) and transverse electric (TE) incident plane wave, and numerical results, including echo width and internal fields, were presented in [2]. Two sets of integral equations for electromagnetic scattering by isotropic two-dimensional chiral bodies embedded in free space which can be attached to a perfect electric conducting body were obtained in [3]. A simple moment solution was presented in [4] for the problem of TE and TM electromagnetic scattering from a homogeneous chiral cylinder of arbitrary cross section. A formal exact full-wave solution for the problem of scattering at a nonchiral–chiral interface in a coaxial waveguide and its numerical results were presented in [5]. The analytic representation of two-dimensional dyadic Green's function of a perfectly conducting cylinder coated with one-layered chiral medium was derived and expanded in terms of the normalized cylindrical vector wave functions, and the integral equation for the current on the loaded strip was formulated in [6]. The electromagnetic scattering by an infinite regular array of thin planar chiral structures disposed on grounded or ungrounded dielectric slabs together with experimental results concerning co-polarized and cross-polarized reflection coefficients from both grounded and ungrounded finite grids of novel planar chiral particles were reported in [7]. Angular scattering from radially stratified spherical chiral objects using a matrix Riccati equation to examine basic scattering properties of spherical chiral structures with radial inhomogeneous in permittivity, permeability, and chirality was formulated in [8]. A TM polarization plane wave scattered by various multiple strip-loaded cylindrical chiral objects, and two-dimensional electric dyadic Green's functions in multi-layered cylindrical chiral media were derived according to the scattering superposition principle in [9-10]. In [11], the back scattering of electromagnetic waves

was investigated for a thin hollow chiral anisotropic conducting cylinder with a longitudinal slot. The measurement results were presented for the radar back-scattering cross section in the microwave band. A semi-analytical solution was presented to the problem of electromagnetic scattering from a collection of parallel chiral cylinder of a circular cross section for a TE and TM incident plane wave in [12]. A conceptual idea for a reciprocal phase shifting using chiral materials was discussed in [13]. In [14], constitutive relations which include electric quadrupole terms, in addition to electric and magnetic dipole terms, were used to describe the optical activity, in particular the circular birefringence of an anisotropic chiral medium. The propagation behavior of a cylindrical waveguide loaded centrally by a coaxial chiral rod was investigated by a boundary value procedure in [15]. A procedure to extract all three constitutive parameters of chiral material from waveguide measurements was presented in [16].

1.3.2 Scattering by Non-Chiral Elliptic Structures

An elliptic cylinder has one extra degree of freedom compared to a circular one which represents an advantage. The TE and TM electromagnetic scattering waves by elliptic cylindrical structures were considered for four configurations, conducting elliptic cylinders, homogeneous elliptic cylinders, dielectric coated conducting elliptic cylinders, and confocal dielectric-coated dielectric elliptic cylinders, and their numerical results were presented in [17]. The problem of electromagnetic scattering from a homogeneous elliptic cylinder coated with a dielectric or magnetic material, and its solutions in terms of elliptical harmonics, i.e. Mathieu and modified Mathieu functions were presented in [18-19]. Near field analysis and coupling of a perfectly conducting slotted elliptic cylinder

excited by an electric line source placed inside or outside the cylinder, and their solutions using separation of variables technique in terms of Mathieu and modified Mathieu functions were presented in [20]. A solution to the boundary value problem of TE multiple scattering by M parallel perfectly conducting elliptic cylinders and its numerical results for the forward and back scattered fields by two cylinders were presented in [21]. In [22], the scattering properties of an impedance elliptic cylinder coated with a homogeneous material were investigated analytically and the method of separation of variables was used to determine the field distributions in each region for both the TM and TE excitations. An exact solution to the electromagnetic scattering by a dielectric multilayer infinite cylinder of elliptic cross section using an efficient recursive procedure for the computation of fields and radar cross sections per unit length under a TM illumination was presented in [23]. A low frequency analysis of current carring elliptic conductors using the point matching method in the elliptic coordinate system was presented in [24]. The scattering of an electromagnetic plane wave by a conducting strip coated with a multilayer elliptic dielectric and its solution by implementing an efficient procedure for the "treatment" of the boundary conditions were presented in [25]. An analytical solution to the electromagnetic scattering by multilayer elliptic cylinders was derived for the case of isorefractive materials, and for these materials, a recursive solution similar to the solution for the multilayer circular cylinder was presented in [26].

1.4 Overview of the Thesis

In Chapter 2, the properties of chiral media and the propagation of electromagnetic waves inside a chiral media are discussed. This includes chiral and chirality, behavior of

electromagnetic fields in chiral media, and chiral wave equation. Chapter 3 reviews the wave equation in elliptic cylinder coordinates. In this chapter the elliptic cylinder coordinates system, and the solution of the wave equations in this system using the separation of variables technique are introduced. Separated wave equations in the elliptic coordinates are named the Mathieu equations and their solutions are the Mathieu and modified Mathieu functions. In Chapter 4 the theoretical solution of TM polarized electromagnetic scattering by a chiral elliptic cylinder is developed. Expression of the wave equation in elliptic coordinates and chiral media, and expression of incident, transmitted and scattered electromagnetic wave are derived. In this chapter the expansion coefficients are found by applying the boundary conditions and the orthogonality of the Mathieu functions. Also the expressions of echo width for co- and cross-polarized are presented. In Chapter 5 validation investigations of the numerical results are presented for several special cases. The numerical results of the bistatic (forward scattering) and monostatic (back-scattered) echo widths for co- and cross-polarized for a variety of cases by changing the incidence angle, the size of cylinders, and the constitutive parameters of the elliptic chiral cylinder are presented and discussed. In Chapter 6, summary, conclusions and suggested future work are presented. Details of the calculation of Mathieu and modified Mathieu functions, such as recurrence relations for the Fourier coefficients, methods of the characteristic value computation and convergence of the Fourier coefficients are given in an appendix.

2. Chiral Media and Electromagnetic Waves

2.1 Chiral and Chirality

The term "*chiral*" is a Greek's word and means "*hand*". The following are some concept definitions of chiral [27-31]:

- Material with either a left or right handed helical arrangement.
- Having different left-handed and right-handed forms, not mirror symmetric.
- A chiral or asymmetric molecule is one that can be distinguished from its mirror image.
- An object whose mirror image is not the same as itself. Compounds with four different substituents on a carbon atom are chiral.
- Any molecule that is not superimposable on its mirror image.

Molecules can be chiral if they contain one or more chiral centers. For the purposes of introductory organic chemistry, a chiral center can be defined as a *hybridized carbon* that is bonded to four different groups. On the other hand chiral molecule has a carbon atom with four different groups attached. A chiral molecule is not superimposable with its mirror image. Like left and right hands (that have a thumb, fingers in the same order, but are mirror images and not the same), chiral molecules have the same things attached in the same order, but are mirror images and not the same (Figure 2.1). The best definition for chiral molecule maybe is one that, "The necessary and sufficient condition for a chiral molecule is one that is not superimposable on its mirror image" [32]. For example, you cannot place your right hand on your left and have all hand parts in the same place. They are related to each other as mirror images in three-dimensional space, and as such they

can not be superimposed on top of each other. All the other description about asymmetric carbon atoms or four different groups, applies only with certain constraints. An object that is not chiral is said to be achiral (or non-chiral). Thus all objects are either chiral or achiral.

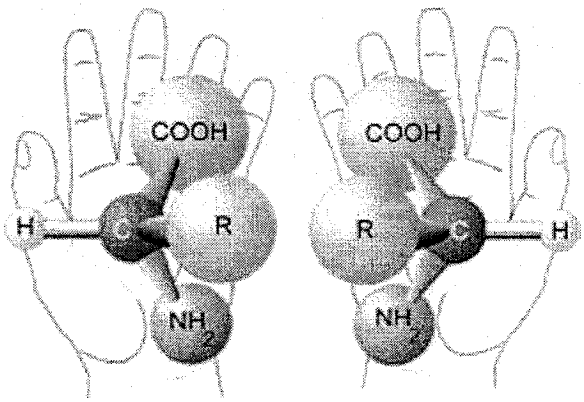

Figure 2.1 – Hands and Chiral Molecules [32]

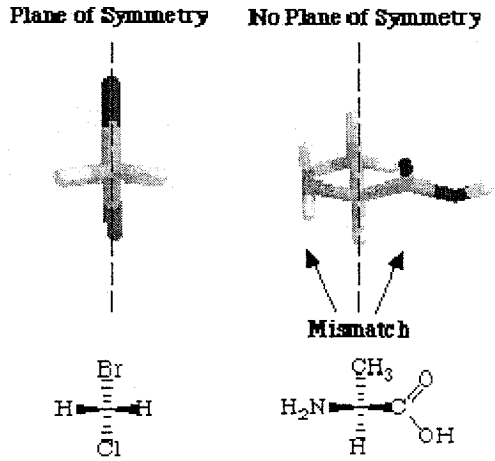

Figure 2.2 – Molecule with 2 & 4 groups [34]

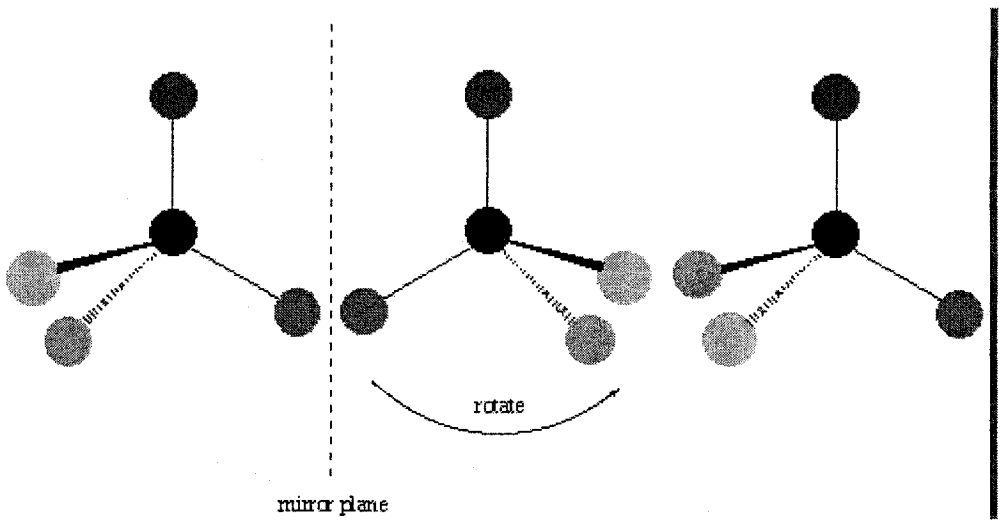

Figure 2.3 – Even after rotation of a chiral molecule, it remains different form [35]

The term "*chirality*" is also Greek's word and refers to the property of "*handness*". Chirality is an important chemical concept. For example the active ingredients in caraway seeds and spearmint demonstrate the concept. Though they have identical molecular structures, the two substances taste differently because they are opposite in chirality [33]. Chirality, resulting from the presence of four different groups around a carbon results from an asymmetry in the molecule. This can be seen by examining the molecules shown in figure 2.2, when two identical groups are on one carbon, there is an internal mirror plane passing through the molecule; when four groups are present, there is no internal mirror plane (no symmetry) and hence the carbon is chiral. Whether or not a molecule or crystal is chiral is determined by its symmetry. Chirality is a special case of asymmetry. Even after rotating one of the molecules it remains different from its stereoisomer and they are not superimposable (Figure 2.3). Chiral molecules are also called *dissymmetric*. They are not necessarily *asymmetric* (i.e. without symmetry), because they can have other types of symmetry [32]. However, all *amino acids* (except *glycine*) and many *sugars* are indeed asymmetric as well as dissymmetric. Non-superimposability on the mirror image is a necessary and sufficient condition for chirality, no exception has ever been found. The non-superimposability can come about in a number of ways, and need not involve a chiral centre or even organic molecules at all [36]. A *tertiary amine* and its apparently non-superimposable mirror image are shown in figure 2.4.

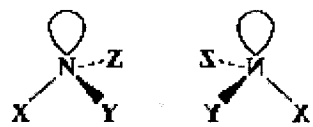

Figure 2.4 - Tertiary Amine [32]

Among the Archimedean solids we find two chiral forms, one turning to the right and the other to the left, respectively. They called *snub polyhedron* (Figure 2.5). The *double helix* is also chiral form (Figure 2.6). Louis Pasteur discovered the chirality of *artaric acid* in 1860 (Figure 2.7). Figure 2.8 shows a model of chiral crystalline structure.

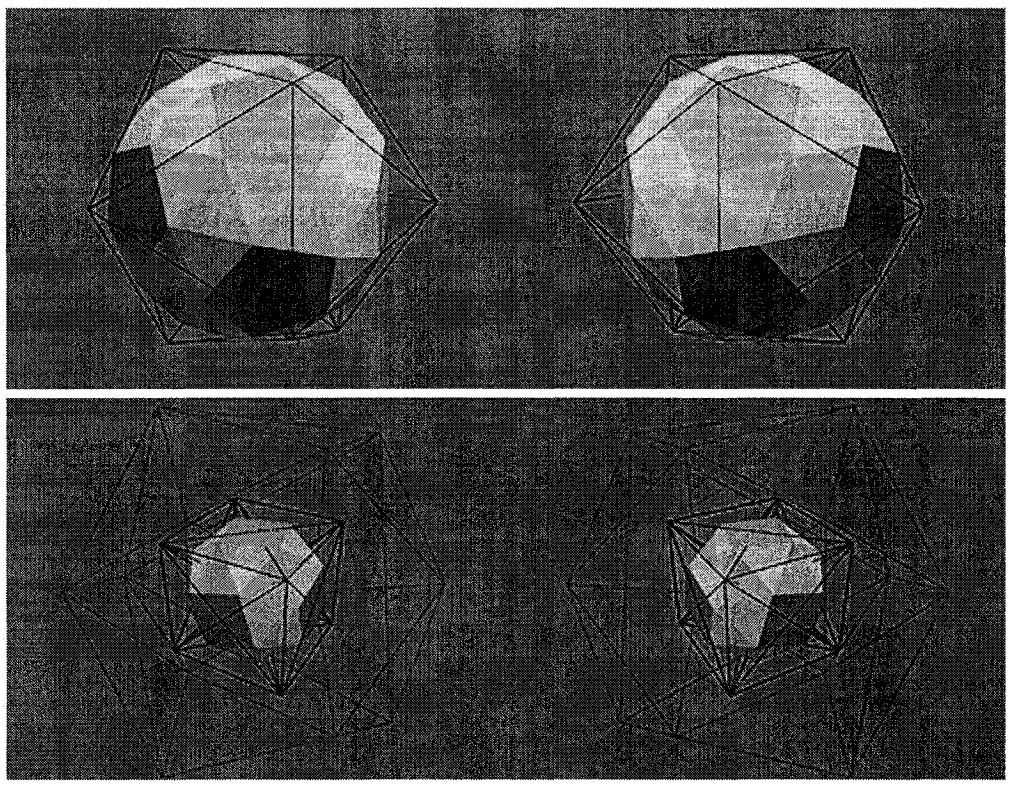

Figure 2.5 – Snub Polyhedron [37]

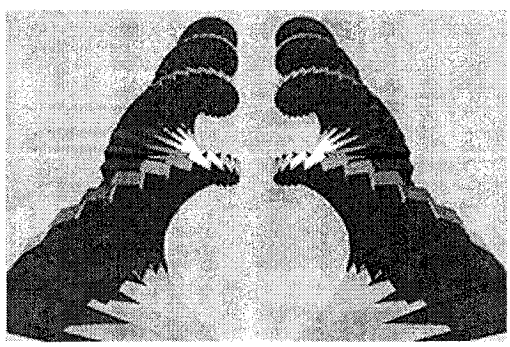

Figure 2.6 - Double Helix [37]

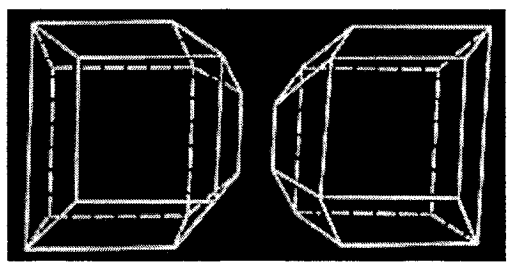

Figure 2.7 - Artaric Acid [37]

A chiral molecule has the property of rotating the plane of polarization of plane-polarized monochromatic light that is passed through it. This phenomenon is called optical activity. The light usually used for the determination of optical activity is sodium light. The rotation will be different, may be zero, and may even reverse in direction compared with the rotation given with sodium light.

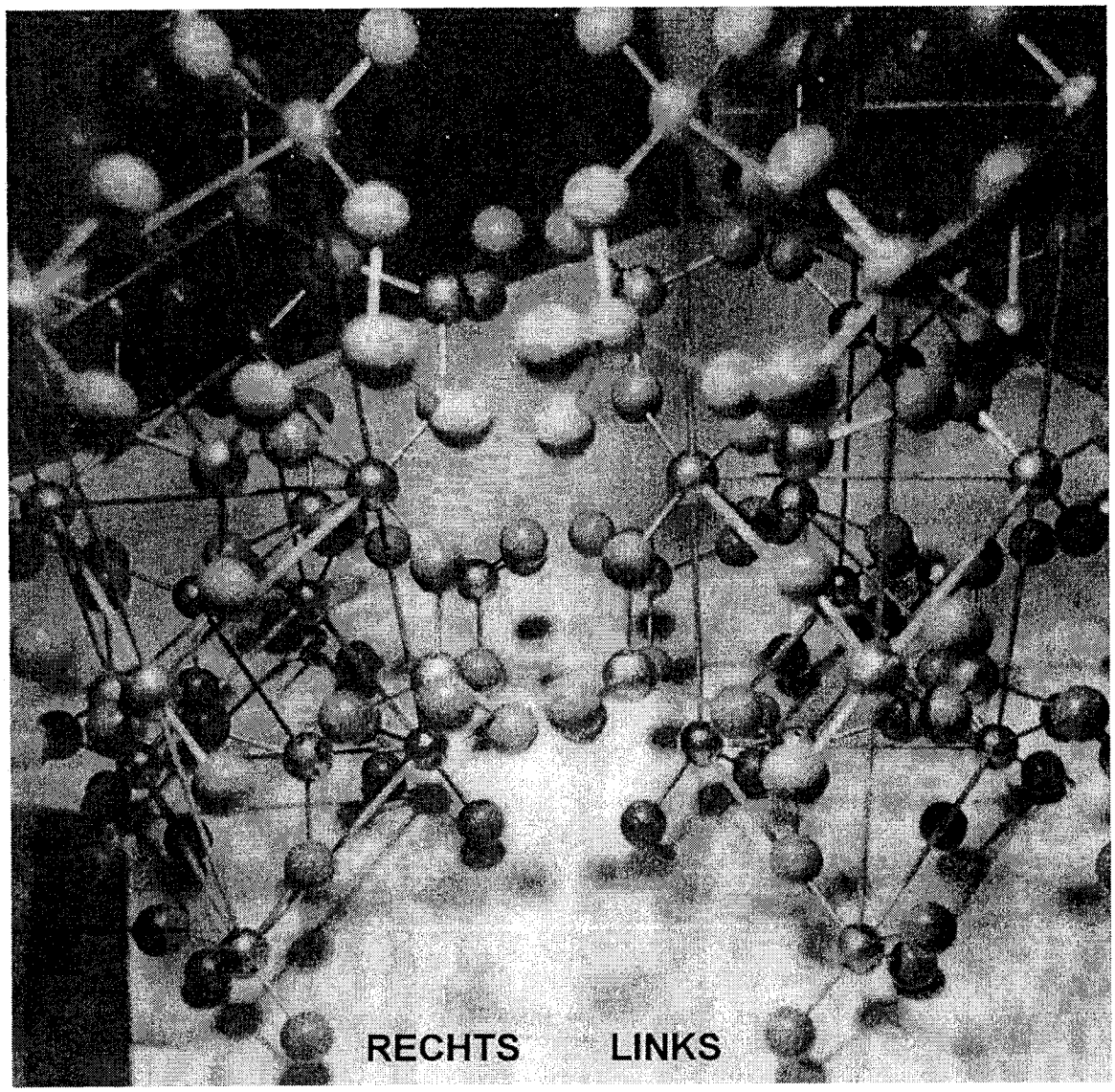

Figure 8 - Model of Chiral Crystalline Structure [37]

Many important molecules required for life exist in two forms. These two forms are non-superimposable mirror images of each other and are called "*enantiomers*" (from the Greek word for opposite) or "*optical isomers*", because they rotate plane-polarized light either to the right or to the left. Nearly all of the biological polymers must be homochiral (all its component monomers having the same handedness or 100 % optically active) to function. All *amino acids* in *proteins* are left-handed, while all *sugars* in DNA and RNA are right-handed [38]. Life on Earth is made of left-handed *amino acids*, almost exclusively. No one knows why but some of the *amino acids* that fall to earth from space are more left than right. Thus, it is known that radiation can also exist in left and right handed forms. There is a theory called the Bonner hypothesis, that proposes that left handed radiation in space (from a rotating neutron star for example) could lead to left handed amino acids in space, which would explain the left handed amino acids in meteorites [39].

Many biological and natural molecules are chiral, such as e.g. amino acids, carbohydrates, nucleic acids, sugars, proteins, hormones, glycine, tertiary amine, artaric acid, snub polyhedron, DNA, and RNA. Some man made chiral objects are irregular tetrahedron, stringed instruments, double helix and hand gloves.

A recent practical work, on chiral materials have been carried out by Gerald Busse, Jens Reinert and Arne F. Jacob [40]. They produced 4.0-mm diameter circular chiral objects by winding a 0.2-mm-diameter copper wire to form right-handed three-turn helices. For electrical insulation and to allow random orientation, each helix was embedded in a 6.0-mm dielectric foam sphere using an injection molding process. To this end, the helices were dispersed in Teflon molds that were injected with conventional two

components polyurethane foam. During each run, 8400 produced chiral objects were enough to fill on average 0.79 m of a circular waveguide with 50-mm diameter used in the experiments. The material was diluted by adding foam spheres randomly, without chiral inclusion. The shape of the chiral slab within the waveguide was fixed by two 7.5-mm thick polystyrene foam plugs. Because of the short length and a low permittivity, $\varepsilon_r=1.03\text{-}j1.28x10^{-4}$, as determined from resonator measurements, their influence on the measured response was neglected. In these experiments some preliminary investigations were presented, delivering important information about homogeneity, chirality, and especially, the resonant behavior of the chiral material.

2.2 Behavior of Electromagnetic fields in Chiral Media

The chiral media is a reciprocal medium characterized by different phase velocities for right and left circularly polarized waves. These are the same properties as an isotropic optically active media, therefore the same constitutive relationships are used. Chiral media responds with both electric and magnetic polarization to either electric or magnetic excitation, and chiral objects can generate both co- and cross-polarized scattered fields. In a lossless chiral medium, any linearly polarized wave undergoes a rotation of its polarization as it propagates. For a chiral cylinder, the chirality results in a coupling between the TM_Z and TE_Z scattering waves. Therefore, the solution of the scattering problem involving chiral medium is more complicated compared to scattering by achiral medium.

An isotropic chiral medium is a macroscopically continuous medium composed of equivalent chiral objects that are uniformly distributed and randomly oriented. The theory

of electromagnetic wave propagation in isotropic chiral media differs from the more common aspects of isotropic achiral media. From the technical point of view, an isotropic chiral medium is characterized by three parameters, in counterpoint to achiral media characterized by two parameters only (the dielectric constant and the magnetic permeability). The new extra parameter, the so-called chirality admittance, is responsible for optical activity. Also the electromagnetic chirality is known as optical activity in the optical regime.

Interaction of electromagnetic waves with bi-anisotropic media offers some novel promising applications in microwave and millimeter-wave technology. The bi-anisotropic medium is a generalization of the well-known isotropic chiral medium and it is described in the general case by four dyadic constitutive parameters and a special type of this medium is the uniaxial bi-anisotropic chiral medium, where the constitutive parameter dyadics are uniaxial.

2.3 The Chiral Wave Equation

This section presents the procedure for transforming the coupled wave equations for chiral media to a set of uncoupled wave equations so that classical eigenfunction techniques can be used [2]. The constitutive relationships for a chiral medium can be written as

$$\vec{D} = \varepsilon \vec{E} - j\gamma \vec{B} \tag{2.1}$$

$$\vec{H} = \frac{1}{\mu} \vec{B} - j\gamma \vec{E} \tag{2.2}$$

where $\vec{D}, \vec{B}, \vec{E},$ and $\vec{H}$ are the electric flux density, magnetic flux density, electric field, and magnetic field, respectively. Also ε is the permittivity, μ is the permeability, and γ is the chiral admittance of the medium. If μ, ε, or γ is complex the media is lossy. If $\gamma = 0$, then (2.1) and (2.2) reduce to the constitutive for an achiral medium. To simplify Equations (2.1) and (2.2) can be rewritten as

$$\vec{D} = \varepsilon_c \vec{E} - j\mu\gamma \vec{H} \tag{2.3}$$

$$\vec{B} = \mu \vec{H} + j\mu\gamma \vec{E} \tag{2.4}$$

where $\varepsilon_c = \varepsilon + \mu\gamma^2$, is the effective permittivity of the chiral medium.

In a chiral media with electric volume current density $\vec{J}$ and electric charge density ρ, the matrix form of Maxwell's equations can be written as

$$\nabla \times \begin{pmatrix} \vec{E} \\ \vec{H} \end{pmatrix} = [K] \begin{pmatrix} \vec{E} \\ \vec{H} \end{pmatrix} + \begin{pmatrix} \vec{0} \\ \vec{J} \end{pmatrix}, \tag{2.5}$$

$$\nabla \cdot \begin{pmatrix} \vec{E} \\ \vec{H} \end{pmatrix} = \frac{\rho}{\varepsilon} \begin{pmatrix} 1 \\ -j\gamma \end{pmatrix}, \tag{2.6}$$

where

$$[K] = \begin{bmatrix} \omega\mu\gamma & -j\omega\mu \\ j\omega\varepsilon_c & \omega\mu\gamma \end{bmatrix}, \tag{2.7}$$

$$\text{and} \qquad \rho = \frac{j}{\omega} \nabla \cdot \vec{J}. \tag{2.8}$$

Using (2.5) and (2.6), the source-free wave equation in chiral media, in terms of ($\vec{E}$, $\vec{H}$), is

$$\nabla^2 \begin{pmatrix} \vec{E} \\ \vec{H} \end{pmatrix} + [K]^2 \begin{pmatrix} \vec{E} \\ \vec{H} \end{pmatrix} = 0. \tag{2.9}$$

The coupling caused by [K] in the wave equation can be removed by diagonalizing [K] such that

$$[A]^{-1}[K][A] = \begin{bmatrix} k_R & 0 \\ 0 & -k_L \end{bmatrix}, \tag{2.10}$$

where

$$[A] = \begin{bmatrix} 1 & 1 \\ j/\eta_c & -j/\eta_c \end{bmatrix}, \tag{2.11}$$

and the chiral wave impedance and wave numbers are given by

$$\eta_c = \sqrt{\frac{\mu}{\varepsilon_c}}\ , \tag{2.12}$$

$$K_R = \omega\sqrt{\mu\varepsilon_c} + \omega\mu\gamma\ , \tag{2.13}$$

$$K_L = \omega\sqrt{\mu\varepsilon_c} - \omega\mu\gamma\ . \tag{2.14}$$

We define ($\vec{E}_R$, $\vec{E}_L$) by

$$\begin{pmatrix} \vec{E} \\ \vec{H} \end{pmatrix} = [A] \begin{pmatrix} \vec{E}_R \\ \vec{E}_L \end{pmatrix}, \tag{2.15}$$

where $\vec{E}_R$ and $\vec{E}_L$ are the electric fields of right and left circularly polarized waves with propagation constants K_R and K_L, respectively. Substituting (2.15) into (2.5) and (2.6) results in a set of uncoupled equations for chiral media

$$\nabla \times \begin{pmatrix} \vec{E}_R \\ \vec{E}_L \end{pmatrix} = \begin{pmatrix} K_R \vec{E}_R \\ -K_L \vec{E}_L \end{pmatrix} + \vec{J} \frac{j\eta_c}{2} \begin{pmatrix} -1 \\ 1 \end{pmatrix} \tag{2.16}$$

$$\textit{and} \qquad \nabla \cdot \begin{pmatrix} \vec{E}_R \\ \vec{E}_L \end{pmatrix} = \frac{\rho}{2\varepsilon} \begin{pmatrix} 1-\eta_c\gamma \\ 1+\eta_c\gamma \end{pmatrix}. \tag{2.17}$$

Then the uncoupled source-free wave equation in chiral media is

$$\nabla^2 \begin{pmatrix} \vec{E}_R \\ \vec{E}_L \end{pmatrix} + \begin{pmatrix} K_R^2 \vec{E}_R \\ K_L^2 \vec{E}_L \end{pmatrix} = 0. \tag{2.18}$$

2.4 Conclusion

In this chapter, we review the properties and wave equation of chiral media. The term "*chiral*" and "*chirality*" are Greek's words and mean "*hand*" and "*handness*", respectively. All objects are either chiral or achiral. Many biological and natural molecules are chiral. Some man made chiral objects are irregular tetrahedron, stringed instruments, double helix and hand gloves. Some waveguide experiments on chiral materials as a practical work is explained. The chiral media is a reciprocal medium characterized by different phase velocities for right and left hand circularly polarized

waves. These are the same properties as an isotropic optically active media, therefore the same constitutive relationships are used. The procedure for transforming the coupled wave equations for chiral media to a set of uncoupled wave equations are also presented.

3. Wave Equation in Elliptic Coordinates

The solution of the problem of electromagnetic scattering wave by an elliptic chiral cylinder should be expressed in terms of elliptic coordinates. That is convenient to find the wave equation and its solutions in the elliptic coordinate system. Thus in this chapter we introduce the elliptic coordinates system and review the wave equation and its solutions in this system.

3.1 Elliptic Cylinder Coordinates System

Consider an elliptical cylinder as shown figure 3.1 with its cross section in the (x, y) plane [41]. The semi-focal distance f is given by $f^2 = a^2 - b^2$ where $2a$ is the largest, and

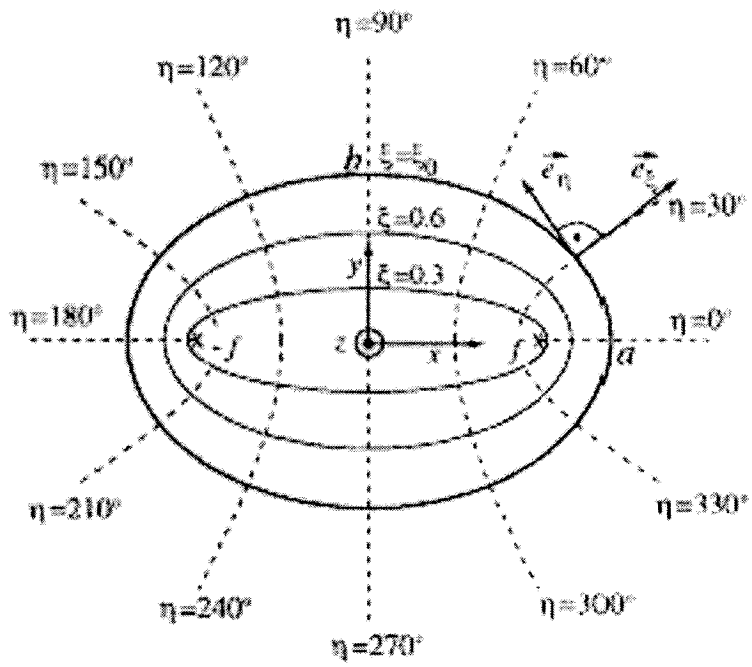

Figure 3.1- Elliptic Coordinates System [41]

$2b$ is the smallest axis of the ellipse. The elliptic coordinates system (ξ,η,z) is defined according to the transformation $x + j\,y = f\,cosh(\xi + j\,\eta)$. By equating the real and the imaginary parts of each side [42], in Cartesian coordinates system (x, y, z), we obtain

$$x = f\,cosh\,\xi\,cos\,\eta, \qquad y = f\,sinh\,\xi\,sin\,\eta, \qquad z = z, \tag{3.1}$$

where ξ works as a radial coordinate, $0 \le \xi \le \infty$, and η works as a angular coordinate, $0 \le \eta \le 2\pi$.

The surface $\xi = \xi_0$ reduces to the elliptic cylinder

$$\left(\frac{x}{f\cosh\xi_0}\right)^2 + \left(\frac{y}{f\sinh\xi_0}\right)^2 = \cos^2\eta + \sin^2\eta = 1, \tag{3.2}$$

with semi-major axis $a = f\,cosh\,\xi_0$ and semi-minor axis $b = f\,sinh\,\xi_0$. The surface $\eta = \eta_o$ reduces to the hyperbolic cylinder

$$\left(\frac{x}{f\cos\eta_0}\right)^2 - \left(\frac{y}{f\sin\eta_0}\right)^2 = \cosh^2\xi - \sinh^2\xi = 1, \tag{3.3}$$

which crosses the x-axis at $\pm f\,cos\,\eta_o$ and has asymptotes $y = \pm x\,tan\,\eta_o$. The corresponding scale factors in the elliptic coordinates system are

$$h_\xi = f\sqrt{\cosh^2\xi - \cos^2\eta}\ , \quad h_\eta = f\sqrt{\frac{1}{2}(\cosh 2\xi - \cos 2\eta)}\ , \quad and \quad h_z = 1. \tag{3.4}$$

3.2 Wave Equations in Elliptic Coordinates

In general the scalar wave equation can be written as

$$\left[\nabla^2 - \frac{1}{v^2}\frac{\partial^2}{\partial t^2}\right]U(r,t) = 0, \tag{3.5}$$

where $v^2 = 1/\mu\varepsilon$ for electromagnetic fields. By assuming a solution of the form $U(r, t) = U(r)\,T(t)$ and replacing it into (3.5) we obtain

$$\left[\frac{d^2}{dt^2} + k^2 v^2\right] T(t) = 0, \tag{3.6}$$

$$\left[\nabla^2 + k^2\right] U(r) = 0, \tag{3.7}$$

where $-k^2$ is the separation constant. The solutions of the harmonic Equation (3.6) are $T(t) = e^{\pm j\omega t}$. Equation (3.7) is three-dimensional Helmholtz equation. For cylindrical systems by using the Laplacian operator and assuming a spatial solution we can separate Equation (3.7) as

$$\nabla^2 = \nabla_t^2 + \partial^2 / \partial z^2, \tag{3.8}$$

$$U(r) = U_t(r_t) Z(z), \tag{3.9}$$

$$\left[\frac{d^2}{dz^2} + k_z^2\right] Z(z) = 0, \tag{3.10}$$

$$\left[\nabla_t^2 + k_t^2\right] U_t(r_t) = 0, \tag{3.11}$$

$$k_t^2 = k^2 - k_z^2. \tag{3.12}$$

The solutions of Equation (3.10) are $Z(z) = e^{\pm jk_z z}$. For (3.11) by replacing the elliptic coordinates scale factors (3.4) into the transverse Laplacian, and taking $r_t = (\xi, \eta)$, we can write

$$\nabla_t^2 = \frac{1}{h_\xi^2}\frac{\partial^2}{\partial \xi^2} + \frac{1}{h_\eta^2}\frac{\partial^2}{\partial \eta^2}, \tag{3.13}$$

$$h_\xi = f\sqrt{\cosh^2 \xi - \cos^2 \eta}\ , \tag{3.14}$$

$$h_\eta = f\sqrt{\frac{1}{2}(\cosh 2\xi - \cos 2\eta)}\ , \tag{3.15}$$

$$\left[\frac{\partial^2}{\partial \xi^2} + \frac{\partial^2}{\partial \eta^2} + \frac{k_t^2 f^2}{2}(\cosh 2\xi - \cos 2\eta)\right] U(\xi, \eta) = 0. \tag{3.16}$$

Equation (3.16) is the two-dimensional Helmholtz equation in elliptic coordinates. We assume a solution of the form $U(\xi, \eta) = R(\xi)\, S(\eta)$. Substitution of $U(\xi, \eta)$ into Equation (3.16) yields

$$\left[\frac{d^2}{d\eta^2} + (\alpha - 2q\cos 2\eta)\right] S(\eta) = 0, \tag{3.17}$$

$$\left[\frac{d^2}{d\xi^2} - (\alpha - 2q\cosh 2\xi)\right] R(\xi) = 0, \quad q = (k_t f)^2 / 4, \tag{3.18}$$

where α is the separation constant, and q is a dimensionless parameter related to the transverse propagation constant k_t.

Equations (3.17) and (3.18) are known in physics and engineering as the angular Mathieu equation, and radial (or modified) Mathieu equation respectively. Their solutions are the angular Mathieu functions and the radial (or modified) Mathieu functions respectively.

3.3 Solution of the Angular Mathieu Equation

Based on physical considerations, the angular Mathieu equation has periodic solution with period π or 2π. The values of α which satisfy these conditions are known as *characteristic values* or *eigenvalues*. When the solutions $S(\eta)$ are even with respect to $\eta=0$, the characteristic values are denoted as $\alpha_m(q)$ where $m=0,1,2,3,\ldots$, whereas for odd solutions they are represented as $\beta_m(q)$ where $m=1,2,3,\ldots$. They generate an infinite set of real values that have the property $\alpha_0 < \beta_1 \leq \alpha_1 < \beta_2 \leq \alpha_2 < \ldots$. Since the characteristic values define the stability of the solutions, they play an important role in the accuracy of these functions.

The periodic solutions of the angular Mathieu equation which are named angular Mathieu functions, are given [42-44] by using the Fourier series

$$S_{e\,2n}(\eta,q) = \sum_{r=0}^{\infty} A_{2r}(q)\cos 2r\eta \qquad \textit{even solution with even char. num. } (\alpha_{2n}) \tag{3.19}$$

$$S_{e\,2n+1}(\eta,q) = \sum_{r=0}^{\infty} A_{2r+1}(q)\cos(2r+1)\eta \quad \textit{even solution with odd char. num. } (\alpha_{2n+1}) \tag{3.20}$$

$$S_{o\,2n+2}(\eta,q) = \sum_{r=0}^{\infty} B_{2r+2}(q)\sin(2r+2)\eta \quad \textit{odd solution with even char. num. } (\beta_{2n+2}) \tag{3.21}$$

$$S_{o\,2n+1}(\eta,q) = \sum_{r=0}^{\infty} B_{2r+1}(q)\sin(2r+1)\eta \quad \textit{odd solution with odd char. num. } (\beta_{2n+1}) \tag{3.22}$$

where A and B are Fourier coefficients and depend on the parameter q in (3.18). The derivative of the angular Mathieu functions (3.19)-(3.22) are

$$\frac{d}{d\eta}[S_{e\,2n}(\eta,q)] = -\sum_{r=0}^{\infty} 2rA_{2r}\sin 2r\eta\ , \tag{3.23}$$

$$\frac{d}{d\eta}[S_{e\,2n+1}(\eta,q)] = -\sum_{r=0}^{\infty}(2r+1)A_{2r+1}\sin(2r+1)\eta\ , \tag{3.24}$$

$$\frac{d}{d\eta}[S_{o\,2n+2}(\eta,q)] = \sum_{r=0}^{\infty}(2r+2)B_{2r+2}\cos(2r+2)\eta\ , \tag{3.25}$$

$$\frac{d}{d\eta}[S_{o\,2n+1}(\eta,q)] = \sum_{r=0}^{\infty}(2r+1)B_{2r+1}\cos(2r+1)\eta\ . \tag{3.26}$$

3.4 Solution of the Radial (Modified) Mathieu Equation

The radial Mathieu equation, in elliptic coordinates plays a similar role as the Bessel equation, in circular coordinates. So, for each kind of Bessel function, there exists a pair of even and odd version of radial Mathieu function. Then, there are eight radial Mathieu functions for four kinds of Bessel functions.

3.4.1 First kind solutions of the Radial Mathieu Equation

First kind solutions of the radial Mathieu equation for $q > 0$, are named J-Bessel type of the radial Mathieu functions. The expressions for the four types of expansion are given [44], by using the Fourier series

$$Je_{2m}(q,\xi) = \left(\sqrt{\pi/2}/A_0\right)\sum_{n=0}^{\infty}(-1)^{n-m} A_{2n} J_n(v_1) J_n(v_2), \tag{3.27}$$

$$Je_{2m+1}(q,\xi) = \left(\sqrt{\pi/2}/A_1\right)\sum_{n=0}^{\infty}(-1)^{n-m} A_{2n+1}[J_n(v_1) J_{n+1}(v_2) + J_{n+1}(v_1) J_n(v_2)], \tag{3.28}$$

$$Jo_{2m+2}(q,\xi) = \left(\sqrt{\pi/2}/B_2\right)\sum_{n=0}^{\infty}(-1)^{n-m} B_{2n+2}[J_n(v_1) J_{n+2}(v_2) - J_{n+2}(v_1) J_n(v_2)], \tag{3.29}$$

$$Jo_{2m+1}(q,\xi) = \left(\sqrt{\pi/2}/B_1\right)\sum_{n=0}^{\infty}(-1)^{n-m} B_{2n+1}[J_n(v_1) J_{n+1}(v_2) - J_{n+1}(v_1) J_n(v_2)], \tag{3.30}$$

where $v_1 = \sqrt{q}e^{-\xi}$, *and* $v_2 = \sqrt{q}e^{\xi}$.

The derivatives of functions (3.27)-(3.30) are

$$\frac{d}{d\xi}Je_{2m}(q,\xi) = \left(\sqrt{\pi/2}/2A_0\right)\sum_{n=0}^{\infty}(-1)^{n-m} A_{2n}\begin{Bmatrix} -v_1 J_n(v_2)[J_{n-1}(v_1) - J_{n+1}(v_1)] \\ +v_2 J_n(v_1)[J_{n-1}(v_2) - J_{n+1}(v_2)] \end{Bmatrix}, \tag{3.31}$$

$$\frac{d}{d\xi}Je_{2m+1}(q,\xi) = -\left(\sqrt{\pi/2}/2A_1\right)\sum_{n=0}^{\infty}(-1)^{n-m} A_{2n+1}\begin{Bmatrix} -v_1 J_{n+1}(v_2)[J_{n-1}(v_1) - J_{n+1}(v_1)] \\ +v_2 J_n(v_1)[J_n(v_2) - J_{n+2}(v_2)] \\ -v_1 J_n(v_2)[J_n(v_1) - J_{n+2}(v_1)] \\ +v_2 J_{n+1}(v_1)[J_{n-1}(v_2) - J_{n+1}(v_2)] \end{Bmatrix}, \tag{3.32}$$

$$\frac{d}{d\xi}Jo_{2m+2}(q,\xi) = -\left(\sqrt{\pi/2}/2B_2\right)\sum_{n=0}^{\infty}(-1)^{n-m} B_{2n+2}\begin{Bmatrix} -v_1 J_{n+2}(v_2)[J_{n-1}(v_1) - J_{n+1}(v_1)] \\ +v_2 J_n(v_1)[J_{n+1}(v_2) - J_{n+3}(v_2)] \\ +v_1 J_n(v_2)[J_{n+1}(v_1) - J_{n+3}(v_1)] \\ -v_2 J_{n+2}(v_1)[J_{n-1}(v_2) - J_{n+1}(v_2)] \end{Bmatrix}, \tag{3.33}$$

$$\frac{d}{d\xi}Jo_{2m+1}(q,\xi) = \left(\sqrt{\pi/2}/2B_1\right)\sum_{n=0}^{\infty}(-1)^{n-m} B_{2n+1}\begin{Bmatrix} -v_1 J_{n+1}(v_2)[J_{n-1}(v_1) - J_{n+1}(v_1)] \\ +v_2 J_n(v_1)[J_n(v_2) - J_{n+2}(v_2)] \\ +v_1 J_n(v_2)[J_n(v_1) - J_{n+2}(v_1)] \\ -v_2 J1(v_1)[J_{n-1}(v_2) - J_{n+1}(v_2)] \end{Bmatrix}. \tag{3.34}$$

3.4.2 Second kind solutions of the Radial Mathieu Equation

Second kind solutions of the radial Mathieu equation for $q > 0$, are named Y-Bessel type of the radial Mathieu functions. The expressions for the four types of expansion and their derivatives are given [44], by using the Fourier series

$$Ye_{2m}(q,\xi) = \left(\sqrt{\pi/2}/A_0\right)\sum_{n=0}^{\infty}(-1)^{n-m}A_{2n}J_n(v_1)Y_n(v_2), \tag{3.35}$$

$$Ye_{2m+1}(q,\xi) = \left(\sqrt{\pi/2}/A_1\right)\sum_{n=0}^{\infty}(-1)^{n-m}A_{2n+1}[J_n(v_1)Y_{n+1}(v_2)+J_{n+1}(v_1)Y_n(v_2)], \tag{3.36}$$

$$Yo_{2m+2}(q,\xi) = \left(\sqrt{\pi/2}/B_2\right)\sum_{n=0}^{\infty}(-1)^{n-m}B_{2n+2}[J_n(v_1)Y_{n+2}(v_2)-J_{n+2}(v_1)Y_n(v_2)], \tag{3.37}$$

$$Yo_{2m+1}(q,\xi) = \left(\sqrt{\pi/2}/B_1\right)\sum_{n=0}^{\infty}(-1)^{n-m}B_{2n+1}[J_n(v_1)Y_{n+1}(v_2)-J_{n+1}(v_1)Y_n(v_2)], \tag{3.38}$$

where $v_1 = \sqrt{q}e^{-\xi}$, *and* $v_2 = \sqrt{q}e^{\xi}$.

$$\frac{d}{d\xi}Ye_{2m}(q,\xi) = \left(\sqrt{\pi/2}/2A_0\right)\sum_{n=0}^{\infty}(-1)^{n-m}A_{2n}\begin{Bmatrix}-v_1Y_n(v_2)[J_{n-1}(v_1)-J_{n+1}(v_1)]\\+v_2J_n(v_1)[Y_{n-1}(v_2)-Y_{n+1}(v_2)]\end{Bmatrix}, \tag{3.39}$$

$$\frac{d}{d\xi}Ye_{2m+1}(q,\xi) = -\left(\sqrt{\pi/2}/2A_1\right)\sum_{n=0}^{\infty}(-1)^{n-m}A_{2n+1}\begin{Bmatrix}-v_1Y_{n+1}(v_2)[J_{n-1}(v_1)-J_{n+1}(v_1)]\\+v_2J_n(v_1)[Y_n(v_2)-Y_{n+2}(v_2)]\\-v_1Y_n(v_2)[J_n(v_1)-J_{n+2}(v_1)]\\+v_2J_{n+1}(v_1)[Y_{n-1}(v_2)-Y_{n+1}(v_2)]\end{Bmatrix}, \tag{3.40}$$

$$\frac{d}{d\xi}Yo_{2m+2}(q,\xi) = -\left(\sqrt{\pi/2}/2B_2\right)\sum_{n=0}^{\infty}(-1)^{n-m}B_{2n+2}\begin{Bmatrix}-v_1Y_{n+2}(v_2)[J_{n-1}(v_1)-J_{n+1}(v_1)]\\+v_2J_n(v_1)[Y_{n+1}(v_2)-Y_{n+3}(v_2)]\\+v_1Y_n(v_2)[J_{n+1}(v_1)-J_{n+3}(v_1)]\\-v_2J_{n+2}(v_1)[Y_{n-1}(v_2)-Y_{n+1}(v_2)]\end{Bmatrix}, \tag{3.41}$$

$$\frac{d}{d\xi}Yo_{2m+1}(q,\xi) = \left(\sqrt{\pi/2}/2B_1\right)\sum_{n=0}^{\infty}(-1)^{n-m}B_{2n+1}\begin{Bmatrix}-v_1Y_{n+1}(v_2)[J_{n-1}(v_1)-J_{n+1}(v_1)]\\+v_2J_n(v_1)[Y_n(v_2)-Y_{n+2}(v_2)]\\+v_1Y_n(v_2)[J_n(v_1)-J_{n+2}(v_1)]\\-v_2J1(v_1)[Y_{n-1}(v_2)-Y_{n+1}(v_2)]\end{Bmatrix}. \tag{3.42}$$

3.4.3 The Third and Fourth Kind Solutions of the Radial Mathieu Equation

The third and fourth kind solutions of the radial Mathieu equation are named the Mathieu-Hankel functions. These functions are used to represent incoming and outgoing waves in propagation problems. They can express by the first and second kind of the radial Mathieu functions. Then,

$$\textit{Third kind solution} = H_1 \textit{ (First kind Hankel)} = \textit{(J-Bessel)} + j \textit{ (Y-Bessel)}, \quad (3.43)$$

$$\textit{Fourth kind solution} = H_2 \textit{ (Second kind Hankel)} = \textit{(J-Bessel)} - j \textit{ (Y-Bessel)}. \quad (3.44)$$

So we can obtain both even and odd functions for each kind.

Equations (3.19)-(3.42) depend on Fourier coefficients A and B. To finding A or B, we have to calculate characteristic value α or β respectively. α and β depend on parameter q which also depends on the wave number k and semi focal length f. More details of these calculations are given in the appendix.

3.5 Conclusion

Elliptic coordinates system and the corresponding wave equation in this system are presented. The solution of the wave equation is expressed in terms of Mathieu and modified Mathieu functions. Expressions for these functions are given. Details of their numerical calculations are given in Appendix A.

4. Scattering by Elliptic Chiral Cylinder

In this chapter the theoretical solution of TM polarized electromagnetic scattering by an elliptic chiral cylinder is developed. Expression of the wave equation in chiral media using elliptic coordinates and expressions of incident, transmitted and scattered electromagnetic waves are derived. Expansion coefficients are found by applying the boundary conditions and the orthogonality of the Mathieu functions. Finally the expressions of echo widths for co- and cross-polarized cases are presented.

4.1 Wave Equation

The general form of the wave equation for a chiral media is given in Section 2.3 while the wave equation in elliptic coordinate system for a non-chiral media is given in Section 3.2. In this section we combine the two formulations to express the wave equation for a chiral media in elliptic coordinates system. We start with the two-dimensional Helmholtz scalar equation in elliptic coordinates,

$$\left[\frac{\partial^2}{\partial\xi^2}+\frac{\partial^2}{\partial\eta^2}+\frac{k^2f^2}{2}(\cosh 2\xi-\cos 2\eta)\right]U(\xi,\eta)=0. \tag{4.1}$$

Assuming a separation solution of the form $U(\xi, \eta) = R(\xi)\, S(\eta)$ and substituting it into Equation (4.1) yields

$$\left[\frac{d^2}{d\eta^2}+(\alpha-2q\cos 2\eta)\right]S(\eta)=0, \tag{4.2}$$

$$\left[\frac{d^2}{d\xi^2}-(\alpha-2q\cosh 2\xi)\right]R(\xi)=0, \tag{4.3}$$

where α is the separation constant, and q is a dimensionless parameter related to the wave number k and semi-focal length f by $q = (kf)^2 / 4$. Equations (4.2) and (4.3) are the angular and radial (or modified) Mathieu equation respectively. Their solutions are the angular and radial (or modified) Mathieu functions. More details of Mathieu functions were given in Chapter 3.

The constitutive relationships for a chiral medium can be written as

$$\vec{D} = \varepsilon_c \vec{E} - j\mu\gamma \vec{H} \tag{4.4}$$

$$\vec{B} = \mu \vec{H} + j\mu\gamma \vec{E} \tag{4.5}$$

where $\vec{D}, \vec{B}, \vec{E},$ and $\vec{H}$ are the electric flux density, magnetic flux density, electric field, and magnetic field respectively. Also $\varepsilon_c = \varepsilon + \mu\gamma^2$, is the effective permittivity of the chiral medium, μ is the permeability, ε is the permittivity, and γ is the chiral admittance of the medium. If μ, ε, or γ are complex the media is lossy. If $\gamma = 0$, then (4.4) and (4.5) reduce to the constitutive relations for an achiral medium. The chiral wave impedance and wave numbers are given by

$$\eta_c = \sqrt{\frac{\mu}{\varepsilon_c}} , \tag{4.6}$$

$$K_R = \omega\sqrt{\mu\varepsilon_c} + \omega\mu\gamma , \tag{4.7}$$

$$K_L = \omega\sqrt{\mu\varepsilon_c} - \omega\mu\gamma . \tag{4.8}$$

We define ($\vec{E}_R$, $\vec{E}_L$) by

$$\begin{pmatrix} \vec{E} \\ \vec{H} \end{pmatrix} = \begin{bmatrix} 1 & 1 \\ j/\eta_c & -j/\eta_c \end{bmatrix} \begin{pmatrix} \vec{E}_R \\ \vec{E}_L \end{pmatrix}, \tag{4.9}$$

where $\vec{E}_R$ and $\vec{E}_L$ are the electric fields of right and left circularly polarized waves with propagation constants K_R and K_L, respectively. Substituting (4.9) into the matrix form of Maxwell's Equations (2.5) and (2.6) results in a set of uncoupled equations for chiral media

$$\nabla \times \begin{pmatrix} \vec{E}_R \\ \vec{E}_L \end{pmatrix} = \begin{pmatrix} K_R \vec{E}_R \\ -K_L \vec{E}_L \end{pmatrix} + \vec{J} \frac{j\eta_c}{2} \begin{pmatrix} -1 \\ 1 \end{pmatrix} \tag{4.10}$$

$$\textit{and} \qquad \nabla \cdot \begin{pmatrix} \vec{E}_R \\ \vec{E}_L \end{pmatrix} = \frac{\rho}{2\varepsilon} \begin{pmatrix} 1-\eta_c\gamma \\ 1+\eta_c\gamma \end{pmatrix}. \tag{4.11}$$

Then the uncoupled source-free wave equation in chiral media is

$$\nabla^2 \begin{pmatrix} \vec{E}_R \\ \vec{E}_L \end{pmatrix} + \begin{pmatrix} K_R^2 \vec{E}_R \\ K_L^2 \vec{E}_L \end{pmatrix} = 0. \tag{4.12}$$

4.2 The Eigenfunction Expansion

Consider an elliptic chiral cylinder with permeability μ_r, permittivity ε_r, and chiral admittance γ. The geometry of this cylinder with TM_Z uniform plane wave incident on it is shown in Figure 4.1. The external fields of the cylinder may be expanded as an infinite sum of vector wave functions, $\vec{M}_m$ and $\vec{N}_m$ [2], which are related by

$$\nabla \times \vec{N}_m = k\vec{M}_m, \tag{4.13}$$

$$\nabla \times \vec{M}_m = k\vec{N}_m. \tag{4.14}$$

These vector wave functions are solutions to

$$\nabla \times \nabla \times \vec{Q} - k^2 \vec{Q} = 0, \tag{4.15}$$

$$\textit{and} \qquad \nabla \cdot \vec{Q} = 0, \tag{4.16}$$

where $\vec{Q} = \vec{M}_m$ or $\vec{N}_m$. According to (4.1) and its separation solution $U(\xi, \eta) = R(\xi)\, S(\eta)$ in elliptical coordinates, using (4.13) $\vec{M}_m$ and $\vec{N}_m$ can be written as

$$\vec{N}_m^{(p)}(k) = \hat{u}_z\, U_m(\xi,\eta) = \hat{u}_z\, R^{(p)e}_{om}(c,\xi) S^e_{om}(c,\eta) \tag{4.17}$$

$$\vec{M}_m^{(p)}(k) = \frac{1}{k}\nabla \times \vec{N}_m^{(p)}(k) = \hat{u}_\xi\, M_\xi + \hat{u}_\eta\, M_\eta$$

$$= \hat{u}_\xi \frac{\sqrt{1-\eta^2}}{kf\sqrt{\xi^2-\eta^2}} R^{(p)e}_{om}(c,\xi) S'^{e}_{om}(c,\eta)$$

$$- \hat{u}_\eta \frac{\sqrt{\xi^2-1}}{kf\sqrt{\xi^2-\eta^2}} R'^{(p)e}_{om}(c,\xi) S^e_{om}(c,\eta) \tag{4.18}$$

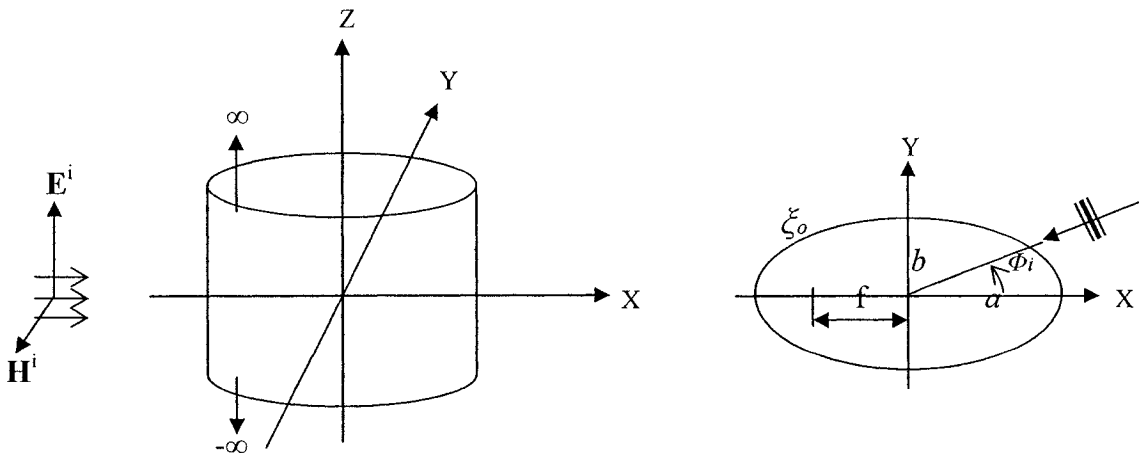

Figure 4.1 – TM_Z uniform plane wave incident on an elliptic chiral cylinder

where $p=1,...,4$, $c = k^2f^2/4$, k is the wave number, f is the semi focal length, $0 \le \xi < \infty$, $0 \le \eta \le 2\pi$, Se_m and So_m are even and odd angular Mathieu functions, Re_m and Ro_m are even and odd radial (modified) Mathieu functions, and the prim indicates the derivative with respect to the argument.

4.2.1 Incident Wave

In the case of a Transverse Magnetic (TM_Z) plane wave normally incident from Φ^i, the incident electric field, with unit amplitude may be written [17] in the form

$$\vec{E}^i = \hat{u}_z e^{-jk_0x} = \sum_m \vec{N}_m^{(1)}(k_0) = \hat{u}_z \sum_m A_{om}^e R^{(1)e}_{om}(c_0,\xi) S^e_{om}(c_0,\eta) \tag{4.19}$$

$$where\ A^e_{om} = \sqrt{8\pi}\, j^m S^e_{om}(c_0,\cos\phi^i)/N^e_{om}(c_0),\ and\ N^e_{on}(c_0) = \int_0^{2\pi}\left[S^e_{on}(c_0,\eta)\right]^2 d\eta. \tag{4.20}$$

$A_{e\,m}$ and $A_{o\,m}$ are the coefficients for a plane wave that is impinging at angle Φ^i with respect to the x-axis, $N_{e\,m}$ and $N_{o\,m}$ are even and odd normalized constants. The corresponding magnetic field is given by

$$\begin{aligned}\vec{H}^i &= -\hat{u}_y \frac{1}{\eta_0} e^{-jk_0x} = \frac{j}{\eta_0}\sum_m \vec{M}_m^{(1)}(k_0) \\ &= \hat{u}_\xi \frac{j}{\eta_0 k_0 f}\sqrt{\frac{1-\eta^2}{\xi^2-\eta^2}}\sum_m A^e_{om} R^{(1)e}_{om}(c_0,\xi) S'^e_{om}(c_0,\eta) \\ &\quad - \hat{u}_\eta \frac{j}{\eta_0 k_0 f}\sqrt{\frac{\xi^2-1}{\xi^2-\eta^2}}\sum_m A^e_{om} R'^{(1)e}_{om}(c_0,\xi) S^e_{om}(c_0,\eta).\end{aligned} \tag{4.21}$$

4.2.2 Transmitted Wave

In the chiral cylinder, the eigenfunction expansion must account for the rotation of polarization inherent to chiral media. In a z-independent problem, these result in a coupling between the TM_Z and TE_Z fields, which prevents the eigenfunction expansion from being written as a simple superposition of TM_Z and TE_Z fields. However, the eigenfunction expansion can be written as a superposition of right and left circularly polarized fields. This is done by combining the vector wave functions $\vec{M}_m$ and $\vec{N}_m$, to form right and left circularly polarized vector wave function

$$\vec{E}_{Rm}^{(p)} = \vec{N}_m^{(p)}(k_R) + \vec{M}_m^{(p)}(k_R), \tag{4.22}$$

$$\vec{E}_{Lm}^{(p)} = \vec{N}_m^{(p)}(k_L) - \vec{M}_m^{(p)}(k_L), \tag{4.23}$$

which satisfy the wave Equation (4.10)-(4.12) in a source-free chiral region. Then the electric field in the elliptic chiral cylinder may be represented as

$$\vec{E}^c = \vec{E}_R^c + \vec{E}_L^c$$

$$= \sum_m c_{om}^e \left[\vec{N}_m^{(1)}(k_R) + \vec{M}_m^{(1)}(k_R) \right] + \sum_m d_{om}^e \left[\vec{N}_m^{(1)}(k_L) - \vec{M}_m^{(1)}(k_L) \right]$$

$$= \hat{u}_z \left[\sum_m c_{om}^e R^{(1)e}_{om}(c_R, \xi) S_{om}^e(c_R, \eta) + \sum_m d_{om}^e R^{(1)e}_{om}(c_L, \xi) S_{om}^e(c_L, \eta) \right]$$

$$+ \hat{u}_\xi \left[\frac{1}{k_R f \sqrt{\frac{1-\eta^2}{\xi^2 - \eta^2}}} \sum_m c_{om}^e R^{(1)e}_{om}(c_R, \xi) S'^e_{om}(c_R, \eta) \right.$$

$$- \frac{1}{k_L f}\sqrt{\frac{1-\eta^2}{\xi^2-\eta^2}}\sum_m d^e_{om} R^{(1)e}_{om}(c_L,\xi) S'^{e}_{om}(c_L,\eta)\Bigg]$$

$$- \hat{u}_\eta\Bigg[\frac{1}{k_R f}\sqrt{\frac{\xi^2-1}{\xi^2-\eta^2}}\sum_m c^e_{om} R'^{(1)e}_{om}(c_R,\xi) S^e_{om}(c_R,\eta)$$

$$- \frac{1}{k_L f}\sqrt{\frac{\xi^2-1}{\xi^2-\eta^2}}\sum_m d^e_{om} R'^{(1)e}_{om}(c_L,\xi) S^e_{om}(c_L,\eta)\Bigg]. \qquad (4.24)$$

where $c_{e\,m}$, $c_{o\,m}$, $d_{e\,m}$, and $d_{o\,m}$ are unknown expansion coefficients. The corresponding magnetic field can be written as

$$\vec{H}^c = \vec{H}^c_R + \vec{H}^c_L$$

$$= \frac{j}{\eta_c}\Bigg[\sum_m c^e_{om}\Big[\vec{N}^{(1)}_m(k_R)+\vec{M}^{(1)}_m(k_R)\Big]-\sum_m d^e_{om}\Big[\vec{N}^{(1)}_m(k_L)-\vec{M}^{(1)}_m(k_L)\Big]\Bigg]$$

$$= \hat{u}_z \frac{j}{\eta_c}\Bigg[\sum_m c^e_{om} R^{(1)e}_{om}(c_R,\xi) S^e_{om}(c_R,\eta)-\sum_m d^e_{om} R^{(1)e}_{om}(c_L,\xi) S^e_{om}(c_L,\eta)\Bigg]$$

$$+ \hat{u}_\xi \frac{j}{\eta_c}\Bigg[\frac{1}{k_R f}\sqrt{\frac{1-\eta^2}{\xi^2-\eta^2}}\sum_m c^e_{om} R^{(1)e}_{om}(c_R,\xi) S'^{e}_{om}(c_R,\eta)$$

$$+ \frac{1}{k_L f}\sqrt{\frac{1-\eta^2}{\xi^2-\eta^2}}\sum_m d^e_{om} R^{(1)e}_{om}(c_L,\xi) S'^{e}_{om}(c_L,\eta)\Bigg]$$

$$- \hat{u}_\eta \frac{j}{\eta_c}\Bigg[\frac{1}{k_R f}\sqrt{\frac{\xi^2-1}{\xi^2-\eta^2}}\sum_m c^e_{om} R'^{(1)e}_{om}(c_R,\xi) S^e_{om}(c_R,\eta)$$

$$+ \frac{1}{k_L f}\sqrt{\frac{\xi^2-1}{\xi^2-\eta^2}}\sum_m d^e_{om} R'^{(1)e}_{om}(c_L,\xi) S^e_{om}(c_L,\eta)\Bigg]. \qquad (4.25)$$

4.2.3 Scattered Wave

Due to elliptic chiral cylinder the scattered fields will have TM_Z and TE_Z components, therefore, the scattered fields are expanded as

$$\vec{E}^s = \sum_m a^e_{om}\, \vec{N}^{(4)}_m(k_0) + b^e_{om}\, \vec{M}^{(4)}_m(k_0)$$

$$= \hat{u}_z \sum_m a^e_{om} R^{(4)e}_{om}(c_0,\xi) S^e_{om}(c_0,\eta)$$

$$+ \hat{u}_\xi \frac{1}{k_0 f}\sqrt{\frac{1-\eta^2}{\xi^2-\eta^2}} \sum_m b^e_{om} R^{(4)e}_{om}(c_0,\xi) S'^e_{om}(c_0,\eta)$$

$$- \hat{u}_\eta \frac{1}{k_0 f}\sqrt{\frac{\xi^2-1}{\xi^2-\eta^2}} \sum_m b^e_{om} R'^{(4)e}_{om}(c_0,\xi) S^e_{om}(c_0,\eta)\ , \qquad (4.26)$$

$$\vec{H}^s = \frac{j}{\eta_0}\sum_m a^e_{om}\, \vec{M}^{(4)}_m(k_0) + b^e_{om}\, \vec{N}^{(4)}_m(k_0)$$

$$= \hat{u}_z \frac{j}{\eta_0}\sum_m b^e_{om} R^{(4)e}_{om}(c_0,\xi) S^e_{om}(c_0,\eta)$$

$$+ \hat{u}_\xi \frac{j}{\eta_0 k_0 f}\sqrt{\frac{1-\eta^2}{\xi^2-\eta^2}} \sum_m a^e_{om} R^{(4)e}_{om}(c_0,\xi) S'^e_{om}(c_0,\eta)$$

$$- \hat{u}_\eta \frac{j}{\eta_0 k_0 f}\sqrt{\frac{\xi^2-1}{\xi^2-\eta^2}} \sum_m a^e_{om} R'^{(4)e}_{om}(c_0,\xi) S^e_{om}(c_0,\eta)\ , \qquad (4.27)$$

where $a_{e\,m}$, $a_{o\,m}$, $b_{e\,m}$, and $b_{o\,m}$ are unknown expansion coefficients.

4.3 Boundary Conditions

We have 4 unknown expansion coefficients, a_m, b_m, c_m, and d_m, for both even and odd modes. In order to compute them, we have to apply the boundary conditions at $\xi=\xi_0$. We know that the tangential components of the electric field across an interface between two media with no impressed magnetic current densities along the boundary of the interface are continuous. Also, the tangential components of the magnetic field across an interface between two media, neither of which is a perfect conductor, are continuous [45]. Thus at $\xi=\xi_0$, the tangential components of the electric field and the tangential components of the magnetic field are continuous and we can write

$$E_z^i + E_z^s = E_z^c \ , \tag{4.28}$$

$$E_\eta^s = E_\eta^c \ , \tag{4.29}$$

$$H_z^s = H_z^c \ , \tag{4.30}$$

$$H_\eta^i + H_\eta^s = H_\eta^c \ . \tag{4.31}$$

By applying the boundary conditions (4.28)-(4.31) we have

$$E_z^i + E_z^s = E_z^c$$

$$\sum_m A_{om}^e R^{(1)e}_{om}(c_0,\xi_0) S_{om}^e(c_0,\eta) + \sum_m a_{om}^e R^{(4)e}_{om}(c_0,\xi_0) S_{om}^e(c_0,\eta)$$

$$= \sum_m c_{om}^e R^{(1)e}_{om}(c_R,\xi_0) S_{om}^e(c_R,\eta) + \sum_m d_{om}^e R^{(1)e}_{om}(c_L,\xi_0) S_{om}^e(c_L,\eta) \ , \tag{4.32}$$

$$E_\eta^s = E_\eta^c$$

$$\frac{1}{k_0}\sum_m b_{om}^e R'^{(4)e}_{om}(c_0,\xi_0) S_{om}^e(c_0,\eta)$$

$$= \frac{1}{k_R}\sum_m c_{om}^e R'^{(1)e}_{om}(c_R,\xi_0) S_{om}^e(c_R,\eta) - \frac{1}{k_L}\sum_m d_{om}^e R'^{(1)e}_{om}(c_L,\xi_0) S_{om}^e(c_L,\eta)\,, \quad (4.33)$$

$$H_z^s = H_z^c$$

$$\frac{1}{\eta_0}\sum_m b_{om}^e R^{(4)e}_{om}(c_0,\xi_0) S_{om}^e(c_0,\eta)$$

$$= \frac{1}{\eta_c}\sum_m c_{om}^e R^{(1)e}_{om}(c_R,\xi_0) S_{om}^e(c_R,\eta) - \frac{1}{\eta_c}\sum_m d_{om}^e R^{(1)e}_{om}(c_L,\xi_0) S_{om}^e(c_L,\eta)\,, \quad (4.34)$$

$$H_\eta^i + H_\eta^s = H_\eta^c$$

$$\frac{1}{k_0\eta_0}\sum_m A_{om}^e R'^{(1)e}_{om}(c_0,\xi_0) S_{om}^e(c_0,\eta) + \frac{1}{k_0\eta_0}\sum_m a_{om}^e R'^{(4)e}_{om}(c_0,\xi_0) S_{om}^e(c_0,\eta)$$

$$= \frac{1}{k_R\eta_c}\sum_m c_{om}^e R'^{(1)e}_{om}(c_R,\xi_0) S_{om}^e(c_R,\eta) + \frac{1}{k_L\eta_c}\sum_m d_{om}^e R'^{(1)e}_{om}(c_L,\xi_0) S_{om}^e(c_L,\eta)\,. \quad (4.35)$$

Multiplying both sides of (4.32)-(4.35) by $S_n(c_0, \eta)$ and applying the orthogonality of Mathieu functions, the terms involving even functions decouple completely from those of odd functions. Thus from (4.32) we have

$$\left[A_n J_n(c_0) + a_n H_n(c_0)\right] N_n(c_0)$$

$$= \sum_m \left[c_m J_m(c_R) M_{mn}(c_0,c_R) + d_m J_m(c_L) M_{mn}(c_0,c_L)\right], \quad (4.36)$$

where

$$J_n(c_i) = J^e_{on}(c_i) = R^{(1)e}_{on}(c_i, \xi_0), \tag{4.37}$$

$$H_n(c_i) = H^e_{on}(c_i) = R^{(4)e}_{on}(c_i, \xi_0), \tag{4.38}$$

$$N_n(c_i) = N^e_{on}(c_i) = \int_0^{2\pi} \left[S^e_{on}(c_i, \eta)\right]^2 d\eta, \tag{4.39}$$

$$M_{mn}(c_i, c_j) = M^e_{omn}(c_i, c_j) = \int_0^{2\pi} S^e_{om}(c_i, \eta) S^e_{on}(c_j, \eta) d\eta, \tag{4.40}$$

for $n = 0, 1, 2, \ldots$ and also for even and odd coefficients. Similarly from (4.33)-(4.35) we can write

$$b_n H_n'(c_0) N_n(c_0)$$

$$= \frac{k_0}{k_R} \sum_m c_m J_m'(c_R) M_{mn}(c_0, c_R) - \frac{k_0}{k_L} \sum_m d_m J_m'(c_L) M_{mn}(c_0, c_L) \ , \tag{4.41}$$

$$b_n H_n(c_0) N_n(c_0)$$

$$= \frac{\eta_0}{\eta_c} \sum_m c_m J_m(c_R) M_{mn}(c_0, c_R) - \frac{\eta_0}{\eta_c} \sum_m d_m J_m(c_L) M_{mn}(c_0, c_L) \ , \tag{4.42}$$

$$\left[A_n J_n'(c_0) + a_n H_n'(c_0)\right] N_n(c_0)$$

$$= \frac{k_0 \eta_0}{k_R \eta_c} \sum_m c_m J_m'(c_R) M_{mn}(c_0, c_R) + \frac{k_0 \eta_0}{k_L \eta_c} \sum_m d_m J_m'(c_L) M_{mn}(c_0, c_L) \ . \tag{4.43}$$

Now multiplying both sides of (4.32)-(4.35) by $S_n(c_R, \eta)$ and applying the orthogonality of Mathieu functions, then we have

$$\sum_m \left[A_m J_m(c_0) + a_m H_m(c_0)\right] M_{mn}(c_R, c_0)$$

$$= c_n J_n(c_R) N_n(c_R) + \sum_m d_m J_m(c_L) M_{mn}(c_R, c_L)\,, \tag{4.44}$$

$$\sum_m b_m H_m'(c_0) M_{mn}(c_R, c_0)$$

$$= \frac{k_0}{k_R} c_n J_n'(c_0) N_n(c_R) - \frac{k_0}{k_L} \sum_m d_m J_m'(c_L) M_{mn}(c_R, c_L)\,, \tag{4.45}$$

$$\sum_m b_m H_m(c_0) M_{mn}(c_R, c_0)$$

$$= \frac{\eta_0}{\eta_c} c_n J_n(c_R) N_n(c_R) - \frac{\eta_0}{\eta_c} \sum_m d_m J_m(c_L) M_{mn}(c_R, c_L)\,, \tag{4.46}$$

$$\sum_m \left[A_m J_m'(c_0) + a_m H_m'(c_0)\right] M_{mn}(c_R, c_0)$$

$$= \frac{k_0 \eta_0}{k_R \eta_c} c_n J_n'(c_R) N_n(c_R) + \frac{k_0 \eta_0}{k_L \eta_c} \sum_m d_m J_m'(c_L) M_{mn}(c_R, c_L)\,. \tag{4.47}$$

Equations (4.36) and (4.41)-(4.47) may be used to solve for the unknown expansion coefficients.

4.4 Finding the Expansion Coefficients

The expansion coefficients a_m, b_m, c_m, and d_m, either even or odd can be written in a matrix form using (4.36) and (4.41)-(4.47). From (4.41) we have

$$[b_n] = [I1_{nm}][c_m] + [I2_{nm}][d_m] \tag{4.48}$$

where

$$I1_{nm} = \frac{k_0}{k_R} \frac{J_m^{'}(c_R) M_{mn}(c_0, c_R)}{H_n^{'}(c_0) N_n(c_0)} \tag{4.49}$$

and

$$I2_{nm} = -\frac{k_0}{k_L} \frac{J_m^{'}(c_L) M_{mn}(c_0, c_L)}{H_n^{'}(c_0) N_n(c_0)}. \tag{4.50}$$

From (4.42) we have

$$[b_n] = [L1_{nm}][c_m] + [L2_{nm}][d_m] \tag{4.51}$$

where

$$L1_{nm} = \frac{\eta_0}{\eta_c} \frac{J_m(c_R) M_{mn}(c_0, c_R)}{H_n(c_0) N_n(c_0)} \tag{4.52}$$

and

$$L2_{nm} = -\frac{\eta_0}{\eta_c} \frac{J_m(c_L) M_{mn}(c_0, c_L)}{H_n(c_0) N_n(c_0)}. \tag{4.53}$$

From (4.44) we have

$$[c_m] = [G1_{mk}][A_k] + [G2_{mk}][a_k] + [P1_{mk}][d_k] \tag{4.54}$$

where

$$G1_{mk} = \frac{J_k(c_0) M_{km}(c_R, c_0)}{J_m(c_R) N_m(c_R)}, \tag{4.55}$$

$$G2_{mk} = \frac{H_k(c_0) M_{km}(c_R, c_0)}{J_m(c_R) N_m(c_R)}, \tag{4.56}$$

and

$$P1_{mk} = -\frac{J_k(c_L) M_{km}(c_R, c_L)}{J_m(c_R) N_m(c_R)}. \tag{4.57}$$

By substituting (4.54) for c_m into (4.48) and (4.51), we have

$$[I1_{nm}]([G1_{mk}][A_k]+[G2_{mk}][a_k]+[P1_{mk}][d_k])+[I2_{nm}][d_m]$$

$$=[L1_{nm}]([G1_{mk}][A_k]+[G2_{mk}][a_k]+[P1_{mk}][d_k])+[L2_{nm}][d_m]$$

$$\{([I1_{nm}]-[L1_{nm}])[G1_{mk}]\}[A_k]=\{-([I1_{nm}]-[L1_{nm}])[G2_{mk}]\}[a_k]$$

$$+\{([L1_{nm}]-[I1_{nm}])[P1_{mk}]+([L2_{nm}]-[I2_{nm}])\}[d_m]$$

$$\Rightarrow \quad [W1_{nk}][A_k]=-[W2_{nk}][a_k]+[T_{nk}][d_k] \tag{4.58}$$

where

$$[W1_{nk}]=([I1_{nm}]-[L1_{nm}])[G1_{mk}], \tag{4.59}$$

$$[W2_{nk}]=([I1_{nm}]-[L1_{nm}])[G2_{mk}], \tag{4.60}$$

$$[T_{nk}]=([L1_{nm}]-[I1_{nm}])[P1_{mk}]+[L2_{nk}]-[I2_{nk}]. \tag{4.61}$$

From (4.44) and (4.47) we have

$$[c_n]=[G1_{nk}][A_k]+[G2_{nk}][a_k]+[P1_{nk}][d_k]$$

$$[c_n]=[F1_{nk}][A_k]+[F2_{nk}][a_k]+[P2_{nk}][d_k]$$

$$([G1_{nk}]-[F1_{nk}])[A_k]=-([G2_{nk}]-[F2_{nk}])[a_k]+([P2_{nk}]-[P1_{nk}])[d_k]$$

$$\Rightarrow \quad [U1_{nk}][A_k]=-[U2_{nk}][a_k]+[W_{nk}][d_k] \tag{4.62}$$

where

$$F1_{nk} = -\frac{\eta_c k_R}{\eta_0 k_0} \frac{J_k^{'}(c_0) M_{kn}(c_R, c_0)}{J_n^{'}(c_R) N_n(c_R)} \tag{4.63}$$

$$F2_{nk} = -\frac{\eta_c k_R}{\eta_0 k_0} \frac{H_k^{'}(c_0) M_{kn}(c_R, c_0)}{J_n^{'}(c_R) N_n(c_R)} \tag{4.64}$$

$$P2_{nk} = -\frac{k_R}{k_L} \frac{J_k^{'}(c_L) M_{kn}(c_R, c_L)}{J_n^{'}(c_R) N_n(c_R)} \tag{4.65}$$

$$[U1_{nk}] = [G1_{nk}] - [F1_{nk}] \tag{4.66}$$

$$[U2_{nk}] = [G2_{nk}] - [F2_{nk}] \tag{4.67}$$

$$[W_{nk}] = [P2_{nk}] - [P1_{nk}]. \tag{4.68}$$

From (4.62) we can find d_k

$$[d_k] = [W_{nk}]^{-1}([U1_{nk}][A_k] + [U2_{nk}][a_k]) \tag{4.69}$$

By substituting (4.69) into (4.58) we have

$$[W1_{nk}][A_k] = -[W2_{nk}][a_k] + [T_{nk}][W_{nk}]^{-1}[U1_{nk}][A_k] + [T_{nk}][W_{nk}]^{-1}[U2_{nk}][a_k]$$

$$\Rightarrow \quad [a_k] = \left([T_{nk}][W_{nk}]^{-1}[U2_{nk}] - [W2_{nk}]\right)^{-1}\left([W1_{nk}] - [T_{nk}][W_{nk}]^{-1}[U1_{nk}]\right)[A_k] \tag{4.70}$$

To finding c_m, substitute (4.69) into (4.54), then we have

$$[c_m] = [G1_{mk}][A_k] + [G2_{mk}][a_k] + [P1_{mk}][W_{nk}]^{-1}([U1_{nk}][A_k] + [U2_{nk}][a_k]) \tag{4.71}$$

We can find b_n by substituting (4.69) and (4.71) into (4.48),

$$[b_n]=[I1_{nm}][G1_{mk}][A_k]+[I1_{nm}][G2_{mk}][a_k]$$

$$+[I1_{nm}][P1_{mk}][W_{nk}]^{-1}[U1_{nk}][A_k]+[I1_{nm}][P1_{mk}][W_{nk}]^{-1}[U2_{nk}][a_k]$$

$$+[I2_{nm}][W_{nm}]^{-1}[U1_{nm}][A_m]+[I2_{nm}][W_{nm}]^{-1}[U2_{nm}][a_m]$$

$$=\left([I1_{nm}]\left([G1_{mk}]+[P1_{mk}][W_{nk}]^{-1}[U1_{nk}]\right)+[I2_{nm}][W_{nm}]^{-1}[U1_{nm}]\right)[A_k]$$

$$+\left([I1_{nm}]\left([G2_{mk}]+[P1_{mk}][W_{nk}]^{-1}[U2_{nk}]\right)+[I2_{nm}][W_{nm}]^{-1}[U2_{nm}]\right)[a_k] \qquad (4.72)$$

Consequently in summary we have the following expressions for the unknown expansion coefficients;

$$[a_k]=\left([T_{nk}][W_{nk}]^{-1}[U2_{nk}]-[W2_{nk}]\right)^{-1}\left([W1_{nk}]-[T_{nk}][W_{nk}]^{-1}[U1_{nk}]\right)[A_k] \qquad (4.73)$$

$$[b_n]=\left([I1_{nm}]\left([G1_{mk}]+[P1_{mk}][W_{nk}]^{-1}[U1_{nk}]\right)+[I2_{nm}][W_{nm}]^{-1}[U1_{nm}]\right)[A_k]$$

$$+\left([I1_{nm}]\left([G2_{mk}]+[P1_{mk}][W_{nk}]^{-1}[U2_{nk}]\right)+[I2_{nm}][W_{nm}]^{-1}[U2_{nm}]\right)[a_k] \qquad (4.74)$$

$$[c_m]=[G1_{mk}][A_k]+[G2_{mk}][a_k]+[P1_{mk}][W_{nk}]^{-1}\left([U1_{nk}][A_k]+[U2_{nk}][a_k]\right) \qquad (4.75)$$

$$[d_k]=[W_{nk}]^{-1}\left([U1_{nk}][A_k]+[U2_{nk}][a_k]\right). \qquad (4.76)$$

The obtained coefficients can be either even or odd. All matrixes in the right hand side of (4.73)-(4.76) are given by Equations (4.20) and (4.49) - (4.68).

4.5 Echo Width

An important parameter in the electromagnetic scattering by a target is usually represented by its echo area or radar cross section (RCS), σ. The echo area or RCS per

unit length is defined as the area intercepting the amount of power that, when scattered isotropically, produces at the receiver a density that is equal to the density scattered by the actual target. For a two-dimensional target the scattering parameter is referred to as the scattering width (SW) or alternatively as the radar cross section per unit length. The equation for the scattering width and the radar cross section, σ of a target takes the form [45],

$$\sigma_{2-D} = \begin{cases} \lim\limits_{\rho\to\infty}\left[2\pi\rho\dfrac{S^s}{S^i}\right] \\ \lim\limits_{\rho\to\infty}\left[2\pi\rho\dfrac{|E^s|^2}{|E^i|^2}\right] \\ \lim\limits_{\rho\to\infty}\left[2\pi\rho\dfrac{|H^s|^2}{|H^i|^2}\right] \end{cases} \qquad \sigma_{3-D} = \begin{cases} \lim\limits_{r\to\infty}\left[4\pi r^2\dfrac{S^s}{S^i}\right] \\ \lim\limits_{r\to\infty}\left[4\pi r^2\dfrac{|E^s|^2}{|E^i|^2}\right] \\ \lim\limits_{r\to\infty}\left[4\pi r^2\dfrac{|H^s|^2}{|H^i|^2}\right] \end{cases} \tag{4.77}$$

where $\sigma_{2\text{-}D}$ is scattering width for two-dimensional target, $\sigma_{3\text{-}D}$ is radar cross section for three-dimensional target, ρ and r are distance from target to observation point, S^s and S^i are scattered and incident power densities, E^s and E^i are scattered and incident electric fields, and H^s and H^i are scattered and incident magnetic fields. For normal incidence the two- and three-dimensional fields and scattering width and radar cross section for a target of length l are related by

$$E_{3-D} \cong \left(E_{2-D}\frac{le^{j\pi/4}}{\sqrt{\lambda\rho}}\right)_{\rho=r}, \tag{4.78}$$

$$\sigma_{3-D} \cong \sigma_{2-D}\frac{2l^2}{\lambda}. \tag{4.79}$$

The unit of the two-dimensional scattering width is length (meter in the MKS system) whereas that of the three-dimensional radar cross section is area (meter squared in the MKS system).

When the transmitter and receiver are at the same location, the radar cross section is usually referred to as monostatic (or backscattered) and it is referred to as bistatic when the two are at different locations. Observations made toward directions that satisfy Snell's law of reflection are usually referred to as specular. Therefore the radar cross section of a target is a very important parameter which characterizes its scattering properties. The definitions of σ indicate that the scattering width SW and radar cross section RCS of a target are defined under plane wave illumination. In practice that can only be approximated when the target is placed in the far field of the source (at least $2D^2/\lambda$) where D is the largest dimension of the target.

To finding echo width for co-polarized in elliptical coordinate we have

$$\sigma = \lim_{\rho\to\infty}\left[2\pi\rho\frac{\left|E_z^s\right|^2}{\left|E_z^i\right|^2}\right]. \tag{4.80}$$

It is useful to use asymptotic expansions for modified Mathieu functions [44]. Then

$$R^{(4)e}_{o\,m}(c_0,\xi) = H^{(2)e}_{o\,m}(c_0,\xi) = J^e_{o\,m}(c_0,\xi) - Y^e_{o\,m}(c_0,\xi), \tag{4.81}$$

$$R^{(4)e}_{o\,m}(c_0,\xi) \overset{\xi\to l\arg e}{\cong} \frac{1}{\sqrt{2\sqrt{q}\cosh\xi}}\left\{\begin{array}{l}\cos\left[\sqrt{2\sqrt{q}\cosh\xi}-\frac{\pi}{2}(M+1/2)\right]\\ -j\sin\left[\sqrt{2\sqrt{q}\cosh\xi}-\frac{\pi}{2}(M+1/2)\right]\end{array}\right\}$$

$$= \frac{1}{\sqrt{k_0\rho}}e^{-jk_0\rho}e^{j\frac{\pi}{2}(M+1/2)} = \frac{j^m}{\sqrt{k_0\rho}}e^{-jk_0\rho}, \tag{4.82}$$

where $k_0\rho = k_0 f \cosh\xi = 2\sqrt{q}\cosh\xi$, and $M = \begin{cases} 2m & \text{for even order,} \\ 2m+1 & \text{for odd order,} \end{cases}$

then $E_z^s = \dfrac{e^{-jk_0\rho}}{\sqrt{k_0\rho}} \sum_m j^m a_{om}^e S_{om}^e(c_0,\eta)$ and

$$\sigma = 2\pi\rho \frac{1}{k_0\rho}\left|\sum_m j^m a_{om}^e S_{om}^e(c_0,\eta)\right|^2 = \lambda\left|\sum_m j^m a_{om}^e S_{om}^e(c_0,\eta)\right|^2, \tag{4.83}$$

or
$$\frac{\sigma}{\lambda} = \left|\sum_m j^m \left[a_{em} S_{em}(c_0,\eta) + a_{om} S_{om}(c_0,\eta)\right]\right|^2. \tag{4.84}$$

To finding echo width for cross-polarized in elliptical coordinate we have

$$\sigma = \lim_{\rho\to\infty}\left[2\pi\rho \frac{\left|E_\eta^s\right|^2}{\left|E_z^i\right|^2}\right]. \tag{4.85}$$

For asymptotic expansion of derivative of modified Mathieu function, we use (4.82), then

$$R'^{(4)e}_{om}(c_0,\xi) = \frac{dR^{(4)}}{d\rho}\frac{d\rho}{d\cosh\xi} = \frac{j^m e^{-jk_0\rho}}{\sqrt{k_0\rho}}\left(-jk_0\sqrt{\rho} - \frac{1}{2\sqrt{\rho}}\right) f$$

$$\overset{\xi\to Large}{\cong} -f\sqrt{\frac{k_0}{\rho}} j^{m+1} e^{-jk_0\rho}, \tag{4.86}$$

then $\sigma = 2\pi\rho\, f^2 \dfrac{k_0}{\rho}\dfrac{1}{k_0^2 f^2}\left(\dfrac{\xi^2-1}{\xi^2-\eta^2}\right)\left|\sum_m j^{m+1} b_{om}^e S_{om}^e(c_0,\eta)\right|^2$

$$= \lambda\left|\sum_m j^{m+1} b_{om}^e S_{om}^e(c_0,\eta)\right|^2, \tag{4.87}$$

where

$$\left(\frac{\xi^2-1}{\xi^2-\eta^2}\right)^{\xi\to Large} \cong 1,$$

$$\Rightarrow \quad \frac{\sigma}{\lambda} = \left|\sum_m j^{m+1}\left[b_{em}S_{em}(c_0,\eta)+b_{om}S_{om}(c_0,\eta)\right]\right|^2. \tag{4.88}$$

Equations (4.84) and (4.88) are used to finding numerical results of the echo width in Chapter 5.

4.6 Conclusion

The theoretical solution of TM polarized electromagnetic scattering by elliptic chiral cylinder is developed. The solution of the wave equation in chiral media using elliptic coordinates together with expressions of incident, transmitted and scattered electromagnetic waves are derived. Unknown expansion coefficients for the transmitted and scattered waves are found by applying the boundary conditions and the orthogonality of Mathieu functions. Expressions of the echo widths for co- and cross-polarized are also presented.

5. Numerical Results

5.1 Introduction

In this chapter selected numerical results are presented for the computed far field and for a variety of geometrical and material parameters. In each case, the infinite series is terminated to include only N terms of both the even and odd functions, where N, in general, is a suitable truncation number proportional to the structure's electrical size and shape. Accuracy of the characteristic values and convergence of the Fourier coefficients are very important for numerical values of the Mathieu functions. The designated software program for this project is able to control the accuracy of computations. For example the developed program checks the accuracy of the Wronskian relation for the radial (modified) Mathieu functions.

To generate numerical results we consider a solid elliptic chiral cylinder with permeability μ (or relative permeability μ_r), permitivity ε (or relative permitivity ε_r), and chirality admittance γ. a is the semi-major axis and b is the semi-minor axis of the ellipse, and a/b is their ratio. We need the incident angle of the plane wave at the given frequency (or wavelength) to compute the echo widths.

These values are necessary to find other parameters to calculate co- and cross-polarized echo widths (4.84) and (4.88). The calculations of echo widths need numerical values of Mathieu functions. Since the Mathieu functions (3.19)-(3.42) use Fourier coefficients A or B we should calculate the characteristic values α or β respectively. The key parameter to finding the characteristic values α or β is q $(= k^2f^2/4)$, where k is the wave number, and f is the semi-focal length of the ellipse. Depending on the location i.e.,

inside or outside the elliptical cylinder, there are three wave numbers. K_0 is the wave number in free space (outside the elliptical cylinder), K_R is the wave number for the right-hand circularity polarized, and K_L is the wave number for the left-hand circularity polarized of the chiral media (inside the elliptical cylinder).

In the following sections some numerical results of the forward and back scattering echo widths for both co- and cross-polarized waves with a TM polarized incident field are presented and discussed. For an elliptic cylinder with incident angle $\Phi^i = m\pi$ or $\Phi^i = (2m+1)\pi/2$ (where $m=0,1,2,...$) we have a symmetry of 180 degrees.

5.2 Validation

Although the designated software program for this thesis is internally able to control the accuracy of computations, more validation of the theoretical formulation and accuracy of the software program, is investigated. In this section we consider many special cases for which other solutions are available. For example a circular cylinder is a limiting case of the present geometry when $a/b=1$. Also a non-chiral (or dielectric) cylinder corresponds to $\gamma=0$ while perfect conducting cylinders can be simulated when $\gamma=0$, $\mu_r \to 0$, and $\varepsilon_r \to \infty$. The following figures in this section show these special cases.

The co-polarized bistatic echo widths with incident angle $\Phi^i=0$ degree, $a=0.08$ m, $\lambda=1$ m, $\mu_r=2$, $\varepsilon_r=4$, $\gamma=0$ and $a/b=1.001$, as a circular dielectric cylinder are shown in Figure 5.1. Also are shown the echo widths for the co- and cross-polarized bistatic with incident angle $\Phi^i=0$ degree, $a=0.1$ m, $\lambda=1$ m, $\mu_r=4$, $\varepsilon_r=1.5$, $\gamma=0.0005$ and $a/b=1.001$, as a circular chiral cylinder. The ratio ($a/b=1.001$) shows the elliptic cylinder is approaching a circular cylinder. Thus the results should be the same as the results of circular dielectric

or circular chiral cylinder (with this size and material). The results in Figure 5.1 are in excellent agreement with the results obtained by others, i.e. [1], [3] and [4].

The co-polarized bistatic echo widths when $\Phi^i=0$ degree, $\gamma=0$, $\lambda=1$ *m*, $a/b=1.001$, and for various a values as circular perfect conducting cylinders are shown in Figure 5.2. These results are in excellent agreement with the results obtained by Balanis in [45].

The co-polarized bistatic echo widths for the elliptic dielectric cylinders when $\Phi^i=90$ degrees, $\gamma=0$, $\lambda=1$ *m*, $\mu_r=1$, $\varepsilon_r=5$, $a/b=2$, and for various ka are shown in Figure 5.3. These results are in good agreement with the results obtained by Sebak and Shafai in [17].

The co-polarized bistatic echo widths for the elliptic perfect conducting cylinders with incident angle $\Phi^i=0$ *and* 90 degrees, $\gamma=0$, $\lambda=1$ *m*, $a/b=2$, and various ka are shown in Figure 5.4. These results are in excellent agreement with the results obtained by Sebak and Shafai in [17].

Figure 5.5 shows the results of another investigation. The cross-polarized echo width for a non-chiral media, i.e. dielectric or perfect conducting cylinders is zero. The cross-polarized bistatic echo widths with incident angle $\Phi^i=0$ degrees, $\gamma=0$, $\lambda=1$ *m*, and for four kinds of cylinders (dielectric and perfect conducting for both circular and elliptic cylinders) are shown in Figure 5.5. The cross-polarized echo widths for these cylinders are almost zero. The results shown in Figure 5.5 verify that the cross-polarized fields are zero for non-chiral media.

Therefore, these validation investigations confirm the accuracy of the theoretical formulation and the associated software program.

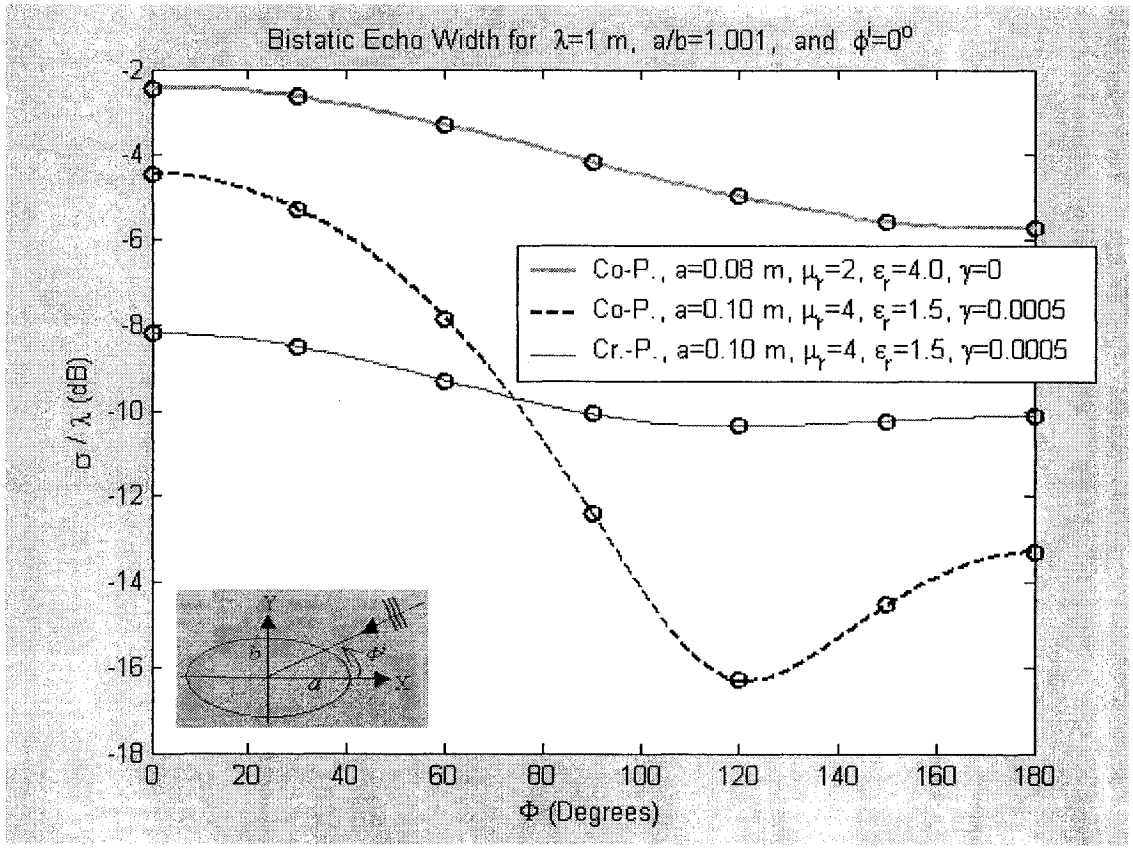

Figure 5.1 – The co- and cross-polarized bistatic (forward scattering) echo widths for the elliptic cylinders approaching circular cylinders. Curves with 'O O O' are the results given in [1], [3] and [4].

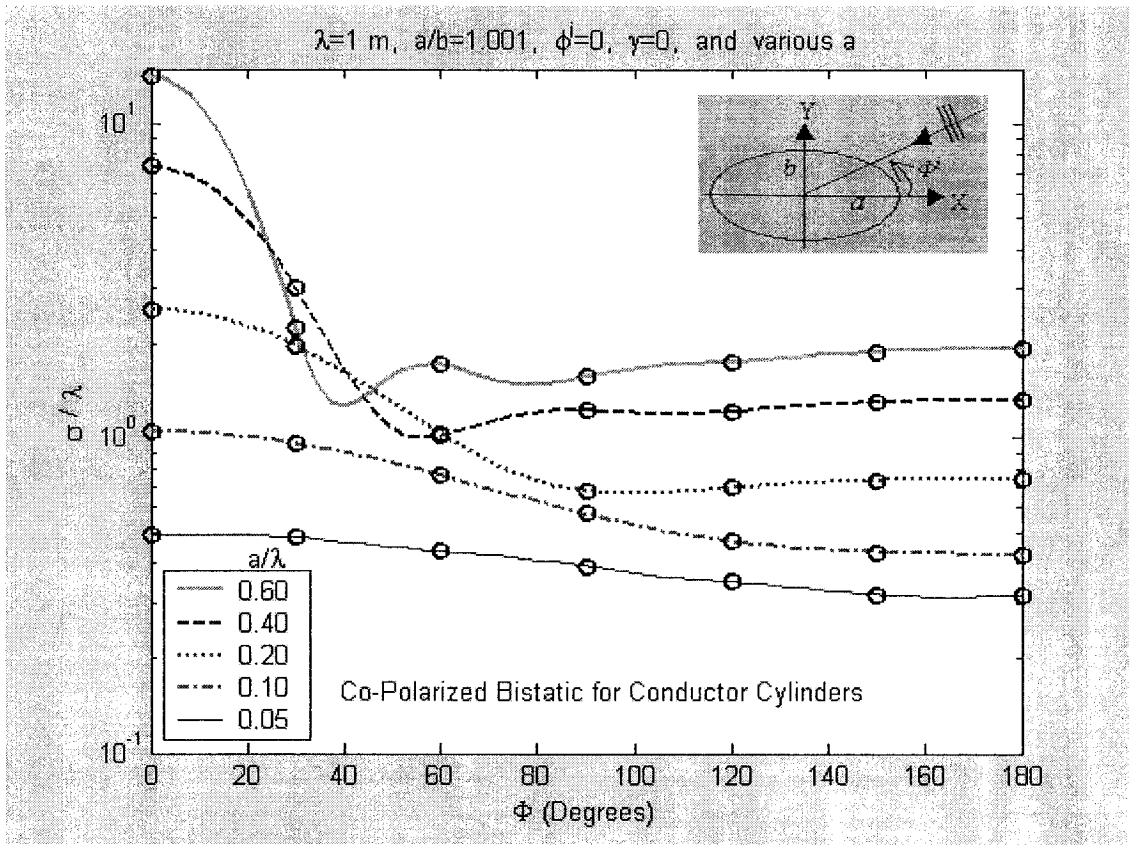

Figure 5.2 – The co-polarized bistatic (forward scattering) echo widths for the elliptic perfect conducting cylinders approaching circular perfect conducting cylinders. Curves with 'O O O' are the results given in [45].

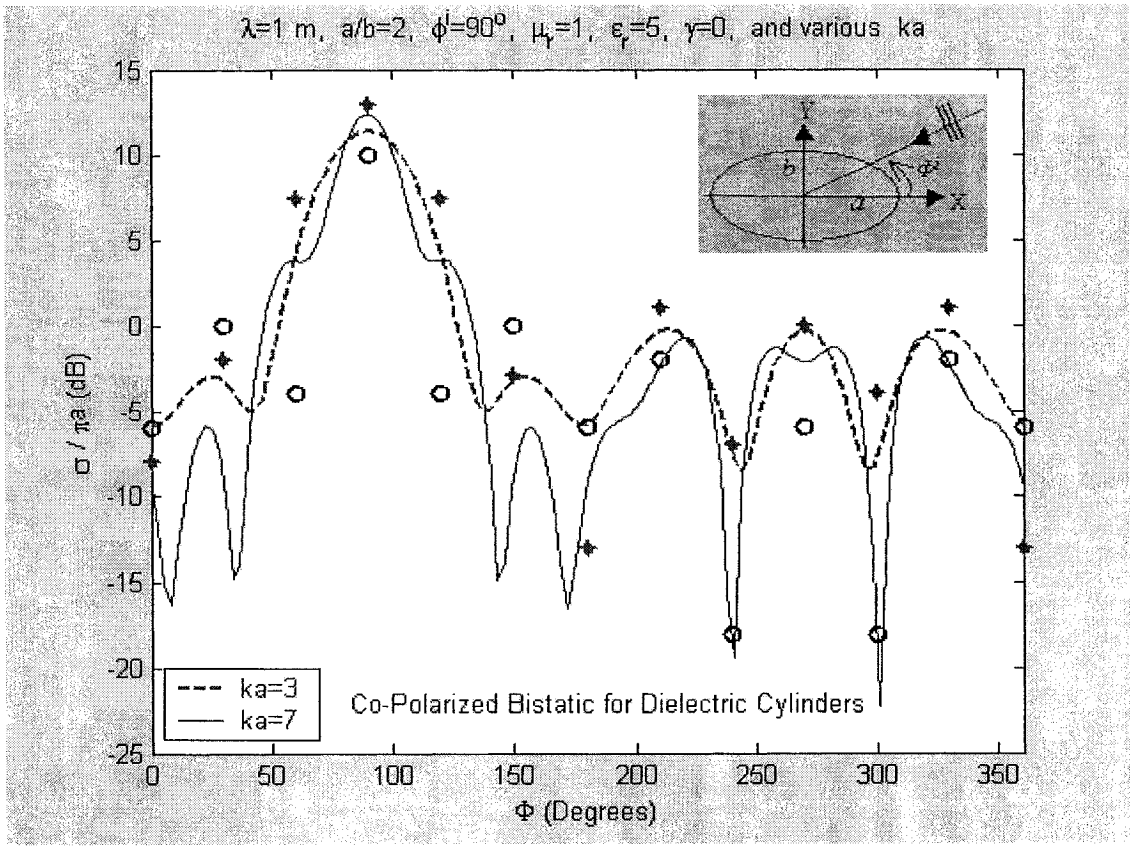

Figure 5.3 – The co-polarized bistatic (forward scattering) echo widths for the elliptic dielectric cylinders. Curve with '* * *' (for ka=3) and curve with 'O O O' (for ka=7) are the results given in [17].

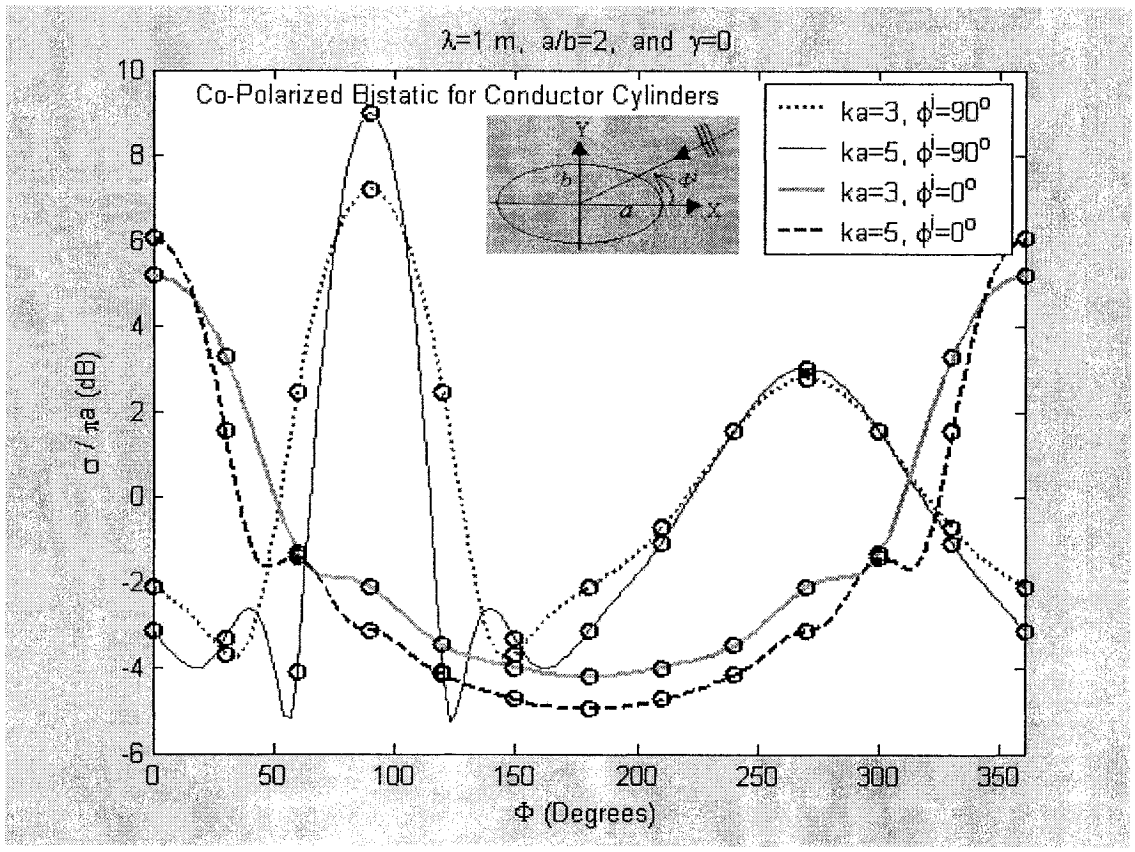

Figure 5.4 – The co-polarized bistatic (forward scattering) echo widths for the elliptic perfect conducting cylinders. Curves with 'O O O' are the results given in [17].

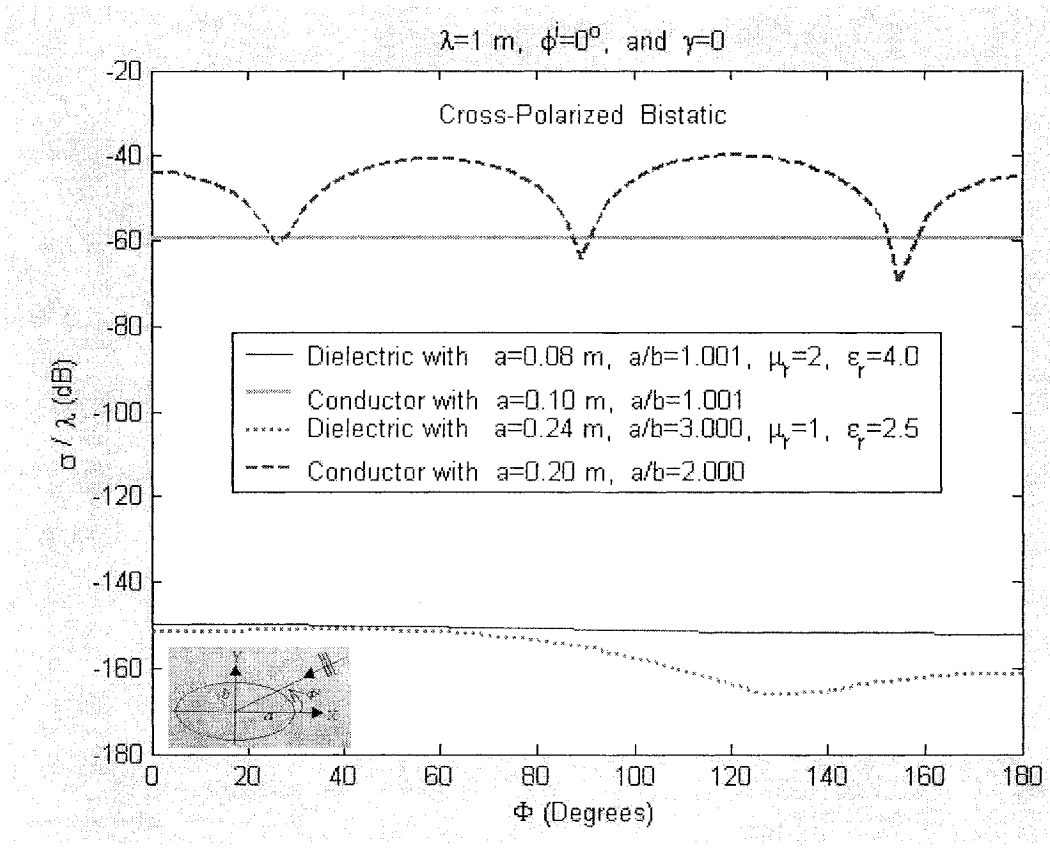

Figure 5.5 – The cross-polarized bistatic (forward scattering) echo widths for the circular and elliptic non-chiral (dielectric and perfect conducting) cylinders.

5.3 Effect of Geometrical and Material Parameters

The validation investigations of five kinds of cylinders in Section 5.2 verify both the theoretical formulation and accuracy of the associated software program. In this section we consider the case of elliptic chiral cylinder that is the main purpose of this thesis. Before discussing the numerical results of the echo widths, i.e. in the far field region, for the elliptic chiral cylinder, the numerical results of the transmitted wave due to an incident wave with $\Phi^i=0$ and $\lambda=1\ m$ into the elliptic chiral cylinder with $f=0.5\ m$, $\xi=1$, $\mu_r=2$, $\varepsilon_r=3$, and $\gamma=0.001$ are computed. Figure 5.6 shows the strength of the near electric field inside the cylinder. For this material the strength of the electric field is up to $70\ V/m$, around the center of the ellipse however around of the major and minor axes it has a small value. And also in the right side of the ellipse (side of the incident wave), the strength of the electric field is higher than the left side. In the first region of the ellipse (for $\Phi<60$ degrees), there are some high values for the electric field.

Numerical results of the forward and back scattering echo widths for both co- and cross-polarized waves with a TM polarized incident field for different geometrical and electrical parameters are discussed in the following paragraphs.

Figures 5.7, 5.8 and 5.9, show co-polarized bistatic echo widths with incident angles $\Phi^i=0,\ 45,\ 90$ degrees respectively, and Figure 5.10 shows the co-polarized monostatic echo width, for $a=0.2\ m$, $\lambda=1\ m$, $a/b=2$, $\mu_r=2$, $\varepsilon_r=3$, and for various γ values. The chirality admittance $\gamma=0$, indicates results for a non-chiral (dielectric) cylinder. For the selected materials these figures show at $\Phi=90$ degrees, the echo width of a chiral media is less than the echo width of a non-chiral media. Also at this angle, a chiral media with higher chirality, has lower echo width. Generally these properties are true for almost

other angles of the monostatic (back-scattered) echo widths in Figure 5.10, however they are not true for the bistatic (forward scattering) echo widths. For example, the bistatic echo width of a non-chiral media in Figures 5.7-5.9 is still higher than the echo width of a chiral media with low chirality ($\gamma=0.005$). But at $\Phi=180$ degrees in these figures, as well as $\Phi=0$ degree in Figure 5.9, the echo width of a chiral media with high chirality ($\gamma=0.025$), is higher than the echo widths of both a non-chiral media and a chiral media with low chiralty. Also at $\Phi=0$ degree in Figure 5.8, the echo width of a chiral media with high chirality ($\gamma=0.025$), is higher than the echo width of a chiral media with low chirality, and it is lower than the echo width of a non-chiral media.

Figures 5.11, 5.12 and 5.13 show the cross-polarized bistatic echo widths for incident angles $\Phi^i=0,\ 45,\ 90$ degrees, respectively. Figure 5.14 shows the cross-polarized monostatic echo width. These results correspond $a=0.24$ m, $\lambda=1$ m, $a/b=3$, $\mu_r=1$, $\varepsilon_r=2.5$, and for various γ values. In these figures we notice a trend that, in general, the echo width decreases by increasing the chirality admittance γ.

Figures 5.15 and 5.16 show the co-polarized bistatic echo widths for incident angle $\Phi^i=0$, and 90 degrees, respectively. Figure 5.17 shows the co-polarized monostatic echo width. These results correspond $a=0.1$ m, $\lambda=1$ m, $\mu_r=4$, $\varepsilon_r=1.5$, $\gamma=0.0005$, and for various values of the ratio (a/b). In these figures the echo width decreases by increasing the axial ratio. Since a is fixed, b decreases as the ratio is increasing and the ellipse becomes narrower. In Figure 5.15, the result for $a/b=1.001$ is the same as that for a circular chiral cylinder.

Figures 5.18 and 5.19 show the cross-polarized bistatic echo widths for incident angle $\Phi^i=0$, and 90 degrees, respectively. Figure 5.20 shows the cross-polarized

monostatic echo width. These results correspond $a=0.1$ m, $\lambda=1$ m, $\mu_r=4$, $\varepsilon_r=1.5$, $\gamma=0.0005$, and for various values of the ratio (a/b). In these figures the echo width decreases by increasing the ratio. Since a is fixed, b decreases and the ellipse becomes narrower by increasing the ratio.

Figure 5.21 shows the co-polarized bistatic echo width for incident angle $\Phi^i=0$ degree. Figure 5.22 shows co-polarized monostatic echo width. These results correspond $\lambda=1$ m, $a/b=2$, $\mu_r=1$, $\varepsilon_r=5$, $\gamma=0.03$, and for various semi-major axis (a). In these figures the echo width increases by increasing a. Since the ratio (a/b) is fixed, b increases with a and the cylinder size becomes larger.

Figure 5.23 shows the cross-polarized bistatic echo width for incident angle $\Phi^i=0$ degree, $\lambda=1$ m, $a/b=2$, $\mu r=1$, $\varepsilon r=5$, $\gamma=0.03$, and for various values of the semi-major axis (a). In this figure the echo width increases by increasing a. Since the ratio (a/b) is fixed, b increases with a and the cylinder size becomes larger.

5.4 Conclusion

All numerical results show that both co- and cross-polarized echo widths can be controlled by changing the frequency of the incident wave, the incidence angle, the axes ratio of the cylinder, and the constitutive parameters of the elliptic chiral cylinder. In the cases for co-polarized monostatic, generally, the echo width of a chiral media is less than the echo width of a non-chiral media, and a chiral media with higher chirality, has lower echo width. The cross-polarized bistatic and monostatic echo widths decrease by increasing the chirality admittance γ. The co- and cross-polarized bistatic echo widths decrease by increasing the axial ratio a/b (for fixed a), however, they increase by

increasing the semi-major axis a (for fixed a/b). These properties are also true for co- and cross-polarized monstatic echo widths.

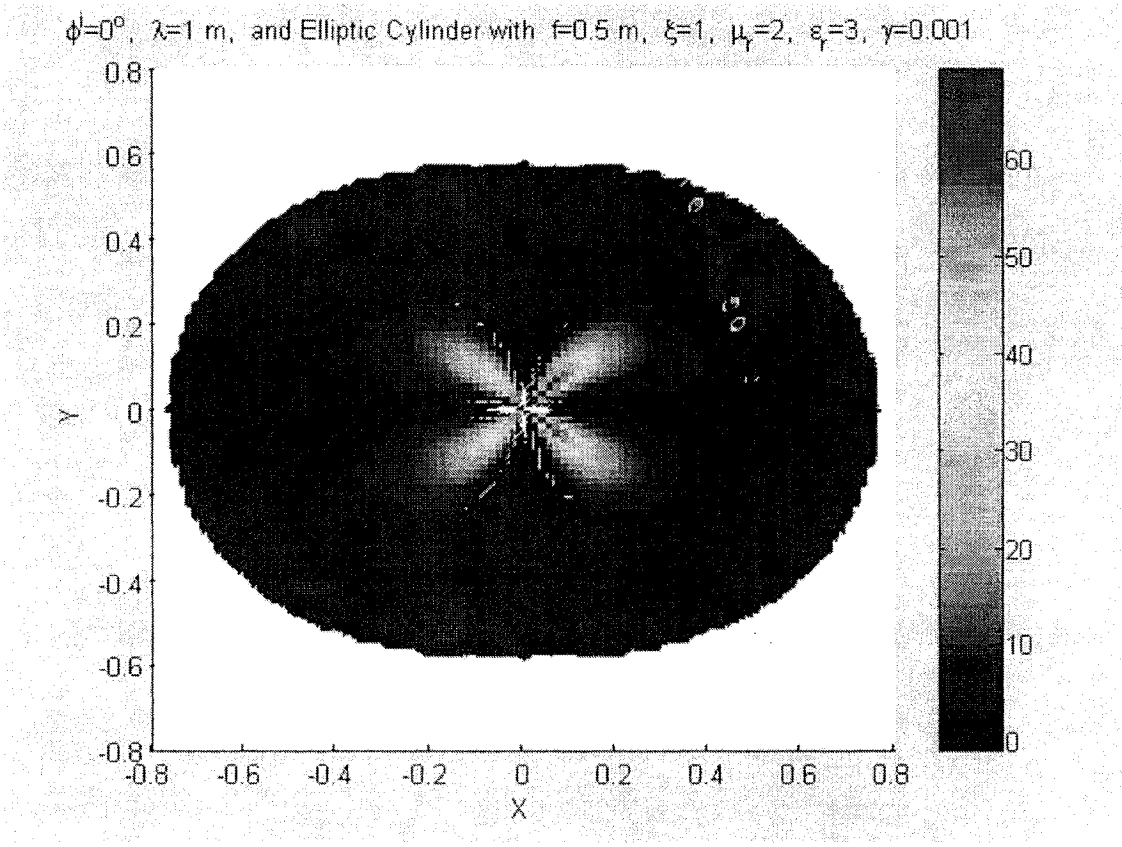

Figure 5.6 - The strength of the electric field inside of the elliptic chiral cylinder.

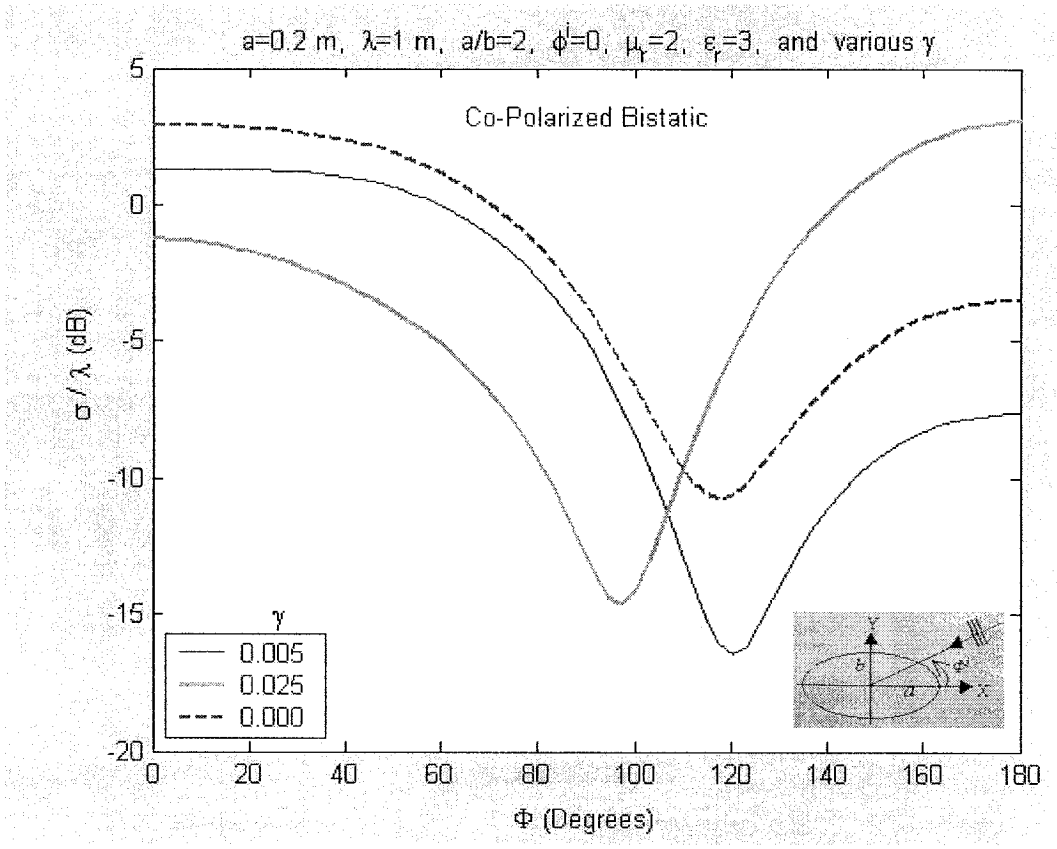

Figure 5.7 - The co-polarized bistatic (forward scattering) echo widths with incident angle $\Phi^i=0$ degree, and various chirality admittance γ.

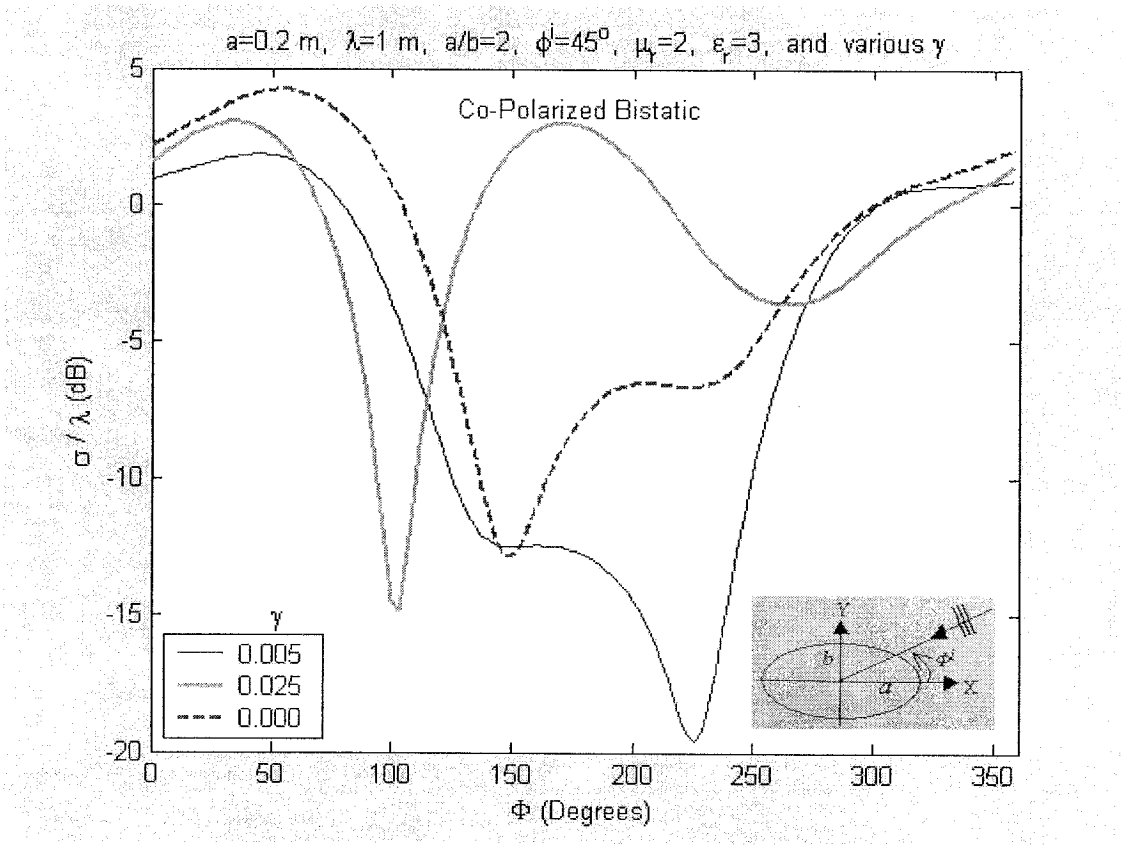

Figure 5.8 - The co-polarized bistatic (forward scattering) echo widths with incident angle $\Phi^i=45$ degrees, and various chirality admittance γ.

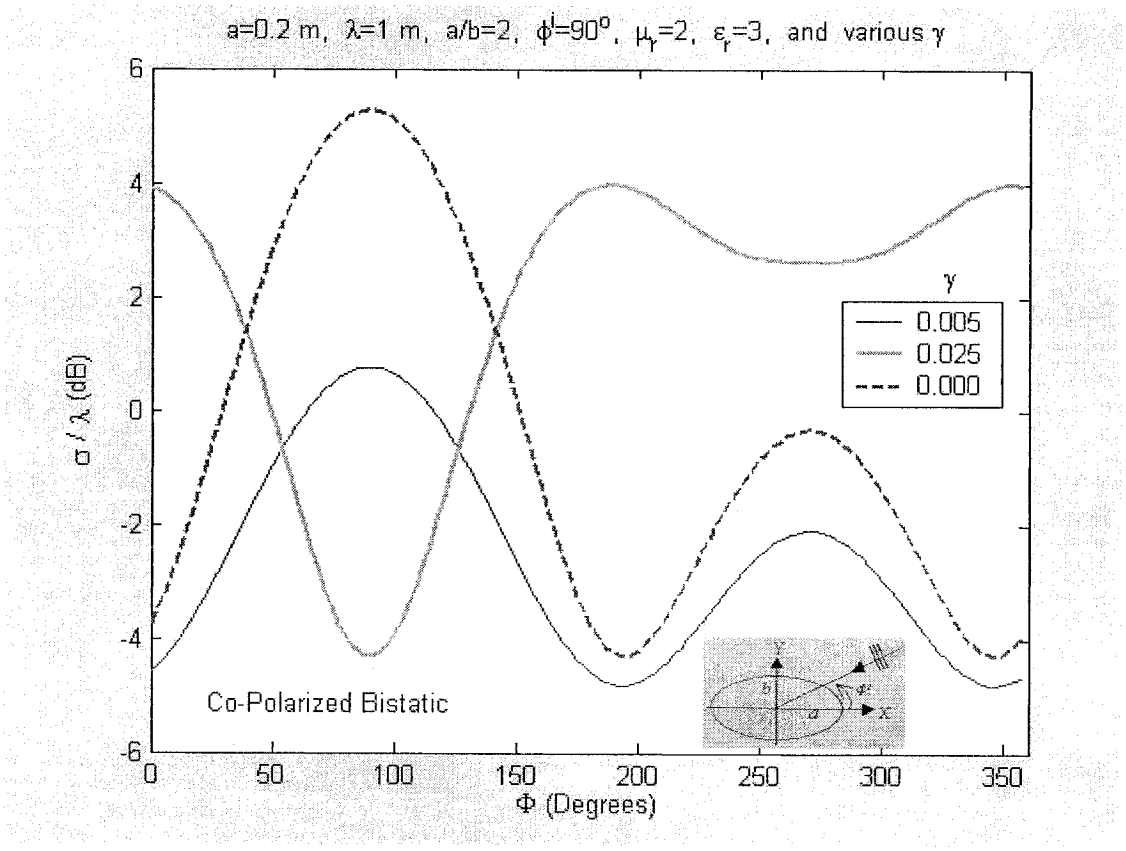

Figure 5.9 - The co-polarized bistatic (forward scattering) echo widths with incident angle $\Phi^i=90$ degrees, and various chirality admittance γ.

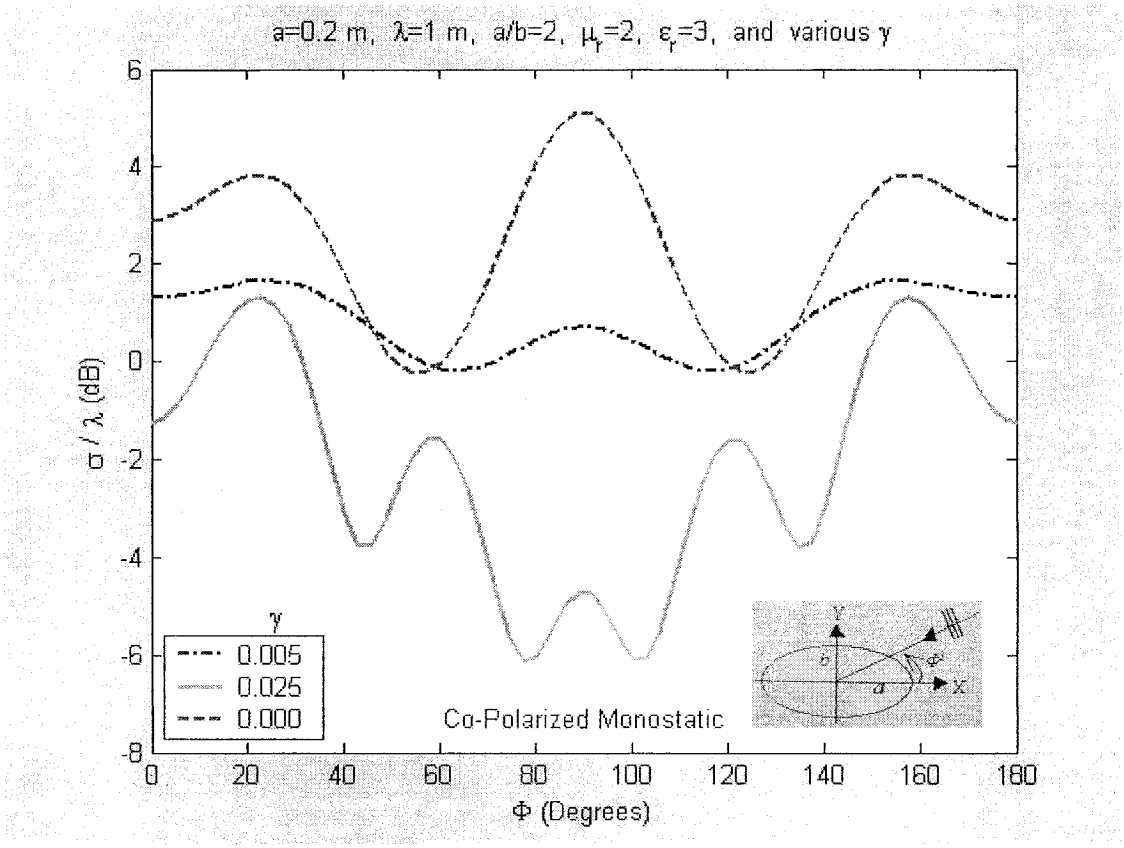

Figure 5.10 - The co-polarized monostatic (back-scattered) echo widths for various chirality admittance γ.

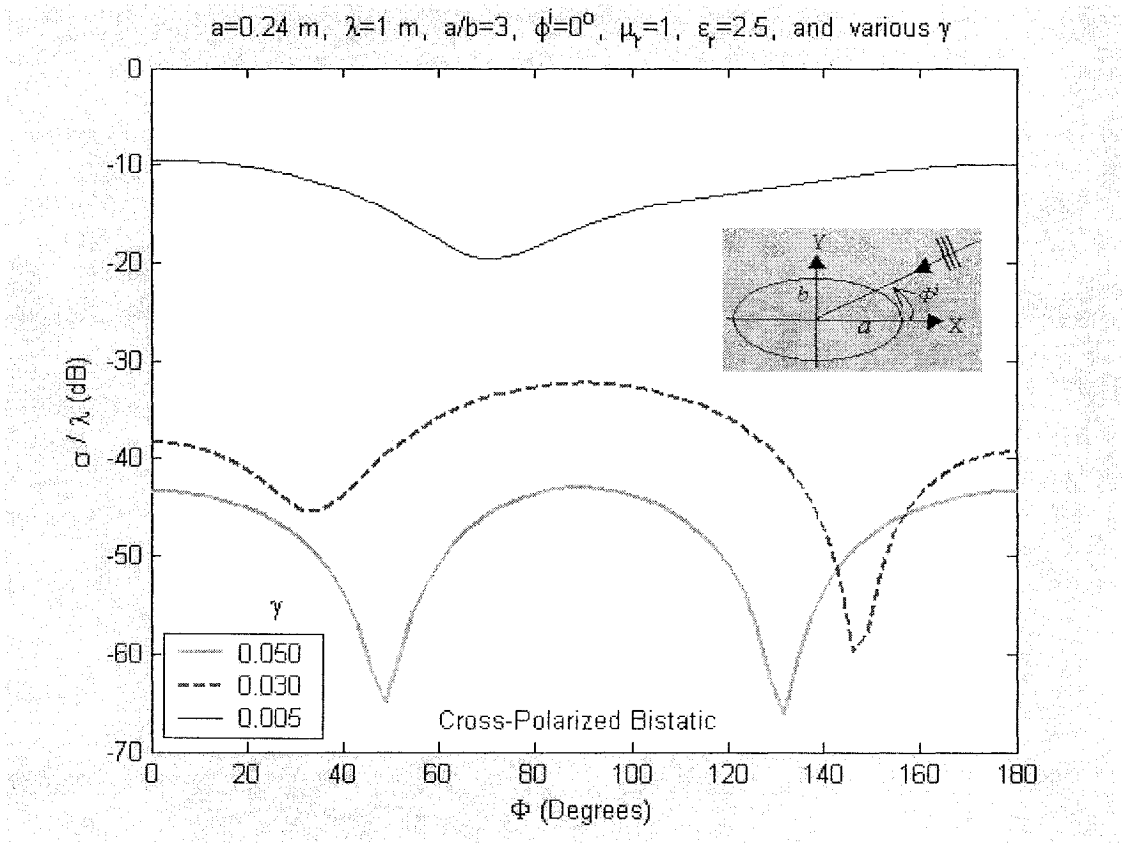

Figure 5.11 - The cross-polarized bistatic (forward scattering) echo widths with incident angle $\Phi^i=0$ degree, and various chirality admittance γ.

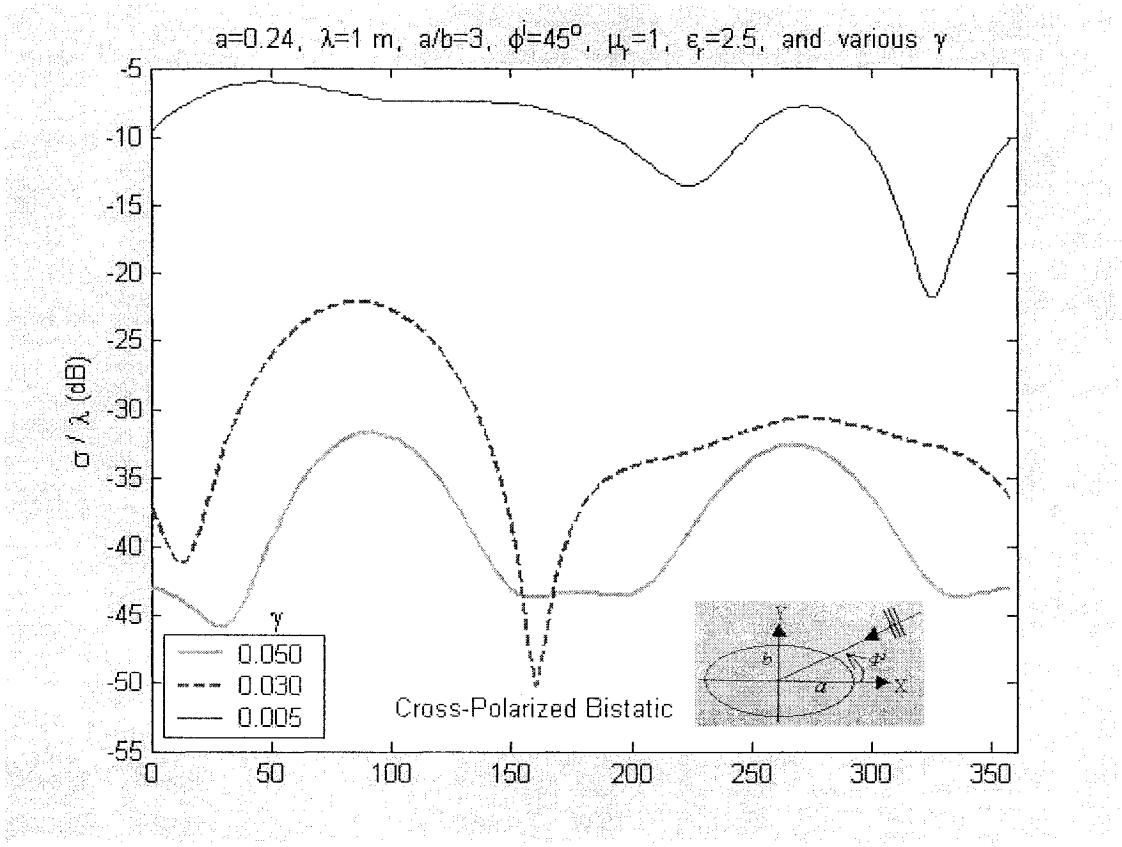

Figure 5.12 - The cross-polarized bistatic (forward scattering) echo widths with incident angle $\Phi^i=45$ degrees, and various chirality admittance γ.

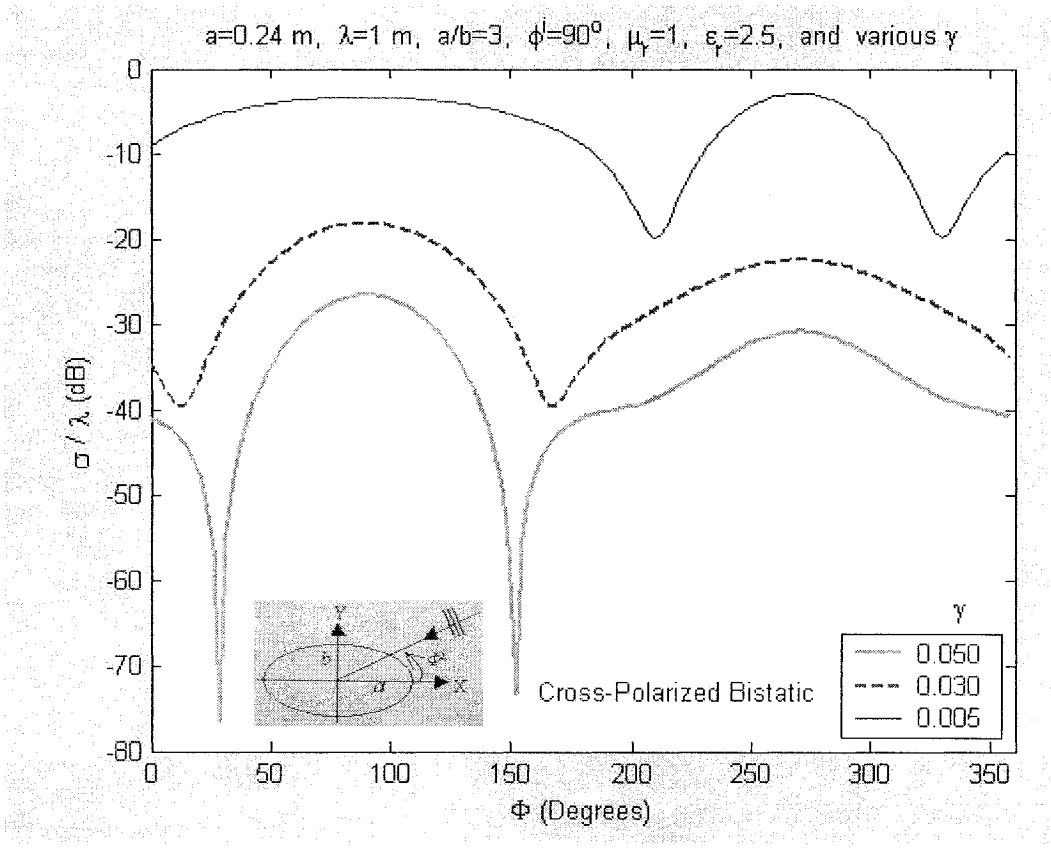

Figure 5.13 - The cross-polarized bistatic (forward scattering) echo widths with incident angle $\Phi^i=90$ degrees, and various chirality admittance γ.

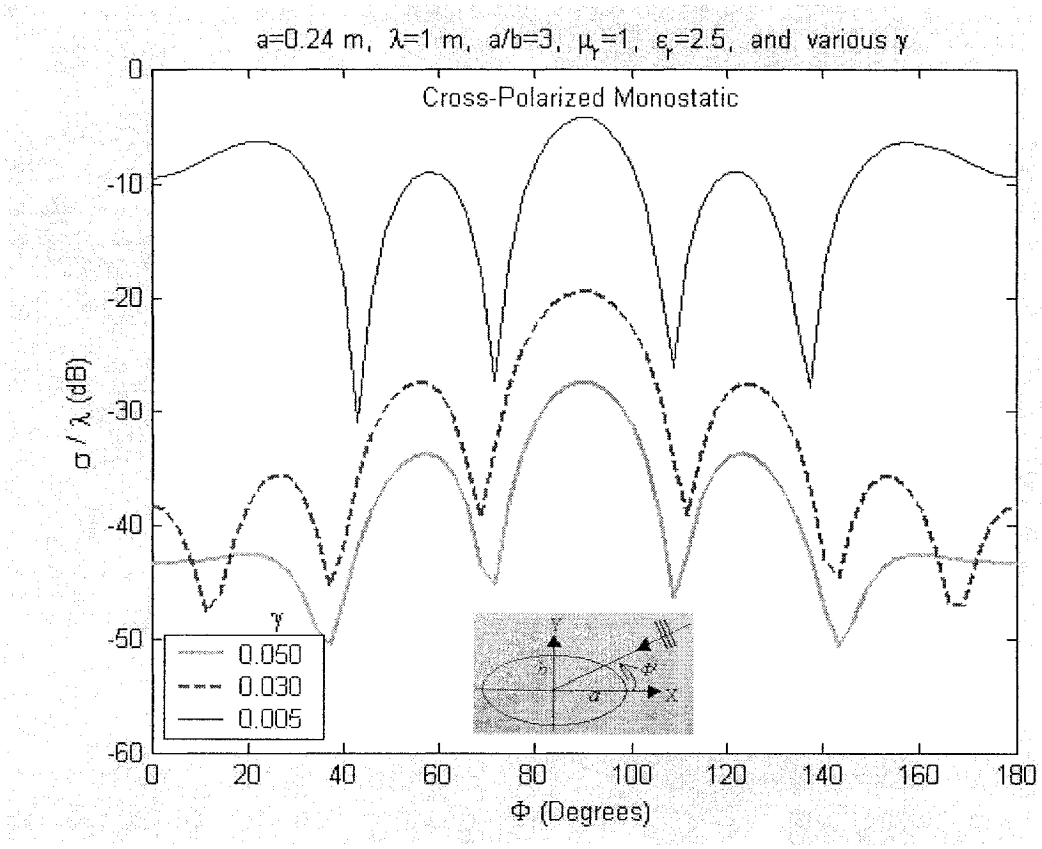

Figure 5.14 - The cross-polarized monostatic (back-scattered) echo widths for various chirality admittance γ.

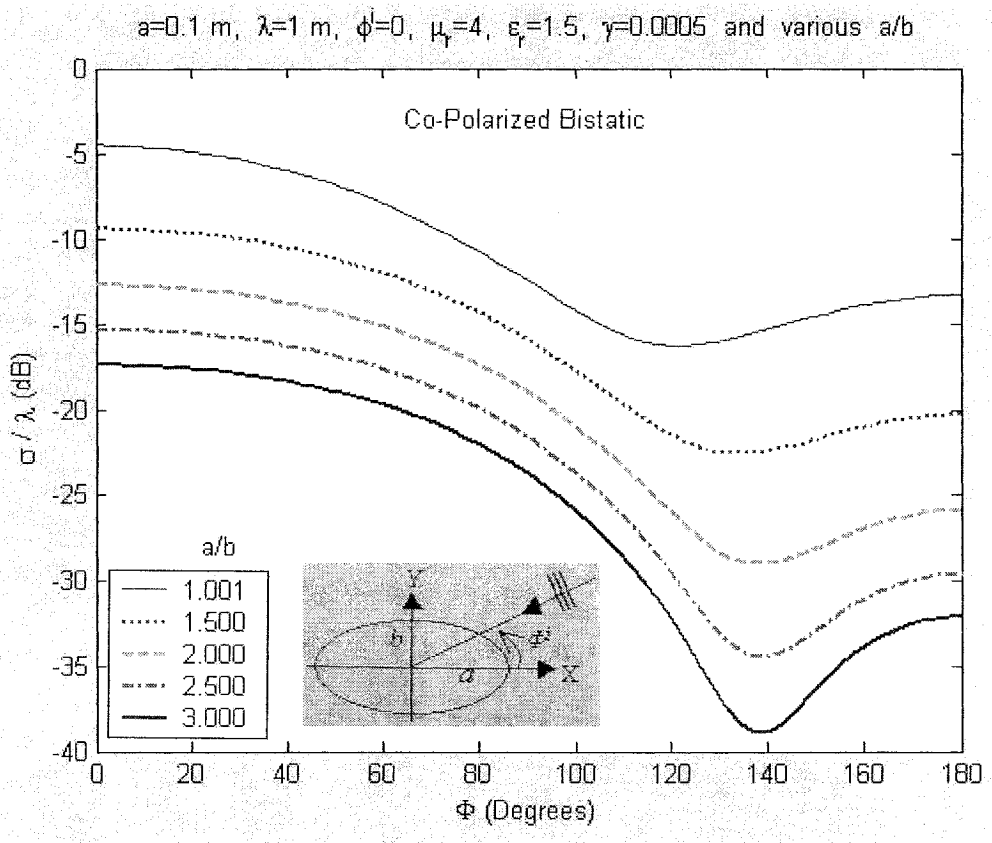

Figure 5.15 - The co-polarized bistatic (forward scattering) echo widths with incident angle $\Phi^i=0$ degree, and various ratio (a/b).

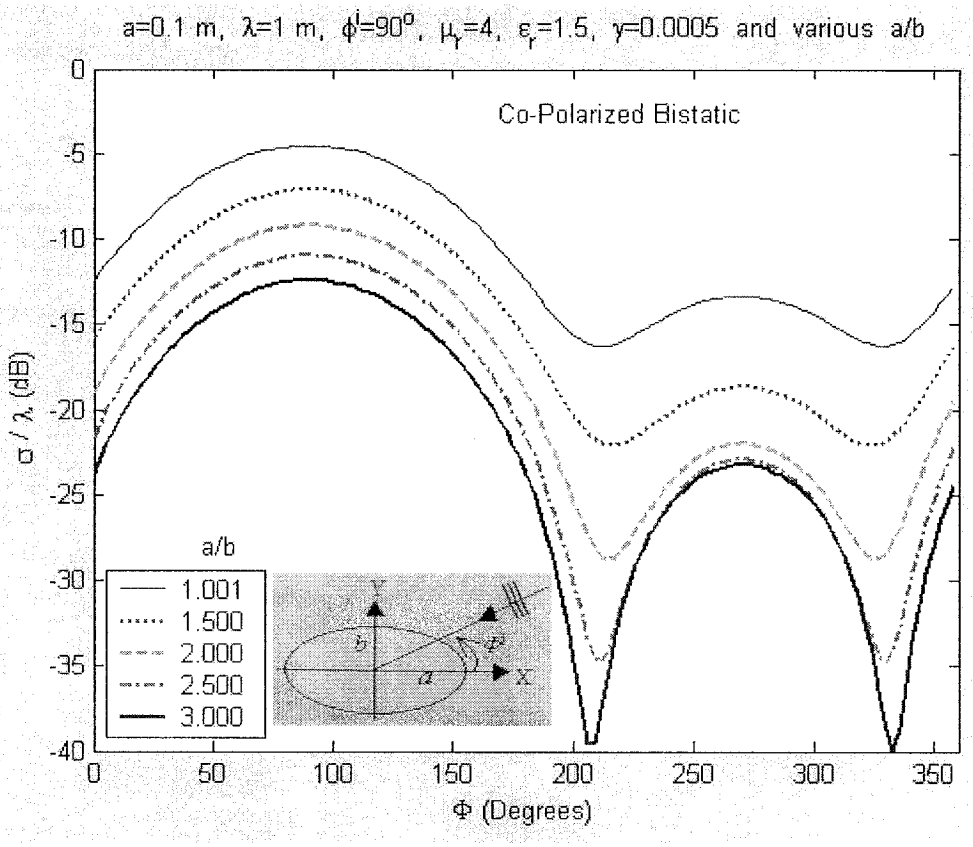

Figure 5.16 - The co-polarized bistatic (forward scattering) echo widths with incident angle $\Phi^i=90$ degrees, and various ratio (a/b).

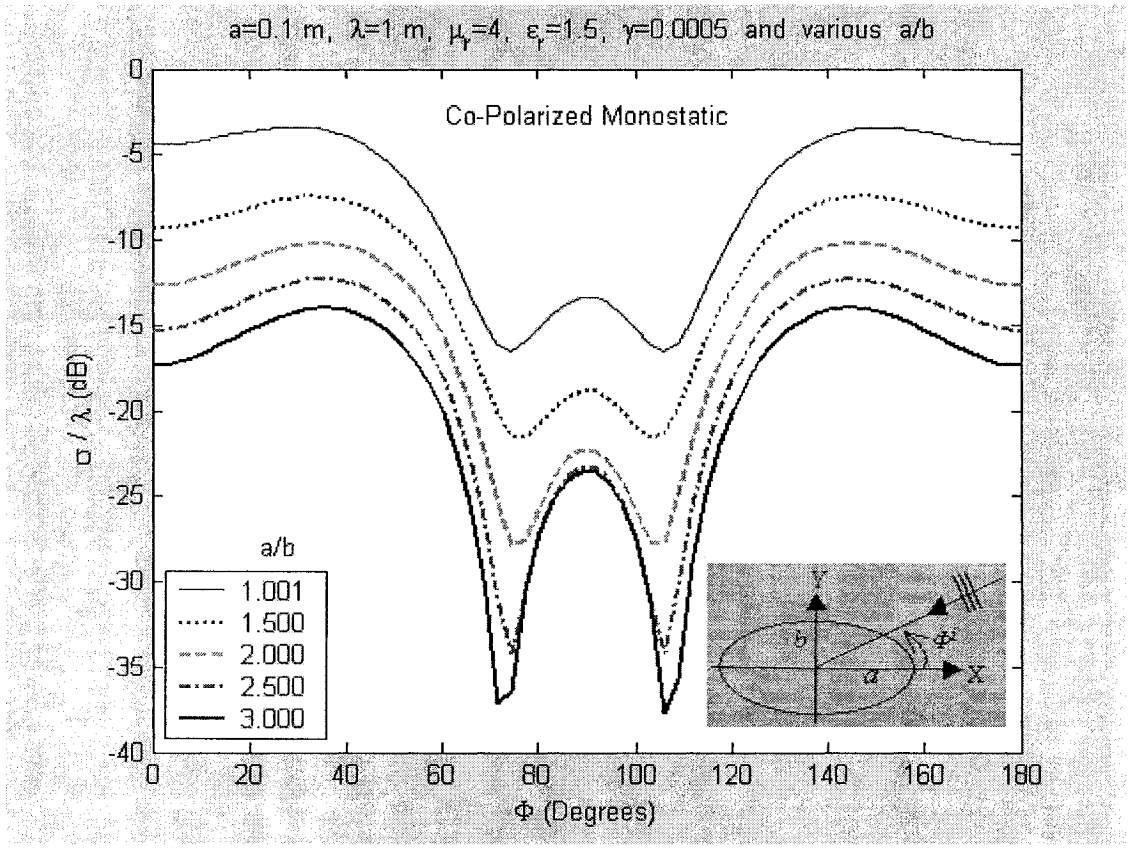

Figure 5.17 - The co-polarized monostatic (back-scattered) echo widths for various ratio (*a/b*).

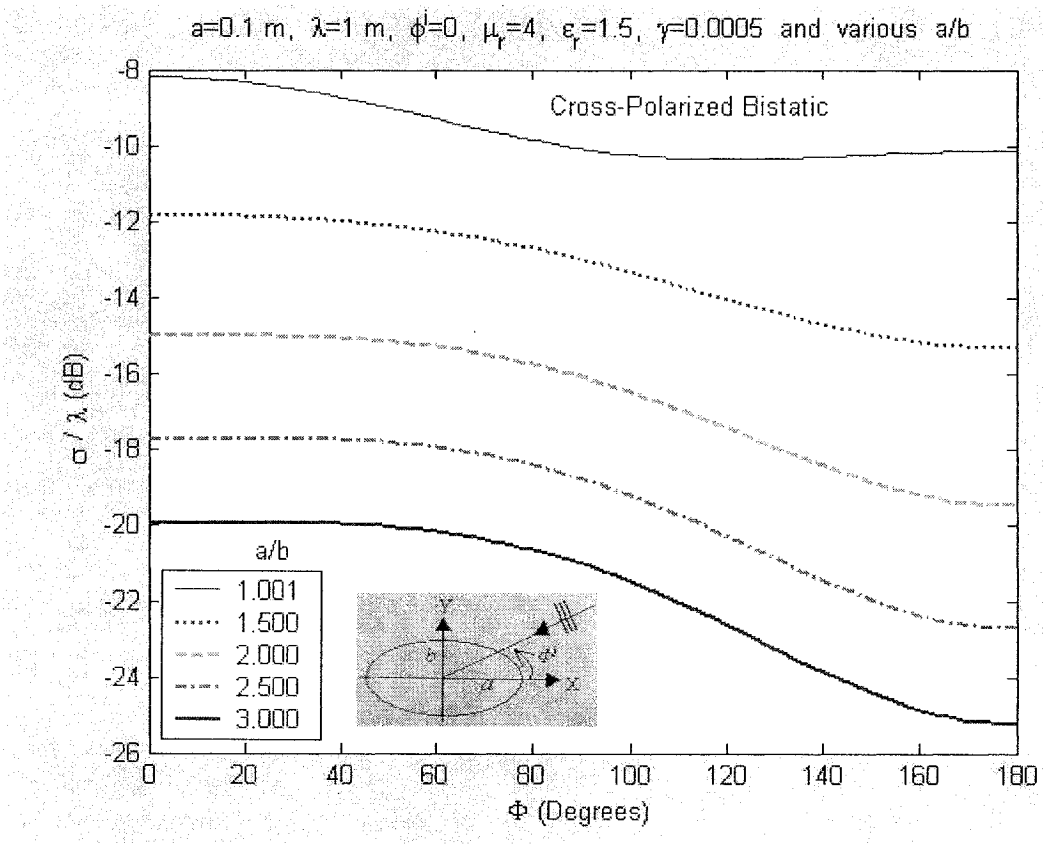

Figure 5.18 - The cross-polarized bistatic (forward scattering) echo widths with incident angle $\Phi^i=0$ degree, and various ratio (a/b).

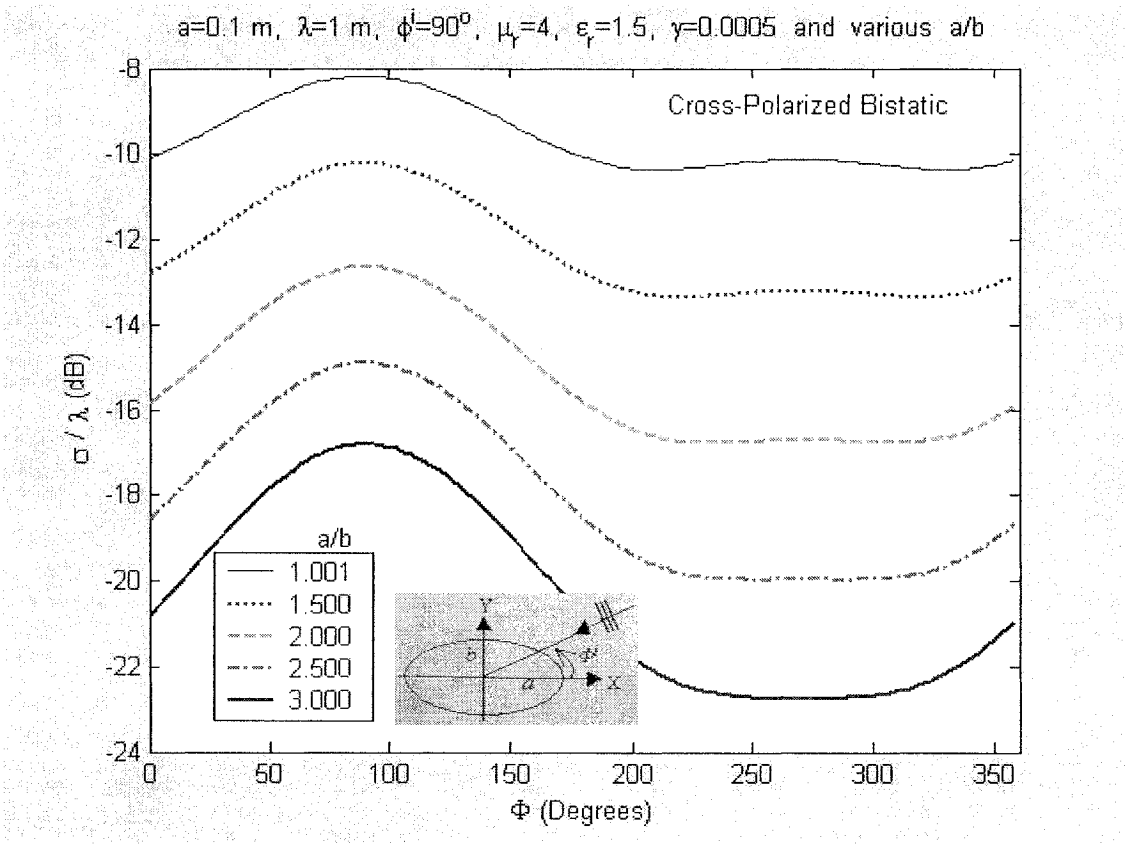

Figure 5.19 - The cross-polarized bistatic (forward scattering) echo widths with incident angle $\Phi^i=90$ degrees, and various ratio (a/b).

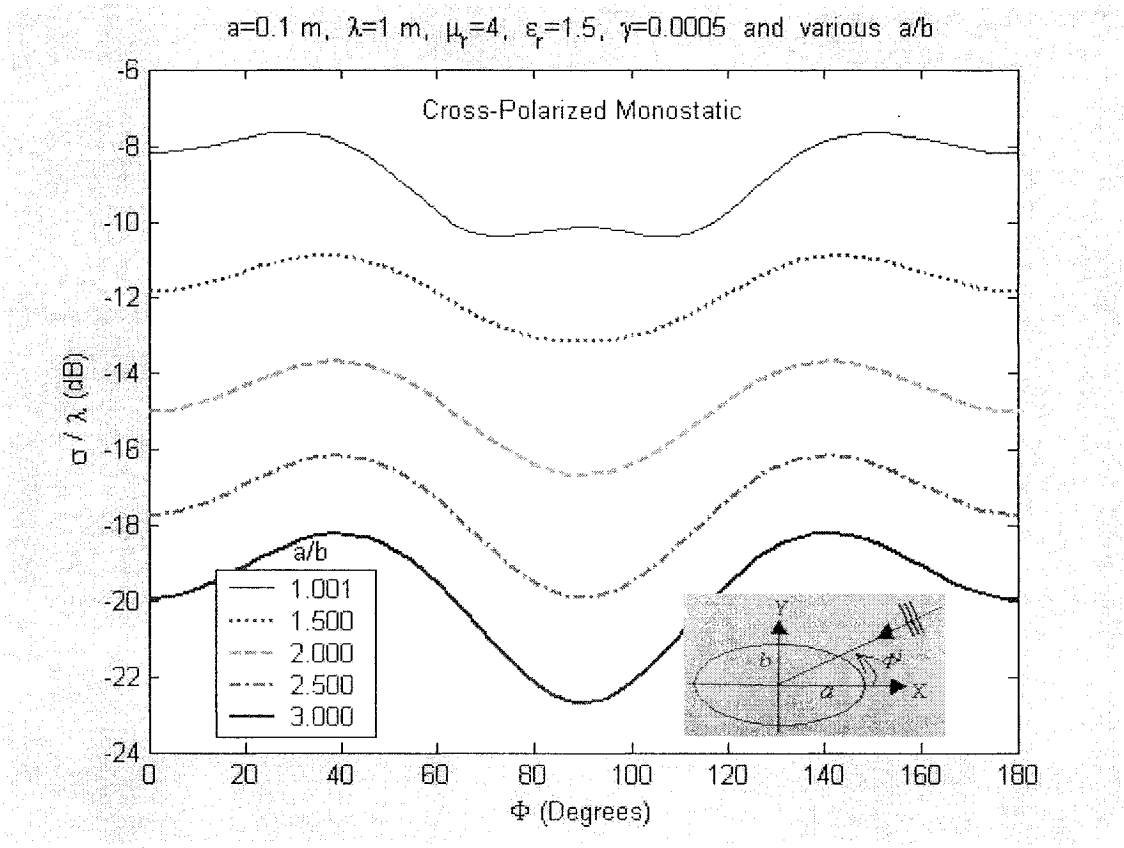

Figure 5.20 - The cross-polarized monostatic (back-scattered) echo widths for various ratio (*a/b*).

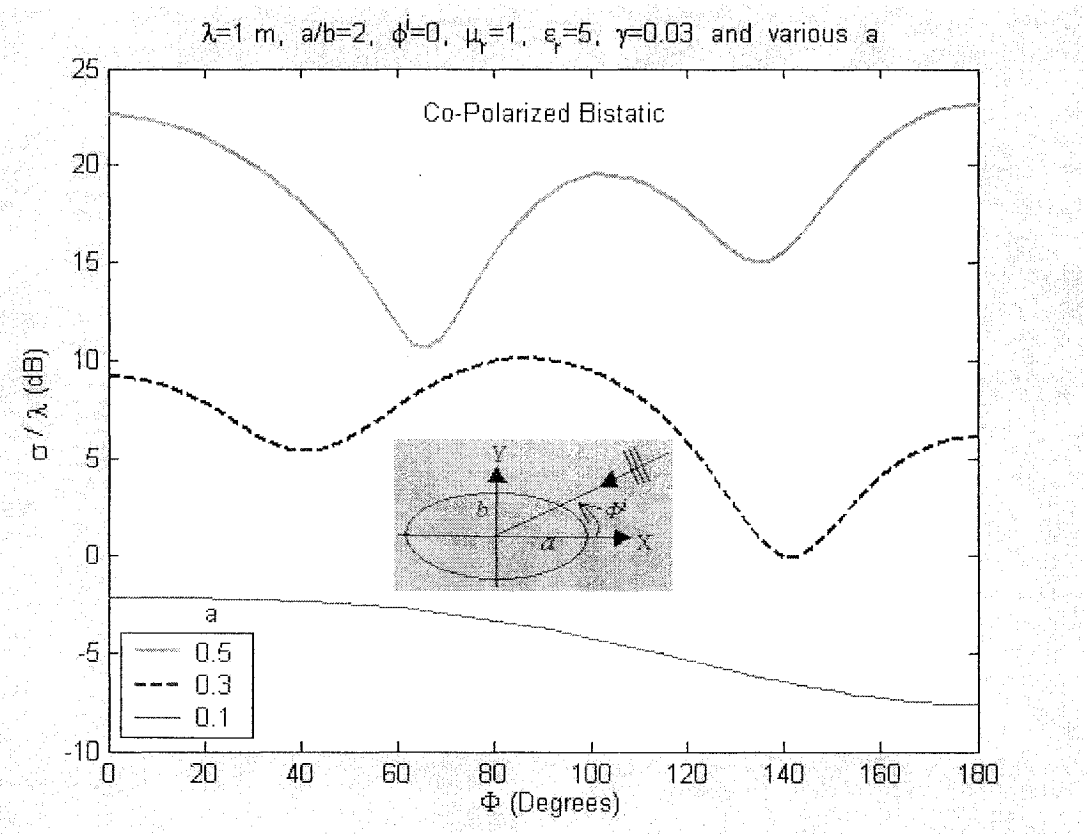

Figure 5.21 - The co-polarized bistatic (forward scattering) echo widths with incident angle $\Phi^i=0$ degree, and various a.

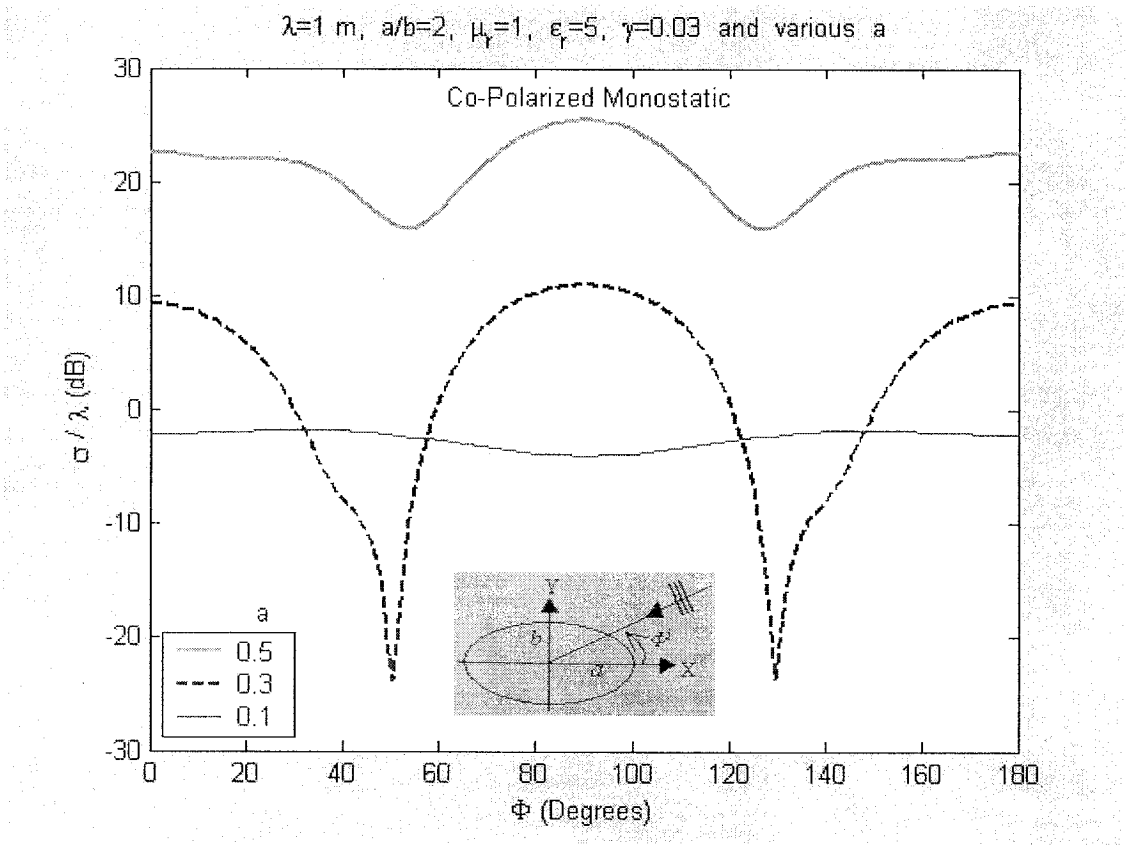

Figure 5.22 - The co-polarized monosatic (back-scattered) echo widths for various *a*.

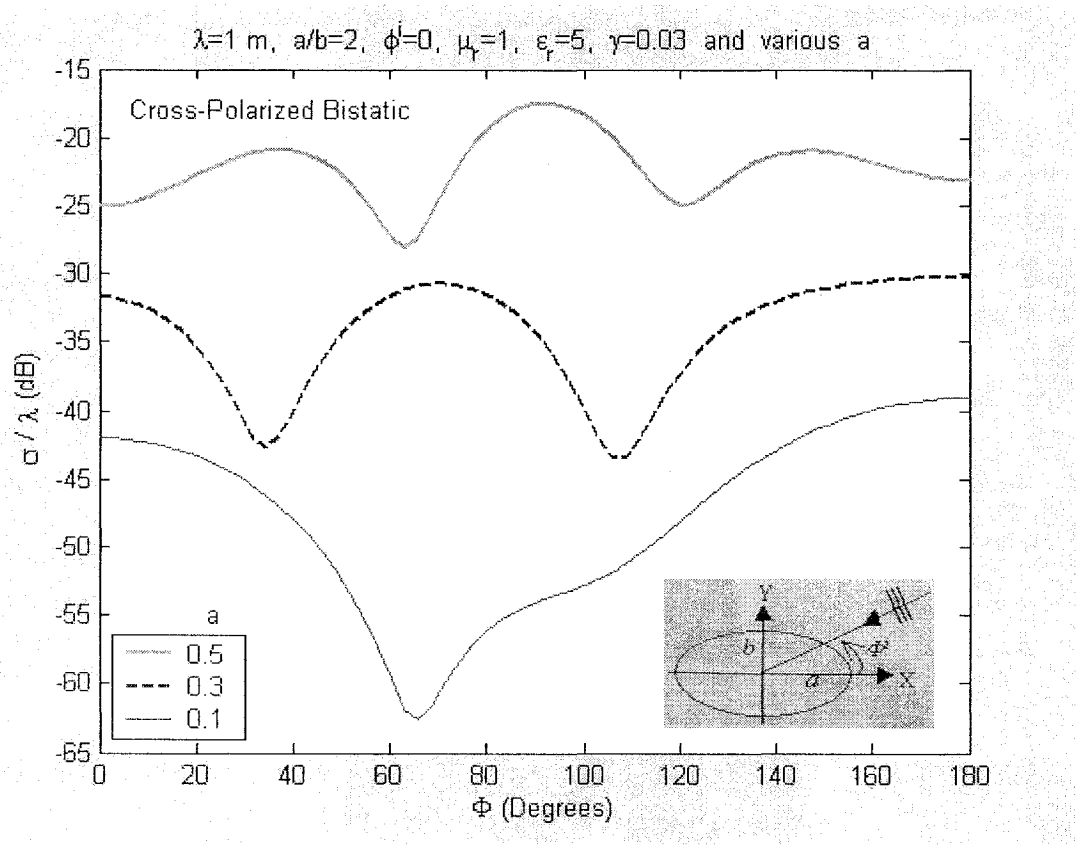

Figure 5.23 - The cross-polarized bistatic (forward scattering) echo widths with incident angle $\Phi^i=0$ degree, and various a.

6. Summary and Conclusions

The problem of electromagnetic scattering by elliptic chiral cylinder has been analyzed and investigated theoretically for TM polarized waves. This problem has been solved as an exact boundary value problem using the separation of variables method.

The chiral media contains an additional material parameter γ, that is an advantage for practical designs. However analysis of this media needs very complicated mathematics. In chiral media, both co- and cross-polarized waves are supported. In Chapter 2 properties of chiral media were discussed and wave equations in this media were presented.

The scattering by elliptic cylinders is more complicated compared to scattering by circular cases and also offers more parameters in controlling the scattering properties of cylindrical objects. The elliptic chiral cylinder geometry is more general and can be used to study the effect of different material and geometrical parameters on the scattering properties of different objects. In Chapter 3 the wave equation in elliptical coordinates system were presented. In this system the solution is based on the separation of variables technique, and expressed in terms of Mathieu and modified Mathieu functions. The accuracy of characteristic values and convergence of Fourier coefficients for Mathieu functions are very important. Expression for the angular and radial (modified) Mathieu functions and their derivatives were also given.

In Chapter 4, TM polarized electromagnetic wave scattering by elliptic chiral cylinder was developed using an exact boundary value problem approach. The solution is based on the separation of variable technique in elliptic cylindrical coordinates system.

The incident, transmitted and scattered electromagnetic waves are expressed in terms of infinite wave functions with expansion coefficients. The matrix forms of the expansion coefficients are found by enforcing the boundary conditions and applying the orthogonality of the Mathieu functions through a lengthy complicated process. The radar cross section (RCS) per unit length or echo width of electromagnetic scattering by elliptic chiral cylinder for co- and cross-polarized waves were computed using the asymptotic expansions for modified Mathieu functions.

Very long computer program were developed and used to generate numerical results. The numerical results of the bistatic (forward scattering) and monostatic (back-scattered) echo widths for co- and cross-polarized and a variety of cases were discussed in Chapter 5. Validation of the developed formulation and computer program were carried out by considering many limiting cases such as circular dielectric, circular perfect conducting, and circular chiral cylinders, as well as elliptic dielectric and elliptic perfect conducting cylinders. These numerical results agreed well with published results, for these special cases.

Based on the numerical results we can note the following conclusions:

- In the case of fixed ellipse axes a, b and various chirality admittance γ, in many cases for co-polarized bistatic field and in general case for co-polarized monstatic field, the echo width decreased by increasing the chirality admittance. And also the echo width of a chiral media was less than the echo width of a non-chiral media.
- In the case of fixed ellipse axes and various chirality admittance, in general, the echo width decreased by increasing the chirality admittance for the cross-polarized component.

- In the case of fixed material parameters and major axis, the echo width decreased by increasing of ratio (or decreasing the minor axis) for both co- and cross-polarized cases. That means when the ellipse becomes narrower (by increase of ratio and fixed major axis), the echo width decreases.
- In the case of fixed material parameters and axial ratio, the echo width increased by increasing the major axis for co- and cross-polarized. Since the ratio is fixed, then the minor axis increases with major axis. Consequently the echo width increases by increasing of cylinder size.
- All numerical results show that both co- and cross-polarized echo widths can be controlled by changing the frequency (or wavelength) of incident wave, the incidence angle, the axes (*a, b,* or ratio) of the cylinder, and the constitutive parameters of the elliptic chiral cylinder. Furthermore the results illustrate that the echo widths are greatly influenced by chirality parameter which may enhance or reduce the echo width.
- To control the echo width, the elliptic chiral cylinder has one extra degree of freedom compared to a circular chiral cylinder, i.e. the two semi-axes a and b compared to the circular radius r.

In future work, the analysis of the electromagnetic scattering problem by elliptic chiral cylinders could be further studied. For example, the theoretical development in this thesis could be extended to study the electromagnetic scattering by two parallel elliptic chiral cylinders. The separation distance is d and the medium of the surrounding cylinders is free space. The incident, transmitted and scattered waves can be expressed with respect to the elliptic cylinder coordinates system of one of them. A translation

theorem can then be used to express field expressions in the local coordinates of each cylinder.

References

1. M. S. Kluskens and E. H. Newman, "Scattering by a Chiral Cylinder of Arbitrary Cross Section," *IEEE Transactions on Antennas and Propagation*, Vol. 38, No 9, September 1990.
2. M. S. Kluskens and E. H. Newman, "Scattering by a Multilayer Chiral Cylinder," *IEEE Transactions on Antennas and Propagation*, Vol. 39, No 1, January 1991.
3. R.G. Rojas, "Integral Equations for EM Scattering by Homogeneous/Inhomogeneous Two-dimensional Chiral Bodies," *IEE Proc.-Microw. Antennas Propagation*, Vol. 141, No 5, October 1994.
4. M. A. Al-Kanhal and E. Arvas, "Electromagnetic Scattering from a Chiral Cylinder of Arbitrary Cross Section," *IEEE Transactions on Antennas and Propagation*, Vol. 44, No 7, July 1996.
5. Z. Shen and R. H. MacPhie, "Scattering at a Nonchiral–Chiral Interface in a Coaxial Waveguide," *IEEE Transactions on Microwave Theory and Techniques*, Vol. 46, No 7, July 1998.
6. W. Y. Yin and L. W. Li, "Scattering from Strip-Loaded Composite Chiral Cylinder Structure," *IEEE*, 1999.
7. S. Zouhdi, G. E. Couenon and A. F. Lamer, "Scattering from a Periodic Array of Thin Planar Chiral Structures – Calculation and Measurement," *IEEE Transactions on Antennas and Propagation*, Vol. 46, No 7, June 1999.

8. D. L. Jaggart and J. C. Liu, "The Matrix Riccati Equation for Scattering from Stratified Chiral Spheres," *IEEE Transactions on Antennas and Propagation*, Vol. 47, No 7, July 1999.

9. W. Y. Yin, L. W. Li, T. S. Yeo, and M. S. Leong, "Direct Singular Integral Equation Method in Scattering from Multiple Strip-Lodded Cylindrical Chiral Objects," *IEEE,* 2000.

10. L. W. Li, D. You, M. S. Leong, and T. S. Yeo, "Electromagnetic Scattering by Multilayered Chiral-Media Structures: a Scattering-to-Radiation Transform," *Progress In Electromagnetics Research, PIER*, 26, 249–291, 2000.

11. V. N. Apletalin, P. A. Malyshkin, A. D. Shatrov and V. S. Solosin, "Back-Scattering from a Chiral Anisotropic Conducting Cylinder with a Longitudinal Slot," *Symposium proceedings, Kharkov, Ukraine*, June, 2001.

12. A. Z. Elsherbeni, M. Al Sarkawy, and S. F. Mahmoud, "Scattering from a Chiral Cylinders of Circular Cross-Sections," *IEEE*, 2003.

13. M. M. I. Saadoun and N. Engheta, "Theoretical Study of Variation of Propagation Constant in a Cylindrical Waveguide Due to Chirality: Chiro-Phase Shifting," *IEEE Transactions on Microwave Theory and Techniques*, Vol. 42, No 6, September 1994.

14. I. P. Theron and J. H. Cloete, "The Electric Quadrupole Contribution to the Circular Birefringence of Nonmagnetic Anistropic Chiral Media: A Circular Waveguide Experiment," *IEEE Transactions on Microwave Theory and Techniques*, Vol. 44, No 8, August 1996.

15. D. Bacon and T. C. K. Rao, "Propagation modes of a cylindrical waveguide loaded by a coaxial chiral cylinder," *IEE Proc.-Microw. Antennas Propag.*, Vol. 145, No 3, June 1998.

16. J. Reinert, G. Busse and A. F. Jacob, "Waveguide Characterization of Chiral Material: Theory," *IEEE Transactions on Microwave Theory and Techniques*, Vol. 47, No 3, March 1999.

17. A. Sebak and L. Shafai, "Generalized solutions for electromagnetic scattering by elliptical structures," *Computer Physics Communications*, 68, 1990.

18. A. Sebak, L. Shafai and H. A. Ragheb, "TM Scattering by a Homogeneous Elliptic Cylinder with Dielectric or Magnetic Coating," *IEEE,* 1990.

19. A. Sebak "Electromagnetic Interaction with a Magnetic Coated Elliptic Cylinder," *IEEE Transactions on Magnetics*, Vol. 27, No 5, September 1991.

20. M. Hussein, A. Sebak and M. Hamid, "Scattering and Coupling Properties of a Slotted Elliptic Cylinder," *IEEE Transactions on Electromagnetic Compatibility*, Vol. 36, No 1, February 1994.

21. A. Sebak and Y. Antar, "Multiple scattering by parallel conducting elliptic cylinders: TE case," *IEE Proc.-Microw. Antennas Propag.*, Vol. 142, No 2, April 1995.

22. A. R. Sebak, "Scattering from Dielectric-Coated Impedance Elliptic Cylinder," *IEEE Transaction on Antennas and Propagation*, Vol. 48, No 10, October 2000.

23. S. Caorsi, M. Pastorino and M. Raffetto, "Electromagnetic Scattering by a Multilayer Elliptic Cylinder Under Transverse-Magnetic Illumination: Series Solution in Terms of Mathieu Functions," *IEEE Transaction on Antennas and Propagation*, Vol. 45, No 6, June 1997.

24. A. M. Hussein and W. Wurjantara, "Analysis of Elliptic Conductors Using the Point Matching Method with Mathieu Functions," *IEEE Transactions on Magnetics*, Vol. 33, No 5, September 1997.

25. S. Caorsi, M. Pastorino and M. Raffetto, "Electromagnetic Scattering by a Conducting Strip with a Multilayer Elliptic Dielectric Coating," *IEEE Transactions on Electromagnetic Compatibility*, Vol. 41, No 4, November 1999.

26. S. Caorsi and M. Pastorino, "Scattering by Multilayer Isorefractive Elliptic Cylinders," *IEEE Transaction on Antennas and Propagation*, Vol. 52, No 1, January 2004.

27. www.wtec.org/loyola/dsply_jp/ac_gloss.htm

28. www.georgehart.com/virtual-polyhedra/glossary.html

29. www.ch.ic.ac.uk/vchemlib/mol/glossary/

30. xenon.che.ilstu.edu/genchemhelphomepage/glossary/c.html

31. www.agsci.ubc.ca/fnh/courses/glossary.htm

32. F. A. Cotton and G. Wilkinson, "Advanced Inorganic Chemistry: a Comprehensive Text," 4th Ed., John Wiley & Sons, Inc, NY, p. 47, 1980.

33. A. Bessette, "Hands On Chemistry: Chirality," *Bryn Mawr Alumnae Bulletin, Bryn Mawr College,* Sep. 2001.

34. P. R. Young, "Organic Chemistry Online: Chirality," *University of Illinois at Chicago,* 1996.

35. web.mit.edu/esgbio/ www/chem/stereo.html

36. J. March, "Advanced Organic Chemistry," Wiley, 4th ed. 1992.

37. http://www.mi.sanu.ac.yu/vismath/schulze/metaeder/metaeder1/geometrie/chiral

38. W. Thiemann, "International Symposium on Generation and Amplification of Asymmetry in Chemical Systems," Jülich, Germany, pp 32–33, 1973, cited in: Wilder-Smith and A. E., *The Natural Sciences Know Nothing of Evolution*, Master Books, CA, 1981.

39. W. A. Bonner and B. D. Bean, "Asymmetric photolysis with elliptically polarized light" *Orig. Life Evol. Biosphere,* 30, 2000.

40. Gerald Busse, Jens Reinert, and Arne F. Jacob, "Waveguide Characterization of Chiral Material: Experiments," *IEEE Transactions on Microwave Theory and Techniques*, Vol. 47, No 3, March 1999.

41. M. Schneider and J. Marquardt, "Fast Computation of Modified Mathieu Functions Applied to Elliptical Waveguide Problems," *IEEE Transactions on Microwave Theory and Techniques*, Vol. 47, No 4, April 1999.

42. N. W. McLachlan, "Theory and Application of Mathieu Functions," *Dover Publications, Inc.,* New York, 1964.

43. M. Abramowitz and I. A. Stegun, "Handbook of Mathematical Functions With Formulas, Graphs, and Mathematical Tables," *National Bureau of Standards Applied Mathematics Series 55,* June 1964.

44. P. M. Morse and H. Feshbach, "Methods of Theoretical Physics," Vols. I and II, *McGraw-Hill,* New York, 1953.

45. C. A. Balanis, "Advanced Engineering Electromagnetics," *John Wiley & Sons,* New York, 1989.

Appendix

A. Details of Mathieu Functions

Mathieu equations and Mathieu functions are given in Chapter 3. Equations (3.19)-(3.42) depend on Fourior coefficients A and B. To finding A or B, we have to calculate characteristic value α or β respectively. α and β depend on parameter q which also depends on the wave number k and semi focal length f. More details of these calculations are given in this appendix.

A.1 Recurrence Relations for the Coefficients

In the expressions of the Sections 3.3 and 3.4, the Fourier coefficients A and B are used. We can find recurrence relations for the Fourier coefficients for a given characteristic value α_m or β_m by substituting Equations (3.9)-(3.12) into (3.7). Then

$$\left.\begin{aligned} \alpha A_0 - qA_2 &= 0 \\ (\alpha-4)A_2 - q(2A_0 + A_4) &= 0 \\ (\alpha - 4r^2)A_{2r} - q(A_{2r-2} + A_{2r+2}) &= 0, \quad r \geq 2 \end{aligned}\right\} \text{for } S_{e\,2n}(\eta, q), \tag{A.1}$$

$$\left.\begin{aligned} (\alpha-1)A_1 - q(A_1 - A_3) &= 0 \\ [\alpha - (2r+1)^2]A_{2r+1} - q(A_{2r-1} + A_{2r+3}) &= 0, \quad r \geq 1 \end{aligned}\right\} \text{for } S_{e\,2n+1}(\eta, q), \tag{A.2}$$

$$\left.\begin{aligned} (\beta-4)B_2 - qB_4 &= 0 \\ (\beta - 4r^2)B_{2r} - q(B_{2r-2} + B_{2r+2}) &= 0, \quad r \geq 2 \end{aligned}\right\} \text{for } S_{o\,2n+2}(\eta, q), \tag{A.3}$$

$$\left.\begin{aligned} (\beta-1)B_1 - q(B1 - B_3) &= 0 \\ [\beta - (2r+1)^2]B_{2r+1} - q(B_{2r-1} + B_{2r+3}) &= 0, \quad r \geq 1 \end{aligned}\right\} \text{for } S_{o\,2n+1}(\eta, q). \tag{A.4}$$

These relations are linear difference equations, and their convergence is important for numerical purposes, since it determines the accuracy of the Fourier coefficients.

A.2 Calculation of the Characteristic Values α_m and β_m

For each q and order m we have a value for α or β. Since the Mathieu functions can be even or odd, and depend on order m which can also be even or odd, we have totally following four kinds characteristic values.

α_{2n} *for even Mathieu functios and even order* m $(m = 0, 2, 4, ...)$,
α_{2n+1} *for even Mathieu functios and odd order* m $(m = 1, 3, 5, ...)$,
β_{2n+2} *for odd Mathieu functios and even order* m $(m = 2, 4, 6, ...)$,
β_{2n+1} *for odd Mathieu functios and odd order* m $(m = 1, 3, 5, ...)$.

To finding α_{2n} from the second formula of (A.1) we have

$$(\alpha - 4)A_2 - q(A_4 + 2A_0) = 0. \qquad (A.5)$$

Writing

$$V_0 = A_2 / A_0, \quad V_2 = A_4 / A_2, \qquad then \quad V_0 V_2 = A_4 / A_0.$$

Dividing (A.5) by A_0 and making these substitutions gives

$$(4 - \alpha)V_0 + q(V_0 V_2 + 2) = 0,$$
$$-V_0 = \frac{1}{2}q / [1 - \frac{1}{4}(\alpha - qV_2)].$$

In the same way from the third formula of (A.1) with

$$V_{2r-2} = A_{2r} / A_{2r-2}, \qquad V_{2r} = A_{2r+2} / A_{2r},$$

we get $\quad (4r^2 - \alpha)V_{2r-2} + q(V_{2r-2}V_{2r} + 1) = 0,$

for $r > 1 \quad -V_{2r-2} = (q/4r^2)/[1-(1/4r^2)(\alpha - qV_{2r})],$ (*A*.6)

or $\quad V_{2r} = \dfrac{\alpha - 4r^2}{q} - \dfrac{1}{V_{2r-2}}.$

Substituting *r* =*2* in (A.6) yields

$$-V_2 = (q/16)/[1-\frac{1}{16}(\alpha - qV_4)],$$

then $\quad -V_0 = \frac{1}{2}q/\{1-\frac{1}{4}\alpha - (q^2/64)/[1-\frac{1}{16}(\alpha - qV_4)]\}.$

Now putting *r* =*3* in (A.6) we can obtain a formula for V_4,

$$-V_4 = \frac{q/36}{[1-\frac{1}{16}(\alpha - qV_4)]}.$$

Continuing this process we get the infinite continued fraction

$$-V_0 = \cfrac{\frac{1}{2}q}{1-\frac{1}{4}\alpha - \cfrac{\frac{1}{64}q^2}{1-\frac{1}{16}\alpha - \cfrac{\frac{1}{576}q^2}{1-\frac{1}{36}\alpha - \cfrac{\frac{1}{2304}q^2}{1-\frac{1}{64}\alpha - \ldots \cfrac{q^2/16r^2(r-1)^2}{1-\alpha/4r^2 - \ldots}}}}}$$

$$= \cfrac{\frac{1}{2}q}{1-\frac{1}{4}\alpha -} \cfrac{\frac{1}{64}q^2}{1-\frac{1}{16}\alpha -} \cfrac{\frac{1}{576}q^2}{1-\frac{1}{36}\alpha -} \cfrac{\frac{1}{2304}q^2}{1-\frac{1}{64}\alpha -} \ldots \cfrac{q^2/16r^2(r-1)^2}{1-\alpha/4r^2 -} \ldots \qquad (A.7)$$

From the first formula of (A.1) and (A.7) we have

$$\alpha = \frac{-\frac{1}{2}q^2}{1-\frac{1}{4}\alpha-}\ \frac{\frac{1}{64}q^2}{1-\frac{1}{16}\alpha-}\ \frac{\frac{1}{576}q^2}{1-\frac{1}{36}\alpha-}\ \frac{\frac{1}{2304}q^2}{1-\frac{1}{64}\alpha-}\ \cdots\frac{q^2/16r^2(r-1)^2}{1-\alpha/4r^2-}\cdots \qquad (A.8)$$

which is characteristic value for α_{2n}.

To finding α_{2n+1} from the first formula of (A.2) we have

$$(\alpha-1-q)A_1 - qA_3 = 0. \qquad (A.9)$$

Writing

$$V_1 = A_3/A_1 = \frac{\alpha-1-q}{q} = \frac{\alpha-1}{q} - 1, \qquad (A.10)$$

then $V_1V_3 = A_5/A_1$.

From the second formula of (A.2) with

$$V_{2r-1} = A_{2r+1}/A_{2r-1}, \qquad V_{2r+1} = A_{2r+3}/A_{2r+1},$$

we get $[\alpha-(2r+1)^2]V_{2r-1} - q(V_{2r-1}V_{2r+1}+1) = 0,$

for $r>0$ $\quad -V_{2r-1} = [q/(2r+1)^2]/\{1-[1/(2r+1)^2](\alpha - qV_{2r+1})\}, \qquad (A.11)$

or $\quad V_{2r+1} = \frac{\alpha-(2r+1)^2}{q} - \frac{1}{V_{2r-1}}.$

Substituting r =*1, 2,* and *3* in (A.11) yields

$$-V_1 = \frac{1}{9}q/[1-\frac{1}{9}(\alpha - qV_3)],$$

$$-V_3 = \frac{1}{25}q/[1-\frac{1}{25}(\alpha - qV_5)],$$

$$-V_5 = \frac{1}{49}q/[1-\frac{1}{49}(\alpha - qV_7)].$$

Continuing this process we get the infinite continued fraction

$$-V_1 = \cfrac{\frac{1}{9}q}{1-\frac{1}{9}\alpha-\cfrac{\frac{1}{225}q^2}{1-\frac{1}{25}\alpha-\cfrac{\frac{1}{1225}q^2}{1-\frac{1}{49}\alpha-\ldots\cfrac{q^2/[(2r-1)^2(2r+1)^2]}{1-\alpha/(2r+1)^2-\ldots}}}}$$

$$= \cfrac{\frac{1}{9}q}{1-\frac{1}{9}\alpha-}\ \cfrac{\frac{1}{225}q^2}{1-\frac{1}{25}\alpha-}\ \cfrac{\frac{1}{1225}q^2}{1-\frac{1}{49}\alpha-}\ \ldots\cfrac{q^2/[(2r-1)^2(2r+1)^2]}{1-\alpha/(2r+1)^2-}\ldots \qquad (A.12)$$

From (A.10) and (A.12) we have

$$\alpha = 1+q-\cfrac{\frac{1}{9}q^2}{1-\frac{1}{9}\alpha-}\ \cfrac{\frac{1}{225}q^2}{1-\frac{1}{25}\alpha-}\ \cfrac{\frac{1}{1225}q^2}{1-\frac{1}{49}\alpha-}\ \ldots\cfrac{q^2/[(2r+1)^2(2r-1)^2]}{1-\alpha/(2r+1)^2-}\ldots \qquad (A.13)$$

which is characteristic value for α_{2n+1}.

To finding β_{2n+2} from the second formula of (A.13) we have

$$(\beta-4)B_2 - qB_4 = 0. \qquad (A.14)$$

Writing

$$V_2 = B_4/B_2 = (\beta-4)/q, \qquad (A.15)$$
$$\textit{then} \quad V_2V_4 = B_6/B_2.$$

From the second formula of (A.3) with

$$V_{2r-2} = B_{2r} / B_{2r-2}, \qquad V_{2r} = B_{2r+2} / B_{2r},$$

we get $\quad (\beta - 4r^2)V_{2r-2} - q(V_{2r-2}V_{2r} + 1) = 0,$

for $r > 1 \quad -V_{2r-2} = (q/4r^2)/[1-(1/4r^2)(\beta - qV_{2r})],$ (*A*.16)

or $\quad V_{2r} = \dfrac{\beta - 4r^2}{q} - \dfrac{1}{V_{2r-2}}.$

Substituting *r* =*2, 3,* and *4* in (A.16) yields

$$-V_2 = \frac{1}{16}q/[1-\frac{1}{16}(\beta - qV_4)],$$
$$-V_4 = \frac{1}{36}q/[1-\frac{1}{36}(\beta - qV_6)],$$
$$-V_6 = \frac{1}{64}q/[1-\frac{1}{64}(\beta - qV_8)].$$

Continuing this process we get the infinite continued fraction

$$-V_2 = \cfrac{\frac{1}{16}q}{1-\frac{1}{16}\beta - \cfrac{\frac{1}{576}q^2}{1-\frac{1}{36}\beta - \cfrac{\frac{1}{2304}q^2}{1-\frac{1}{64}\beta - \ldots \cfrac{q^2/16r^2(r-1)^2}{1-\beta/4r^2 - \ldots}}}}$$

$$= \cfrac{\frac{1}{16}q}{1-\frac{1}{16}\beta -} \cfrac{\frac{1}{576}q^2}{1-\frac{1}{36}\beta -} \cfrac{\frac{1}{2304}q^2}{1-\frac{1}{64}\beta -} \ldots \cfrac{q^2/16r^2(r-1)^2}{1-\beta/4r^2 -} \ldots \qquad (A.17)$$

From (A.15) and (A.17) we have

$$\beta = 4 - \cfrac{\frac{1}{16}q^2}{1-\frac{1}{16}\beta -} \cfrac{\frac{1}{576}q^2}{1-\frac{1}{36}\beta -} \cfrac{\frac{1}{2304}q^2}{1-\frac{1}{64}\beta -} \ldots \cfrac{q^2/16r^2(r-1)^2}{1-\beta/4r^2 -} \ldots \qquad (A.18)$$

which is characteristic value for β_{2n+2}.

To finding β_{2n+1} from the first formula of (A.4) we have

$$(\beta - 1 + q)B_1 - qB_3 = 0. \qquad (A.19)$$

Writing

$$V_1 = B_3 / B_1 = \frac{\beta - 1 + q}{q} = \frac{\beta - 1}{q} + 1, \qquad (A.20)$$

$$then \qquad V_1 V_3 = B_5 / B_1.$$

From the second formula of (A.4) with

$$V_{2r-1} = B_{2r+1} / B_{2r-1}, \qquad V_{2r+1} = B_{2r+3} / B_{2r+1},$$

$$we\ get \qquad [\beta - (2r+1)^2]V_{2r-1} - q(V_{2r-1}V_{2r+1} + 1) = 0,$$

$$for\ \ r > 0 \qquad -V_{2r-1} = [q/(2r+1)^2]/\{1 - [1/(2r+1)^2](\beta - qV_{2r+1})\}, \qquad (A.21)$$

$$or \qquad V_{2r+1} = \frac{\beta - (2r+1)^2}{q} - \frac{1}{V_{2r-1}}.$$

Substituting $r = 1, 2,$ and 3 in (A.21) yields

$$-V_1 = \frac{1}{9}q/[1 - \frac{1}{9}(\beta - qV_3)],$$

$$-V_3 = \frac{1}{25}q/[1 - \frac{1}{25}(\beta - qV_5)],$$

$$-V_5 = \frac{1}{49}q/[1 - \frac{1}{49}(\beta - qV_7)].$$

Continuing this process we get the infinite continued fraction

$$-V_1 = \cfrac{\frac{1}{9}q}{1-\frac{1}{9}\beta-\cfrac{\frac{1}{225}q^2}{1-\frac{1}{25}\beta-\cfrac{\frac{1}{1225}q^2}{1-\frac{1}{49}\beta-\ldots\cfrac{q^2/[(2r-1)^2(2r+1)^2]}{1-\beta/(2r+1)^2-\ldots}}}}$$

$$= \cfrac{\frac{1}{9}q}{1-\frac{1}{9}\beta-}\ \cfrac{\frac{1}{225}q^2}{1-\frac{1}{25}\beta-}\ \cfrac{\frac{1}{1225}q^2}{1-\frac{1}{49}\beta-}\ \ldots\cfrac{q^2/[(2r-1)^2(2r+1)^2]}{1-\beta/(2r+1)^2-}\ldots \qquad (A.22)$$

From (A.20) and (A.22) we have

$$\beta = 1-q-\cfrac{\frac{1}{9}q^2}{1-\frac{1}{9}\beta-}\ \cfrac{\frac{1}{225}q^2}{1-\frac{1}{25}\beta-}\ \cfrac{\frac{1}{1225}q^2}{1-\frac{1}{49}\beta-}\ \ldots\cfrac{q^2/[(2r+1)^2(2r-1)^2]}{1-\beta/(2r+1)^2-}\ldots \qquad (A.23)$$

which is characteristic value for β_{2n+1}.

Since α, β and q are finite, the denominator of the general term of the Equations (A.8), (A.13), (A.18), and (A.23) approach unity as r goes to infinite, while the numerator of them tends to zero. Hence (A.8), (A.13), (A.18), and (A.23) are convergent.

A.3 Calculation of the Fourier Coefficients *A* and *B*

Calculation of the Fourier coefficients is more complicate than the computation of the characteristic values. Since convergence of the series is very important. Once the characteristic values α or β have been determined, the recurrence relations (A.1)-(A.4) can be applied to calculate the Fourier coefficients A or B.

Now assume the characteristic value α computed for a given q and even order m. To calculate Fourier coefficient A, we can use recurrence relation (A.1) and get

$$V_0 = A_2 / A_0 = \alpha / q, \quad and \quad V_2 = A_4 / A_2 = (\alpha - 4)/q - 2q/\alpha, \quad then$$
$$V_{2r} = A_{2r+2} / A_{2r} = (\alpha - r^2)/q - 1/V_{2r-2} \qquad for \quad r > 1. \qquad (A.24)$$

In practice, r in (A.24) for calculations is limited and can not be infinite. To finding the maximum value of r we have to consider convergence of the series. For do that from the third relation of (A.1) writing $(r+1)$ for r, we have

$$[\alpha - 4(r+1)^2]A_{2r+2} - q(A_{2r} - A_{2r+4}) = 0,$$
$$or \quad [\alpha - 4(r+1)^2]V_{2r} - q(V_{2r}V_{2r+2} + 1) = 0, \quad where \quad V_{2r} = A_{2r+2} / A_{2r},$$
$$so \qquad V_{2r+2} + \frac{1}{V_{2r}} = [\alpha - 4(r+1)^2]/q.$$
$$Then \qquad V_{2r+2} + \frac{1}{V_{2r}} \to -\infty \qquad as \qquad r \to +\infty,$$

it is evident that V_{2r} can not oscillate boundedly, and can not tend to a unique finite limit other than zero. For convergence of the series representing $S_{e\,2n}(\eta, q)$, $A_{2r} \to 0$ as $r \to +\infty$, so V_{2r} must also tend to zero. Consequently, as $r \to +\infty$, one solution tends to zero, and other to infinity. Thus for control of the convergence of series, the maximum value of r in (A.24) must indicate when V_{2r} tend to zero. Then, in practice we must put a condition in (A.24) and find r_max while V_{2r} approach to zero. So in the following formulas r_max is the maximum value of r such that the obtained coefficients with this r will converge the series.

$$Take \quad G_0 = A_2 / A_0 = V_0, \quad and \quad G_2 = A_4 / A_0 = V_2 V_0, \quad then$$
$$G_{2r} = A_{2r+2} / A_0 = V_{2r}V_{2r-2} \ldots V_2 V_0, \quad for \quad 2 \le r \le r\_\max. \qquad (A.25)$$

By (A.25) we have the relation of all coefficients A to A_0, but we can not obtain them since A_0 is unknown. Another knowledge about the coefficients is normalization. We can normalize the series $S_{e\,2n}(\eta, q)$ by the condition that

$$\frac{1}{\pi}\int_0^{2\pi} S_{e\,2n}^2(\eta,q)d\eta = 2A_0^2 + \sum_{r=1}^{r\_\max} A_{2r}^2 = 1, \qquad (A.26)$$

for all real values of q. So from (A.25) and (A.26) we have

$$sum = 2 + \sum_{r=0}^{r\_\max} G_{2r}^2,$$
$$A_0 = \sqrt{\frac{1}{sum}}, \quad and \quad A_{2r+2} = G_{2r}A_0, \quad for\ 0 \le r \le r\_\max. \qquad (A.27)$$

Thus (A.27) is coefficients A for a known characteristic value α, which computed with a given value q and even order m.

The same way we can find Fourier coefficients A for a known characteristic value α, which computed with a given value q and odd order m. So from (A.2) we have

$$V_1 = A_3 / A_1 = (\alpha - 1)/q - 1,$$
$$V_{2r+1} = A_{2r+3} / A_{2r+1} = [\alpha - (2r+1)^2]/q - 1/V_{2r-1} \quad for\ 1 \le r \le r\_\max,$$
$$G_1 = A_3 / A_1 = V_1,$$
$$G_{2r+1} = A_{2r+3} / A_1 = V_{2r+1}V_{2r-1} \ldots V_3V_1 \quad for\ 1 \le r \le r\_\max. \qquad (A.28)$$

We can normalize the series $S_{e\,2n+1}(\eta, q)$ by the condition that

$$\frac{1}{\pi}\int_0^{2\pi} S_{e\,2n+1}^2(\eta,q)d\eta = \sum_{r=0}^{r\_\max} A_{2r+1}^2 = 1, \qquad (A.29)$$

for all real values of q. So from (A.28) and (A.29) we have

$$sum = 1 + \sum_{r=0}^{r\_\max} G_{2r+1}^2,$$
$$A_1 = \sqrt{\frac{1}{sum}}, \quad and \quad A_{2r+3} = G_{2r+1}A_1, \quad for\ 0 \le r \le r\_\max. \qquad (A.30)$$

Thus (A.30) is coefficients A for a known characteristic value α, which computed with a given value q and odd order m.

To finding the Fourier coefficients B for a known characteristic value β, which computed with a given value q and even order m, from (A.3) we have

$$
\begin{aligned}
&V_2 = B_4 / B_2 = (\beta - 4)/q, \\
&V_{2r} = B_{2r+2} / B_{2r} = (\beta - 4r^2)/q - 1/V_{2r-2} \qquad for\ \ 2 \le r \le r\_\max, \\
&G_2 = B_4 / B_2 = V_2, \\
&G_{2r} = B_{2r+2} / B_2 = V_{2r} V_{2r-2} \ \ldots\ V_4 V_2 \qquad for\ \ 2 \le r \le r\_\max.
\end{aligned} \tag{A.31}
$$

We can normalize the series $S_{o\,2n+2}\ (\eta, q)$ by the condition that

$$
\frac{1}{\pi} \int_0^{2\pi} S^2_{o\,2n+2}(\eta, q) d\eta = \sum_{r=0}^{r\_\max} B^2_{2r+2} = 1, \tag{A.32}
$$

for all real values of q. So from (A.31) and (A.32) we have

$$
\begin{aligned}
&sum = 1 + \sum_{r=1}^{r\_\max} G^2_{2r}, \\
&B_2 = \sqrt{\frac{1}{sum}}, \quad and \quad B_{2r+2} = G_{2r} B_2, \qquad for\ 1 \le r \le r\_\max.
\end{aligned} \tag{A.33}
$$

Thus (A.33) is coefficients B for a known characteristic value β, which computed with a given value q and even order m.

Finally for finding the Fourier coefficients B for a known characteristic value β, which computed with a given value q and odd order m, from (A.4) we have

$$
\begin{aligned}
&V_1 = B_3 / B_1 = (\beta - 1)/q + 1, \\
&V_{2r+1} = B_{2r+3} / B_{2r+1} = [\beta - (2r+1)^2]/q - 1/V_{2r-1} \qquad for\ \ 1 \le r \le r\_\max, \\
&G_1 = B_3 / B_1 = V_1, \\
&G_{2r+1} = B_{2r+3} / B_1 = V_{2r+1} V_{2r-1} \ \ldots\ V_3 V_1 \qquad for\ \ 1 \le r \le r\_\max.
\end{aligned} \tag{A.34}
$$

We can normalize the series $S_{o\,2n+1}(\eta, q)$ by the condition that

$$\frac{1}{\pi}\int_0^{2\pi} S^2_{o\,2n+1}(\eta,q)d\eta = \sum_{r=0}^{r\_\max} B^2_{2r+1} = 1, \qquad (A.35)$$

for all real values of q. So from (A.34) and (A.35) we have

$$sum = 1 + \sum_{r=0}^{r\_\max} G^2_{2r+1},$$

$$B_1 = \sqrt{\frac{1}{sum}}, \quad and \quad B_{2r+3} = G_{2r+1}B_2, \quad for\ 0 \le r \le r\_\max. \qquad (A.36)$$

Thus (A.36) is coefficients B for a known characteristic value β, which computed with a given value q and odd order m.